FINAL REPORT

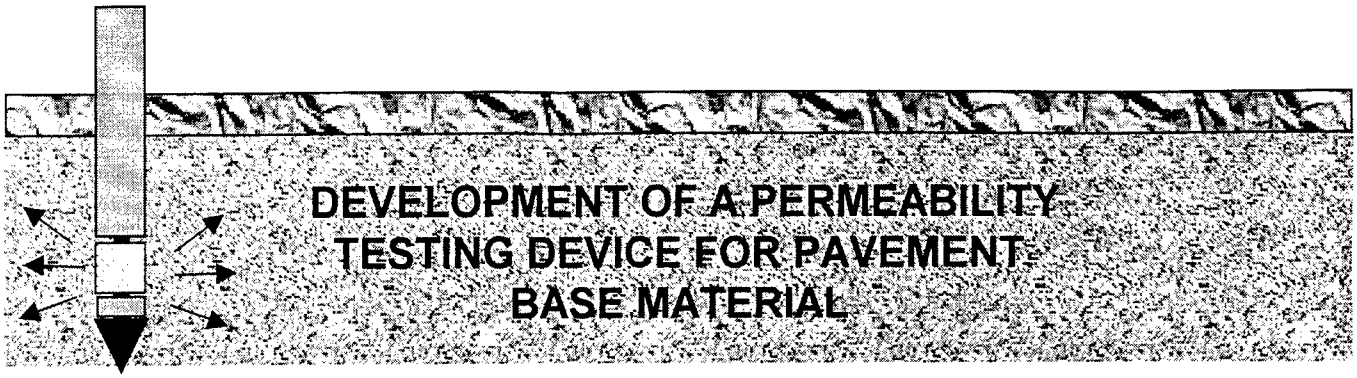

DEVELOPMENT OF A PERMEABILITY TESTING DEVICE FOR PAVEMENT BASE MATERIAL

Submitted by: David Bloomquist Ph.D., PE
University of Florida
Department of Civil Engineering
345 Weil Hall
PO Box 116580
Gainesville, Fl 32611

Submitted to: **Florida Department of Transportation**

Agency ID Nos. WPI 0510715
99700-7619-119
B-9082
HPR 0715
UF Contract No. 4910450449612

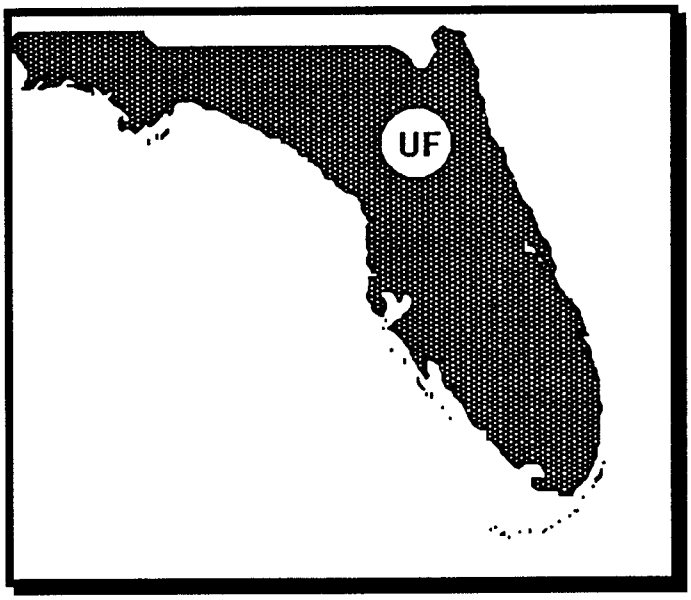

Technical Report Documentation Page

1. Report No.		3. Recipient's Catalog No.
WPI # 0510715	PB99-106650	

4. Title and Subtitle	5. Report Date
Development of a Permeability Testing Device for Pavement Base Material	October 1998
	6. Performing Organization Code: 49104504 496-12
7. Author(s): D. Bloomquist	8. Performing Organization Report No.
9. Performing Organization Name and Address: University of Florida, Department of Civil Engineering, 345 Weil Hall / P. O. Box 116580, Gainesville, FL 32611-6580	10. Work Unit No. (TRAIS): 99700-7619-119
	11. Contract or Grant No.: B-9082
12. Sponsoring Agency Name and Address: Florida Department of Transportation, Research Management Center, 605 Suwannee Street, MS 30, Tallahassee, FL 32301-8064	13. Type of Report and Period Covered: Final Report, 9/1/94 - 3/31/98
	14. Sponsoring Agency Code

15. Supplementary Notes

Prepared in cooperation with the Federal Highway Administration

16. Abstract

This report describes the design, construction and initial field tests of a device capable of measuring the insitu permeability of base, subgrade, and subbase material.

The insitu permeability device consists of a trailer mounted probe that is hydraulically pushed into the ground. Located at the end of the probe is a 1.74 cm cylindrical porous element. Once inserted, water is forced out through the element and either constant or falling head permeability tests can be conducted. The trailer is ballasted with twin polyethylene water tanks and is equipped with hydraulic leveling jacks. A coring device and portable generator are also included.

Results to date indicate a trend may exist between standard laboratory and this insitu permeability test. Thus, the FDOT plans to conduct extensive field tests on a variety of new and existing pavement bases in order to develop a correlation between pavement performance and insitu permeability.

17. Key Words	18. Distribution Statement
Permeability, Pavement Design, Base Material	No restrictions. This document is available to the public through the National Technical Information Service, Springfield, VA, 22161

19. Security Classif. (of this report)	20. Security Classif. (of this page)	21. No. of Pages	22. Price
Unclassified	Unclassified	143	

DISCLAIMER

"The opinions, findings and conclusions expressed in this publication are those of the authors and not necessarily those of the Florida Department of Transportation or the U.S. Department of Transportation.

Prepared in cooperation with the State of Florida Department of Transportation and the U.S. Department of Transportation."

SI* (MODERN METRIC) CONVERSION FACTORS

APPROXIMATE CONVERSIONS TO SI UNITS

Symbol	When You Know	Multiply By	To Find	Symbol
	LENGTH			
in	inches	25.4	millimeters	mm
ft	feet	0.305	meters	m
yd	yards	0.914	meters	m
mi	miles	1.61	kilometers	km
	AREA			
in^2	square inches	645.2	square millimeters	mm^2
ft^2	square feet	0.093	square meters	m^2
yd^2	square yards	0.836	square meters	m^2
ac	acres	0.405	hectares	ha
mi^2	square miles	2.59	square kilometers	km^2
	VOLUME			
fl oz	fluid ounces	29.57	milliliters	ml
gal	gallons	3.785	liters	l
ft^3	cubic feet	0.028	cubic meters	m^3
yd^3	cubic yards	0.765	cubic meters	m^3
NOTE: Volumes greater than 1000 l shall be shown in m^3.				
	MASS			
oz	ounces	28.35	grams	g
lb	pounds	0.454	kilograms	kg
T	short tons (2000 lb)	0.907	megagrams	Mg
	TEMPERATURE (exact)			
°F	Fahrenheit temperature	5(F-32)/9 or (F-32)/1.8	Celcius temperature	°C
	ILLUMINATION			
fc	foot-candles	10.76	lux	l
fl	foot-Lamberts	3.426	candela/m^2	cd/m^2
	FORCE and PRESSURE or STRESS			
lbf	poundforce	4.45	newtons	N
psi	poundforce per square inch	6.89	kilopascals	kPa

APPROXIMATE CONVERSIONS FROM SI UNITS

Symbol	When You Know	Multiply By	To Find	Symbol
	LENGTH			
mm	millimeters	0.039	inches	in
m	meters	3.28	feet	ft
m	meters	1.09	yards	yd
km	kilometers	0.621	miles	mi
	AREA			
mm^2	square millimeters	0.0016	square inches	in^2
m^2	square meters	10.764	square feet	ft^2
m^2	square meters	1.195	square yards	yd^2
ha	hectares	2.47	acres	ac
km^2	square kilometers	0.386	square miles	mi^2
	VOLUME			
ml	milliliters	0.034	fluid ounces	fl oz
l	liters	0.264	gallons	gal
m^3	cubic meters	35.71	cubic feet	ft^3
m^3	cubic meters	1.307	cubic yards	yd^3
	MASS			
g	grams	0.035	ounces	oz
kg	kilograms	2.202	pounds	lb
Mg	megagrams	1.103	short tons (2000 lb)	T
	TEMPERATURE (exact)			
°C	Celcius temperature	1.8C + 32	Fahrenheit temperature	°F
	ILLUMINATION			
lx	lux	0.0929	foot-candles	fc
cd/m^2	candela/m^2	0.2919	foot-Lamberts	fl
	FORCE and PRESSURE or STRESS			
N	newtons	0.225	poundforce	lbf
kPa	kilopascals	0.145	poundforce per square inch	psi

* SI is the symbol for the International System of Units. Appropriate rounding should be made to comply with Section 4 of ASTM E380.

(Revised August 1992)

TABLE OF CONTENTS

LIST OF TABLES

LIST OF FIGURES

EXECUTIVE SUMMARY

Each year the Florida Department of Transportation (FDOT) spends millions of dollars maintaining the state's highway system. Since pavements constitute a major subset of this infrastructure and are often exposed to deleterious environmental conditions and as increased traffic loads, their integrity and serviceability is often jeopardized. Since FDOT's goal is to provide a quality system that will minimize the public's cost in road repairs, vehicle maintenance, traffic delays, and accidents, the agency invests heavily in applied research to ameliorate these problems.

Even though the designers of ancient Roman roads apparently recognized the need for adequate drainage, many of today's roads are not well drained, and as a result, the cost of repairing pavements has risen to approximately $30 to $40 billion a year worldwide (1986 est.). Highway officials estimate that pavements constructed on poorly drained base and subbase material may be twice as costly to maintain as well-drained pavements when compared on a long-term basis. Even with this statistic, primary emphasis in current pavement design continues to focus on density and stability criteria rather than on drainability.

The FDOT was one of the first to recognize the importance of constructing pavements on well drained material and in 1995, a two year research project was initiated with the University of Florida's Department of Civil Engineering. The objective was to design and build a device capable of measuring the permeability of base, subgrade, and subbase material in-place.

The insitu permeability device consists of a trailer mounted probe that is hydraulically pushed into the ground. Located at the end of the probe is a 1.74 cm cylindrical porous element. Once inserted, water is forced out through the element and

either constant or falling head permeability tests can be conducted. A weather resistant control panel is installed on the trailer that houses the solenoids, switches, flow meters, and pressure gauges, thereby, allowing the test to be run by one operator from a single location. The trailer is ballasted with twin polyethylene water tanks and is equipped with hydraulic leveling jacks. A coring device and portable generator are also included.

Results to date indicate a trend may exist between standard laboratory and this insitu permeability test. While it was not the objective of this research to correlate the two, and indeed, due to the dissimilarity in the test procedures and boundary conditions, a strong correlation may not exist. Thus, the FDOT plans to conduct extensive field tests on a variety of new and existing pavement bases in order to develop a correlation between pavement performance and insitu permeability. These would include pavements that have failed (primarily due to pumping), in addition to those performing well. Once a data base is established the FDOT should then be able to asses:

- New pavement designs in terms of stability, density, and permeability (drainability).
- Recently constructed pavements (prior to wearing surface placement) for QA/QC verification.
- The condition of existing in service pavements. Location of potential drainage problem areas could result in more efficient use of funds for preventative maintenance as opposed to repair expenditures.

CHAPTER 1
INTRODUCTION

Background

Each year the Florida Department of Transportation (FDOT) spends millions of dollars to maintain the state roadways. Because all pavement systems are exposed to both adverse environmental conditions as well as ever increasing traffic loads, their quality and serviceability are often at risk. For example, in fiscal year 95/96, the FDOT resurfaced 1,891 lane miles of roads. The FDOT's ultimate goal is to provide a quality system that will minimize the public's cost for road repairs, vehicle maintenance, traffic delays, and accidents. In order to meet this goal, the FDOT invests heavily in research to reduce or ameliorate costly repairs.

Road builders have known that water is the greatest threat to a stable, long-lasting pavement. The ancient Romans in fact knew of the damaging effects of water and tried to maintain their roads above the level of the surrounding terrain. In addition to constructing these roads with thick sections, they often provided a sand layer on top of the subgrade and below the first course of flat stones that were generally cemented together. The fact that many of them still exist today attests to the durability of those highways.

Little progress was made during the subsequent 20 centuries after the Romans until the first half of the nineteenth century. One of the most important principles rediscovered was the necessity of keeping roadbeds dry. Although the significance of good roadbed drainage has been acclaimed on and off through the centuries, it has often been unheeded by road designers, and little attention was given to drainage of roadbeds during the latter half of the nineteenth century.

From 1910 to about 1940, pavement engineers widely proclaimed the need for drainage and nearly every textbook on road building and many published articles contained a statement to that effect. However, with the advent of the so called "rational methods" for designing pavements that included laboratory testing of saturated samples of subgrade and base course materials, the emphasis shifted to density and stability criteria rather than drainability.

Even though the builders of the Ancient Roman Roads seemed to recognize the need for good drainage, many modern roads are not well drained, and largely because of this practice, the cost of pavement repair has risen to $30 to $40 billion a year world-wide (1986 est.). Estimates indicate that poorly drained pavements may be more than twice as costly as well-drained ones when compared on a long-term basis.

Objective

The FDOT's Standard Specifications for Road and Bridge Construction (1991) provides guidelines on composition, liquid and plastic limits, gradation and size requirements, density, and bearing ratio. These parameters primarily deal with the base material stress/strain relationship, deformation, volume change, and fatigue under repeated loading.

The Florida Department of Transportation State Materials Office has recognized the need to provide well-drained pavements and in 1995 a two year research project was initiated with the University of Florida to design and build an insitu permeability device. Their primary requirements for the device include ease of operation, repeatability, cost effectiveness, and reliability.

Methodology

In order to meet the FDOT's requirements, an extensive literature search was compiled and is provided in Chapter 2. This chapter further discusses the need for well-drained roadways, the effects that water has on pavements (such as pumping), and the current methods of testing soil permeability. The rational for designing an insitu device is that laboratory test results may be influenced by sample disturbance, various laboratory errors, and by a general tendency to select the most uniform, intact samples for testing.

Once the failure mechanisms are identified as well as the efforts by others to solve them are determined, a prototype design could be formulated. Chapter 3 outlines the design of the insitu permeability device. The probe theory is discussed and equations are provided for the calculation of constant head and falling head permeability. A tentative shape factor for the probe is also computed. The individual components that comprise the device are discussed and schematics of the various sub-systems are presented. A section that indicates the optimum placement of the major components on the device is included.

After construction of a prototype device, the next task was to conduct preliminary testing to verify that the operational requirements were met. This testing procedure is presented in Chapter 4. Instructions on how to use the insitu permeability device and sample permeability calculations (constant and falling head) for insitu and laboratory permeability determination are provided. Preliminary testing of the device was performed at various locations on the University of Florida campus. Testing was also accomplished at the FDOT test pit at the State Materials Office and on two highway construction sites. The results of these tests are presented at the end of the chapter.

Appendix A includes data from the insitu and laboratory constant head testing while Appendix B contains the data obtained from the insitu and laboratory falling head tests.

Results

The final chapter (5) summarizes the results and provides recommendation for further testing. An important parameter, the shape factor is provided for the device probe. This factor can then be used in the calculation of the insitu permeability. It is anticipated that after further testing this device will eventually be used to evaluate the permeability of both base and subbase material. Ultimately new specification standards for roadway design may be generated.

CHAPTER 2
LITERATURE REVIEW

Water Damage to Pavement

Most of the pavements built in the past several decades are made up of stratified bodies of two or more layers, such as portland cement concrete (PCC) or asphalt concrete (AC) on either stabilized or unstabilized bases. Because these systems are not designed for the rapid elimination of infiltrating water, they have the potential for major distress. When water gets into the boundaries between the structural layers, the multilayered systems act as diaphragm pumps under heavy wheel loads. Water moves in the interface voids between a wearing course and its base due to traffic causing the material to degenerate and eject through cracks and joints. This action eventually produces channels and cavities that undermine the supported pavement, resulting in faulting that may eventually lead to total failure. The sketches in Figure 2-1 illustrate some of the possible ways that heavy wheel impact loads on saturated pavements can damage both AC pavements and PCC pavements. For clarity, the vertical dimensions and deformations have been exaggerated.

The dynamic effects of excess water are largely ignored in the design process. Instead the assumption is that the controlling factors are stress and strain, deformation, volume change, and fatigue under repeated loadings. Erosion between a primary pavement layer and its base can occur regardless of the thickness or rigidity of the base, if conditions conductive to erosion exist at their interface. Erosion and ejection of fines due to excessive pore pressures cannot occur in the absence of free water; hence the need for well-drained roadways.

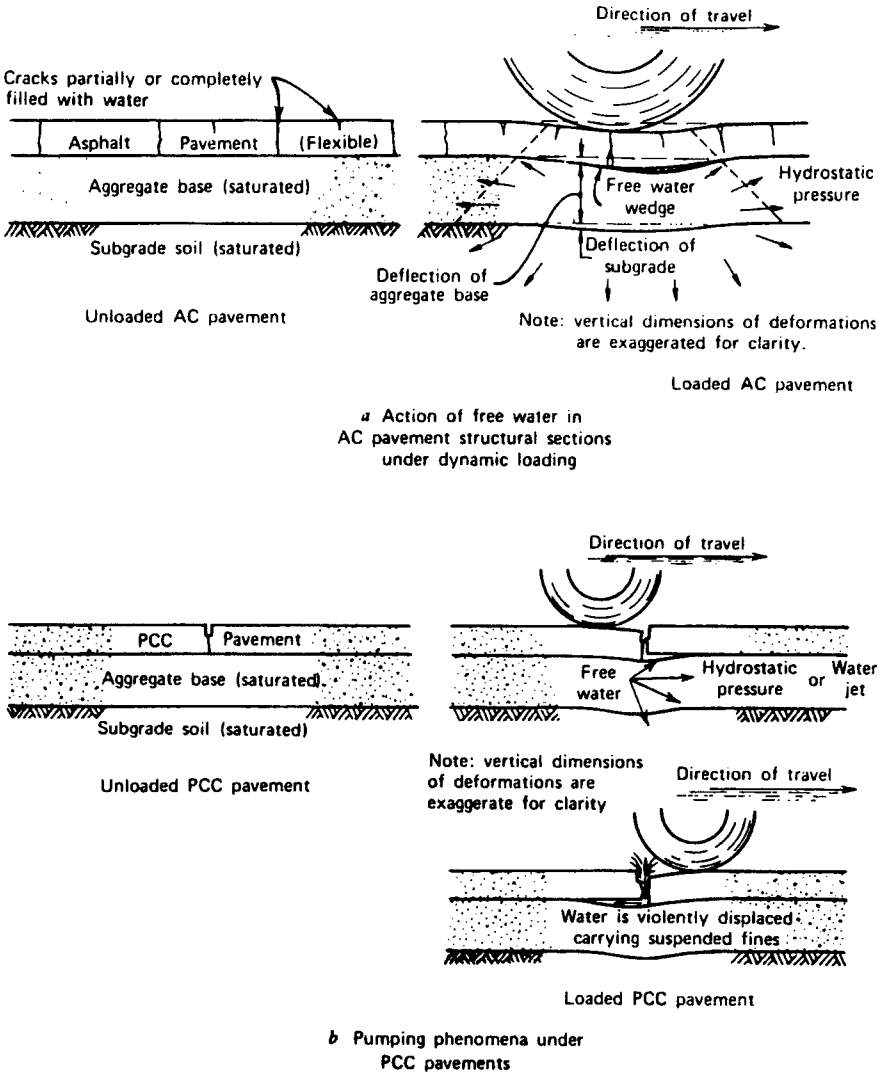

Figure 2-1. The ways that traffic impacts can damage saturated pavements (both rigid and flexible). (Cedergren, 1987, p. 48.)

During construction of roadways, subdrains are used to take care of groundwater, spring inflows, and the like. While it is important to control these factors, consideration needs to be made for surface infiltration. At least 90 to 95 percent of the pavements in the United States are in areas where the rainfall rates are greater than the subgrade capabilities, with very few having drainage systems that can handle this problem.

Surface water infiltration occurs after a pavement is completed and placed into service. Problems usually do not show up initially because the influences of water take

time to reach a critical condition. Although surface water infiltration may eventually reduce the life of a pavement by half were it well drained, this is a gradual process, and during the first few years its effects may go unnoticed. The only outward evidence for several years may only be a dry residue showing up as stains near cracks, joints and across shoulders, and faulting at joints and cracks. Whenever water can be seen flowing out of joints and across shoulders there must be sufficient head or pressure under the adjacent pavement to force the water out. In many cases, it flows out by a combination of artesian head and the pressure of traffic loads.

Because drainability has rarely been considered in the past, many subgrades have a coefficient of permeability that is lower than the rainfall rates that occur each year. This causes any cavities or voids between the pavement and the base to fill with water, placing the structural section in a virtual "bathtub." To determine the importance of this "bathtub" condition, several experimental road tests have been made since 1950. These tests have documented that during times when the pavements contained large amounts of free water, the rates of deterioration in the various tests ranged from 10 to 20 up to hundreds and thousands of times greater than when they contained little or no free water.

During the past several decades, the primary emphasis in pavement design has been on base course density and stability. Since pavement designs are based on the strength of the subgrade and supporting layers in a saturated condition (without evaluating the dynamic effects of wheel impact on any free water trapped beneath structural sections), it has been widely assumed that drainability is not an important attribute. Even though for centuries road builders agreed on the virtues of good drainage, and understood that free water greatly accelerated the rate of damage, nearly all pavements built during the last decades are located on slowly draining systems often containing free water. If premature damage develops after a particular design chart or formula has been used for a number of years, it has been common practice to simply modify the design. For example, the thickness of the structural layers are increased, the percentage of cement or other

stabilizers is raised in an attempt to improve the design. However drainability is not addressed. Many feel that it is neither practical nor economical, nor perhaps even necessary, to speed up the removal of water from structural sections. As a consequence compacted, stabilized bases and subbases nearly all have low permeabilities. Likewise, the materials used in shoulder construction usually act as dams or barriers that prevent the lateral movement of water out of structural sections (Cedergren, 1987).

It might be theoretically possible to build a pavement that is sufficiently "stout" to withstand any specified volume and traffic load for a specified number of repetitions or years of service without providing for good drainage. Unfortunately, some of the most damaging actions caused by traffic load on sections containing free water (pumping, erosion, pulsating pore pressures, etc.) are not significantly reduced by any amount of thickening of base or subbase. The Highway Research Board's Project Committee No. 1, Maintenance of Concrete Pavements as Related to the Pumping Actions of Slabs (Highway Research Board, 1948), says, "The data available show that neither cross section nor thickness have had any effect on pumping. Studies to date have not shown that pavement thickness in excess of that required for imposed loads and the normal supporting value of the subgrade will be either helpful or economically justified."

Spellman (1972) found that heavy wheel loading on PCC pavements constructed on cement treated bases (CTB) caused, "violent water actions" at the interface between the pavement and the base. This caused erosion and formation of cavities under the PCC pavements, ejection of material through the cracks and joints, and the migration of base material from the leading edges and its buildup under trailing edges. This caused loss of support and also produced the "faulting" or "step-off" that is so common in PCC pavements that are damaged by traffic and excess water (Cedergren, 1987).

A comprehensive study made for the Federal Highway Administration (FHWA, 1973) to develop a set of Guidelines for the Design of Subsurface Drainage Systems for Highway Structural Sections, concluded that if free water (primarily from surface

infiltration) is contained within structural sections, the rates of damage from heavy wheel loads are much greater when compared to dry conditions. Subsequent reports prepared for this investigation concluded that poor drainage (slow drainability) of heavy-duty pavements throughout most of the United States is a major contribution to the premature damage in addition, well-drained pavements will almost always be more economical in the long term than poorly drained pavements.

Basic Factors

Many factors contribute to pavement deterioration and failure. Because of this, the subject of distress and failure of pavements is very complex. For example, the aging and oxidation of asphalt films promote deterioration of asphalt concrete pavements and bases. Certain deterioration processes and fatigue under repeated strains are major factors in the cracking and disintegration of PCC pavements. When excess water forms in the spaces between successive lifts of AC pavements, in pore spaces or at the boundaries between PCC pavements and their bases and in joints and cracks, some of the most detrimental actions occur more rapidly.

Large surface areas of pavements are exposed to weather and traffic. Under the combined actions of temperature changes, rainfall, freezing and thawing, oxidation, the stresses and strains of traffic loads, etc., damaging actions occur that shorten life, increase roughness, deposit loosened material on surfaces, and eventually destroy many pavements. Some of the most harmful actions of traffic and water occur entirely within the structural section of a pavement and are unrelated to subgrade strength or behavior (Cedergren, 1987).

As the water content of bases and subbases increases, there is a reduction in the structural support and an increase in the rate of loss of serviceability. When free water completely fills these layers and voids or heavy wheel loads applied to the pavement

surfaces produce impacts in the water that are comparable to a water-hammer. The pulsating water pressures that can build up at such times under wheel impacts not only cause erosion and ejection of material out of pavements, but can strip the asphalt coating from bituminous-stabilized bases and subbases. The water actions can disintegrate cement-treated bases, weaken base courses by rearranging the internal structure of fine-grained materials in aggregate mixtures, overstress subgrades where total thicknesses are inadequate, and cause a number of other detrimental actions.

A special Highway Research Board report (HRB, 1952) describes the sequence of damage to concrete pavement containing free water (cited in Cedergren, 1987, p. 30):

> The first step in the development of pumping is the breaking of the seals of adjoining slab ends and the loss of intimate contact between the free edges of the pavement and the shoulders, which of course, allows surface water to reach the subgrade soil. Seals at transverse joints and open cracks are broken by contraction of the adjoining slabs as the temperature of the pavement drops, by relative deflection (deflection of the slab on one side of the joint or crack with respect to that on the other) as vehicles pass over the pavement and by other factors, such as weathering and poor initial bonding. The loss of intimate contact between the shoulders and the edges of the pavement is caused by (1) shrinkage of the shoulder material, (2) excessive deflections of the slab edges, (3) rutting of the shoulders and (4) in pumping pavements, the ejection of water from the subgrade to the surface.
>
> A vehicle in moving over the pavement develops pressure between the bottom of the slab and the subgrade which causes water, if present on the subgrade, to surge or flow in the direction in which it might escape. The magnitude of the pressure is, of course, dependent upon the deflection of the pavement slab and the degree of confinement or open cracks, but in time, if susceptible pumping conditions obtain, it generally develops an avenue of escape between the shoulder and the edges of the pavement. In pavements constructed on a fine-grained subgrade soil this surging and flow of water beneath the slab causes fines in the soil to mix with the water, which, in escaping, carries the fines with it. A void, becoming progressively larger with repetition of traffic, then forms beneath the pavement slab.
>
> In the early stages of pumping the escape of the water or slurry between the shoulder and the edge of the pavement is, as a rule, confined within several feet of a transverse joint or open crack; but as pumping progresses, an escape channel frequently develops along the full length of the pavement slab. As edge pumping

increases a greater volume of water is permitted to reach the subgrade thus increasing the amount and the intensity of pumping.

With free water completely filling pavements, buoyancy of supersaturated layers reduces unit weights to submerged weights, thereby reducing frictional strengths. Free water provides the medium for the erosion of material at boundaries between pavements and bases and for the physical ejection of material out of cracks and joints, leading to faulting or step-off and ultimately to total failure of PCC pavements, and serious damage to AC pavements. Free water in AC pavements contributes to shrinkage cracking and to oxidation and loss of flexibility, which can lead to cracking and general deterioration of wearing courses and stabilized bases. The breaking out of chunks of pavements constructed of two or more successive layers of similar paving material is almost always associated with free water. In nearly every area of the country, the effects of excess pore pressure and erosional actions are among the most severe causes of loss of pavement life.

Since some of the damaging action in pavements are caused by the high velocity of water in structural sections, an indication of the probable rates of damage with age can be inferred by examining the fundamental equations of flow in enclosed channels, pipes, etc. According to fundamental hydraulics, velocities vary with the square root of pipe or channel diameter. Therefore, when a pavement is new and channel dimensions small, velocities of the trapped water will be lower than after the channels have been enlarged by erosion. Consequently, as a pavement ages, the rate of movement and quantity of water moved can be expected to increase geometrically with time and traffic. Other deteriorating factors such as fatigue, oxidation, and increased volume of traffic add to the propensity for accelerated rates of damage with age.

Importance of Environmental Factors

Among the well-documented tests providing factual information about environmental conditions and loss in serviceability rates of are Road Test One-MD (in

1950), the WASHO Road Test (in 1954), and the AASHO Road Test (in 1958-1960). These road tests provide records of much faster losses in serviceability during unfavorable environmental conditions than during more favorable times.

Even though all of these road test had much greater rates of pavement damage during wet periods, this has not led to any significant change in pavement design practices beyond the use of stronger pavements and "erosion-resistant" types of bases. Until the issuance of the FHWA Guidelines in 1973, there had been no coordinated effort in several decades to improve drainability and reduce exposure of structural sections to excess water.

Detailed studies for the preparation of the FHWA Guidelines, which includes exhaustive discussions with highway engineers in nine selected states and examination of hundreds of miles of "typical" pavements from coast to coast, led to a number of conclusions (Cedergren, 1987):

1. Water can get into most pavements through joints, cracks, porous surfaces, high shoulders, and so on, since the present state of the art does not assure watertightness of pavements for long periods of time. Thermal changes, traffic, and other environmental changes are continuously occurring that develop openings in pavements.

2. The rates of damage to most pavements are much greater when excess water is in structural sections than when there is little or no excess water there.

3. Rainfall rates in most parts of the United States are greater than coefficients of permeability of subgrades (natural or compacted); hence the well-known "bathtub" condition tends to exist in most pavements for significant amounts of time each year.

4. As a consequence of items 2 and 3, most modern roads, airfields, and other important pavements are actually very slow draining systems, and many contain excess water for extensive periods of time a number of times each year. This greatly accelerates loses in serviceability and increases repair and replacement costs.

Possible Remedies

Altering the design of pavements to reduce the damage caused by traffic on structural sections that contain excess water without increasing the drainability does not remove the basic cause of deterioration. This is a costly method that consumes large amounts of essential materials in relation to the benefits obtained. On the whole, efforts to change details without improving drainability are having only little effect on the amount of deterioration and failure in relation to cost.

The studies made in developing the FHWA Guidelines led to the following basic conclusions regarding the prevention of water-induced damage to pavements (Cedergren, 1987):

1. When all cost over the useful life of an important pavement are considered, a well-drained pavement will almost always be more economical than the same pavement designed as a slowly draining structure.

2. The design of a subsurface drainage system should be on a rational basis using seepage principles to calculate probable inflow quantities and to determine required outflow conductivity.

3. If a pavement is to be drained fast enough to significantly reduce water-induced damage, a highly permeable macadam type of base drainage layer is needed under the full width of the heavy traffic lanes, fitted with longitudinal collector pipes and outlet pipes to ensure free gravity drainage out of the system and thus prevent harmful accumulations of water within the structural sections.

4. The special base drainage layer needed for rapid drainage of a roadbed generally can be substituted on an inch-for-inch basis for the nondraining bases and subbases being replaced by the drainage layer. Frequently the only added cost for a well-drained highway or airfield pavement will be the cost of the collector pipes and outlet pipes.

5. The fast-draining layer should be constructed of strong, durable aggregates, generally in the range of 1/4- to 1-inch particle size. No particles smaller than about 1/4 inch should be allowed in any base drainage layer because smaller sizes can seriously cut permeability, and the upper size should be kept within the range of 1/2 up to a maximum of 1 1/2 inch.

6. Crushed durable rock or gravel with high frictional strength and high interlocking properties will often be sufficiently stable without the use of additives or binders; however, if the aggregates are largely rounded, or if added cohesion is needed for the structural requirements, construction stability, or permanent stability, it may be necessary to stabilize these materials by plant-mixing them with 2 to 4 percent hot paving-grade asphalt or other suitable binders.

A leading engineer has said that well-drained structures are nearly always more economical and efficient than their undrained counterparts. A good deal of evidence suggests this is just as true of pavements as of other engineering structures that are subjected to the influences of free water.

Coefficient of Permeability

Analysis of water flow in saturated soils are usually based on Darcy's law which, in turn, is based on the experimental observation of a linear relationship between the rate of flow and the driving forces. Depending on the discipline of the user, Darcy's law can be written in many forms. The form most commonly used in geotechnical engineering is

$$q = -k\, i\, A$$

where q = the flow rate (L^3/T)
i = the hydraulic gradient (dimensionless)
A = the total cross-sectional area of flow (L^2)
k = the constant of proportionality (L/T).

The constant of proportionality is termed the hydraulic conductivity in most disciplines but is often termed the coefficient of permeability or permeability by civil engineers and will be referred to as such in this report. The coefficient of permeability is defined as the discharge velocity through unit area under hydraulic gradient. It can also be thought of as the ease with which a fluid passes through a porous medium.

The common form is to solve for k, where the other variables are known

$$k = \frac{Q}{i\,A\,t}$$

where Q = the quantity of seepage (L^3)
t = the length of time (T).

Factors Influencing Permeability

Although the coefficient of permeability is often considered to be a constant for a given soil or rock, it can vary widely for a given material, depending on a number of factors. Its absolute values depend, first of all, on the properties of water, of which viscosity is the most important. For individual materials and formations its value depends primarily on the dimensions of the finest pore spaces through which water must travel and on the size and continuity of cracks and joints in rocks and fissured clays. In short, the ease with which water can travel through soils and rocks depends largely on the following (Cedergren, 1989):

1. The viscosity of the pore fluid (usually water).
2. The size and continuity of the pore spaces or joints through which the fluid flows, which depend in soils on
   a. the size and shape of the soil particles,
   b. the density,
   c. the detailed arrangement of the individual soil grains, called the structure.
3. The presence of discontinuities.
4. The degree of saturation.
5. The composition of the soil.

Viscosity

Whenever a fluid is in motion, layers of the fluid slip and move in relation to each other. The ease with which they slip depends on the viscosity of the fluid, which is the

resistance or drag offered to motion. As the temperature increases, the viscosity of water decreases and the coefficient of permeability increases. Although the viscosity of water is reduced at high temperatures, the range is much narrower than for other fluids. It is customary to standardize permeability values at 20°C or 70°F and make a correction if field temperatures are substantially different. To standardize the permeability to any temperature the following ratio is used

$$k_{20} = k_T \frac{\eta_T}{\eta_{20}}$$

where k_{20} = coefficient of permeability at 20°C
k_T = coefficient of permeability at test temperature
η_T = viscosity of fluid at test temperature
η_{20} = viscosity of fluid at 20°C.

Size and shape of the soil particles

From theoretical considerations it has been shown that permeability can be expected to vary with the squares of the diameters of pore spaces and the squares of the diameters of the soil particles, see Figure 2-2. The permeability of soils varies significantly with grain size and is extremely sensitive to the quantity, character, and distribution of the finest fractions. Angular and platy particles tend to reduce the permeability more than when rounded and spherical particles predominate in the soil.

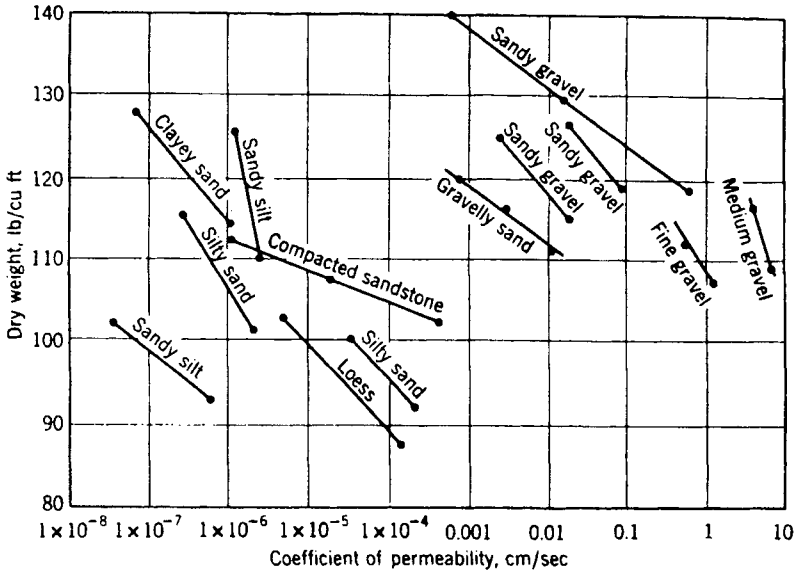

Figure 2-2. Relation between coefficient of permeability and soil type and density (log scale). (Cedergren, 1989, p. 31.)

Density of the soil

The denser a soil and the smaller the pores, the lower its permeability. As a rule the narrower the range of particle sizes, the less permeability is influenced by density. If a soil is compacted in a relatively dry state, a comparatively harsh permeable structure is usually formed. On the other hand, when blends of sand and gravel are thoroughly compacted with ample water, so that the particles tend to slide over one another, their permeabilities can be drastically reduced.

Structure of the soil

Natural soil deposits are always more or less stratified or non-uniform in structure. Water-deposited soils are usually constructed in a series of horizontal layers that vary in grain-size distribution and permeability. These deposits are generally more permeable in a horizontal than vertical direction. Windblown sands and silts are often more permeable vertically than horizontally because of tubular voids believed to be left by rotted plant or grass roots.

If the soil consists of clay particles the more dispersed the particles the lower the permeability will be. This is because the disbursement causes several small channels for the water to flow through. With flocculated soil there are fewer channels that are larger in size, this causes less surface contact for friction.

Presence of discontinuities

Undetected joints, seams, or strata of openwork gravel can lead to serious trouble from excessive seepage and hydrostatic pressures that are likely of develop. Compact clays often contain shrinkage or shear cracks that render such formations thousands of times more permeable than the clay between the cracks. Limestone, gypsum, or other water-soluble rock or mineral constituents can lead to the development of solution channels that can get larger with time. If discontinuities exist the effective permeability will be much greater than the permeability found by performing laboratory test on the material.

Degree of saturation

As the degree of saturation increases, the apparent coefficient of permeability also increases. This is in part due to the breaking of surface tension. The remainder is an unknown quantity, since it is difficult to determine permeability unless one considers the continuity of flow through the medium. If air bubbles are present in the soil they could block or restrict the flow channels causing a reduction in the permeability of the soil.

Soil composition

In silts, sands, and gravels the soil composition has little effect on the permeability. However, for clays the permeability depends on the clay family and on the exchangeable ions present. Kaolinite will have a greater permeability than montmorillonite, even though the void ratio for montmorillonite is very high. Exchangeable cations influence permeability by their influence on the nature and thickness of water absorbed on the clay mineral surface, when there is a thick layer of water on the surface the flow of water is impeded.

Methods for Determining Permeability

There are three methods for determining the coefficient of permeability of a soil:

1. Laboratory Methods
2. Indirect Methods
3. Field or Insitu Methods

The following will look at each method and briefly discuss how each is used and applied.

Laboratory methods for determining coefficient of permeability

The laboratory methods include permeability cells, standard test methods which consist of constant and falling head tests, and special test methods which include radial flow test and low flow test.

Permeability cells. The standard laboratory test for saturated fine-grained soils generally have the soil in the form of a disk with radial boundaries of metal, or occasionally plastic, and with the flow vertically upward. Consolidation cells work well for undisturbed samples, whereas compaction molds are used directly for compacted soils. The permeability of both undisturbed and compacted soil samples can be found using triaxial cell or flexible wall permeameters.

A simple design for a consolidation-cell permeameter is shown in Figure 2-3. The ring has a sharpened upper edge and is used for trimming the sample. With the use of mechanical devices, tilting of the ring is eliminated and the possibility of voids between the soil and ring is minimized. With this method, values of k less than 1 X 10^{-12} cm/s have been measured.

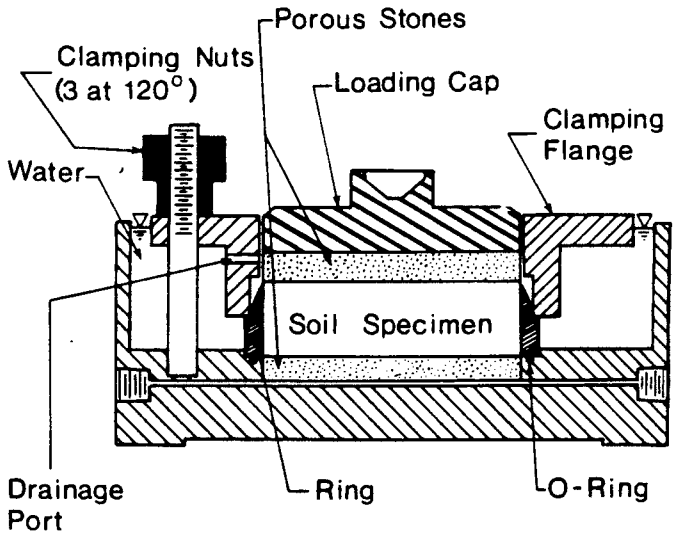

Figure 2-3. Consolidation cell permeameter.
(Olson and Daniel, 1981, p. 21.)

For compacted soils, a standard 10-cm (4-in.) diameter mold can be used with a special base containing a porous stone. A vacuum may be applied during the saturation

stage by sealing a top plate against the top of the mold. It is common practice to prevent soil swelling by clamping a plate against the top of the sample, but calibrated springs may also be used.

The standard triaxial cell has the advantage that back pressure can be used to promote saturation. Triaxial cells can also control the applied total stresses and the drainage of the soil sample. Similar advantages accrue from the use of back-pressure consolidation cells. The triaxial cell is recommended for soil samples that have a hydraulic conductivity less than or equal to 1×10^{-3} cm/s.

Standard test methods. The permeability of a soil is the determining factor for using the constant head or falling head test. The constant head test is most applicable to relatively permeable soils and aggregates. If the permeability is low, the time becomes excessive and evaporation during the test introduces errors in the results. The falling head test is used for low-permeability or fine-grained soils. Terzaghi and Peck suggest that if the permeability is not less than 1×10^{-3} cm/s the constant test should be used and if the permeability is not greater than 1 cm/s then the falling head test can be used.

In the constant head test a specimen of soil is placed in a cylindrical mold. A continuous supply of water is fed through the sample with the hydraulic gradient being held constant. Figure 2-4 is a simple constant head permeameter. As the water flows through the sample and into an overflow container it is collected, that volume is then recorded. The time it takes to collect the water is also recorded. Such equipment is designed to apply only small heads, a few feet of water, so it is most useful with rather pervious soils. The main advantage of the constant head test is the simplicity of interpretation of data.

From the Figure 2-4 the coefficient of permeability can be calculated.

$$k = \frac{QL}{hAt} = \frac{qL}{hA}$$

where Q = total volume of flow (L^3)
q = the flow rate (L^3/T)
L = length of the sample (L)
h = head loss (L)
A = the total cross-sectional area of the cylinder (L^2)
t = time period flow is measured (T).

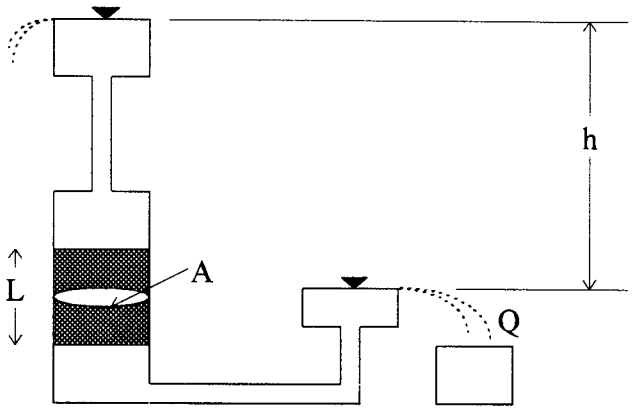

Figure 2-4. Constant head apparatus.

For fine-grained soils the more common test is the falling head test. This test is run in an apparatus with the general features shown in Figure 2-5. The soil sample is placed in a tubular chamber with an overflow arrangement. A small-diameter standpipe tube is connected to the top or bottom of the apparatus. The test is run by filling the standpipe above a marked level. When the water flows past that mark a stopwatch is started, as the water level drops to one or more lower marks the time is recorded. This test can be performed with upward or downward flow through the soil specimen. The main advantage of this method is that small flows can be measured easily using a buret or pipet.

From Figure 2-5, the following relationships can be set up:

$$dQ = -a\,dh = k\frac{h}{L}A\,dt$$

by integrating and transposing terms we obtain

$$k = \frac{a\,L}{A\,t} \log_e \frac{h_i}{h_f}$$

where dQ = change in volume of flow (L^3)
a = cross-sectional area of standpipe (L^2)
L = length of the sample (L)
dh = length of incremental volume in burette (L)
A = the total cross-sectional area of the cylinder (L^2)
dt = change in time the flow is measured (T)
h_i = initial height of water above overflow (L)
h_f = final height of water above overflow (L)
t = time period flow is measured (T).

Several precautions need to be taken when performing the constant or falling head tests. Care should be taken to avoid segregation during placement of soil in the permeameter. The use of deaired pure water will prevent air locking that will cause the permeability to became progressively smaller. Deaerated pure water is also recommended to prevent the influence of minerals in the water which can cause changes in the soil. Considering the inaccuracies of these tests and the fact that insitu water is neither deaired nor distilled it does not seem reasonable to use except for precise research.

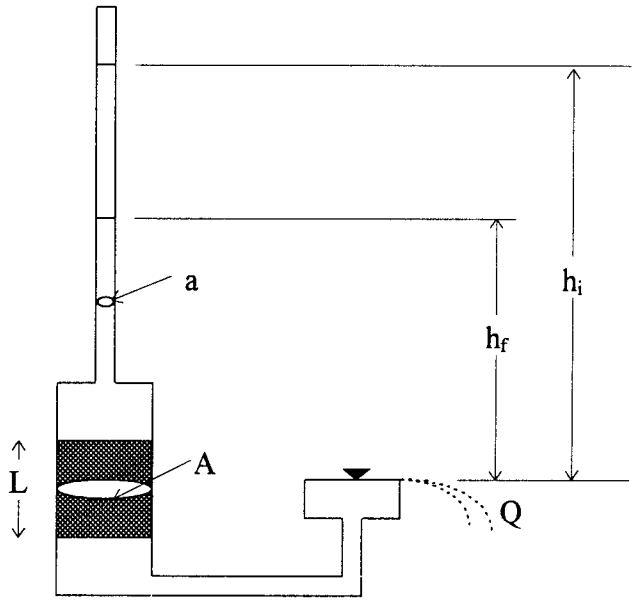

Figure 2-5. Falling head apparatus.

Special test methods. By using the radial flow test the horizontal conductivity can be measured in the laboratory using a cell with a central sand drain and a porous outer boundary (See Figure 2-6). This test can be performed in the triaxial apparatus using a central sand drain and a continuous outer filter paper drain. A disadvantage of using the triaxial apparatus is that the permeability of the paper may not be high enough to provide free drainage except for fairly impervious clays. Advantages of using the triaxial cell is that no special apparatus is needed and that large enough samples may be used to include the effects of macrostructure, such as fissures.

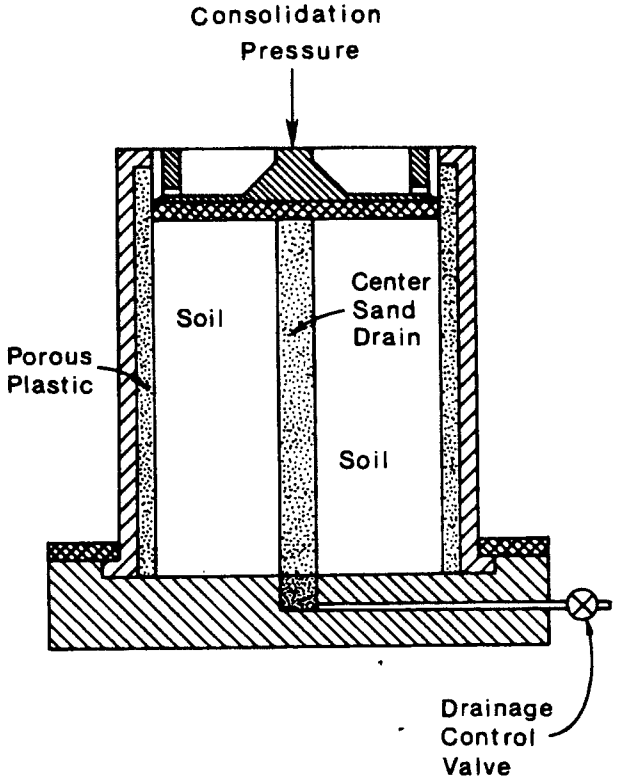

Figure 2-6. Radial flow permeameter.
(Olson and Daniel, 1981, p. 26.)

For a constant head the permeability is calculated as

$$k = \frac{Q}{2\pi L h t} \ln \frac{r_o}{r_w}$$

and for a falling head test the equation used is

$$k = \frac{a}{2\pi L t} \ln \frac{h_1}{h_2} \ln \frac{r_o}{r_w}$$

where Q = volume of flow (L^3)
L = sample height (L)
h = head on the sand drain (L)
t = time period (T)
r_o = radius of porous outer boundary (L)
r_w = radius of central sand drain (L).

The low flow test can be used in the case of relatively impervious clays where substantial time may be needed to obtain measurable flows. One way is to perform the equivalent of a falling head test by replacing the pipet with a compliant pressure transducer. The pressure on the upstream (transducer) side is elevated suddenly, thus deflecting the diaphragm of the transducer. The pressure is measured as water slowly leaks out of the transducer through the sample. The volume is determined from calibrations of volume change versus transducer readings.

Laboratory testing errors. The overriding source of error in laboratory permeability tests involves the use of samples that are not representative of actual field conditions. The problem of unrepresentative sampling is best minimized by thorough field investigation, by attention to details (sampling along faults, fissures, sand partings), by prudent selection of samples for testing, and by use of large samples.

For undisturbed samples, voids may be formed around the edges due to inadequate control of trimming, and fissures may open as a result of stress relief. This could lead to unrealistically high measured permeabilities. Solutions are to use proper trimming techniques and by subjecting the sample to stresses approximating those in the field.

If the sample contains such features as thin sand partings or root holes, the trimming operation may smear clay across the surface and tend to block entrance to these zones. To minimize the effects of smear, (1) use a sharp knife for final trimming and cut

the soil rather than trowel it; (2) include open root holes and other visible zones of higher permeability in the specimen to be tested; and (3) use as large a specimen as possible.

A belief held by some is that the permeability test should be performed using distilled water because such water is inert. Actually, leaching a sample with distilled water may cause expansion of the diffuse cloud of absorbed cations around clay particles and reduce permeability. A solution is to use a permeant of the same chemistry as the original pore water but this is time consuming and expensive. Alternatively, samples of groundwater may be obtained in the field and used as a permeant. Some prefer to use tap water, which, though not ideal, generally seems a much better choice than distilled water.

Problems can arise with air entrapped in the soil sample. In testing compacted samples, engineers often assume that soaking from the bottom, with the top open to the atmosphere, will lead to saturated samples. Because water cannot flow through an air bubble, the bubbles effectively reduce the void space that can be occupied by water and thus reduce permeability. The use of a vacuum pump for a minimum of 15 minutes followed by slow saturation of the sample from the bottom up under vacuum will help free any remaining entrapped air.

Prolonged performance of permeability tests may result in a substantial reduction in permeability due to clogging of the flow channels by organic matter that grows in the soil during testing. The implications of these tests for field problems depends on the application of interest. For some problems, such as ponding of water on the surface, it might be best to try not to prevent growth of organisms in the laboratory tests. In other applications growth of microorganisms may be unlikely, in which case a disinfectant should be added to the permeant and testing times should be minimized.

In an effort to reduce the testing time, large hydraulic gradients may be imposed on the samples. If Darcy's law is valid, such gradients will have no effect on the permeability of the soil sample. It is desirable to use gradients close to those encountered in the field.

On occasion, engineers correct the measured permeability to a standard temperature by adjusting for the effect of temperature on the viscosity and density of pure water. However, the permeability of fine-grained soils is probably influenced by complex interaction between the water, absorbed and free ions, and the mineral surfaces. Consequently, it is a good idea to perform permeability tests at approximately the relevant temperature when the results are to be applied to the solution of problems in the field.

If a volume change in pore pressure is imposed on a sample under a constant total stress, the resulting change in effective stress must result in a change in volume of the sample. Thus in a constant head test some of the initial measured inflow is making up for volume change rather than steady-state seepage. In a falling head test the apparent k would depend on the current applied head.

It is nearly always easier to perform laboratory permeability tests with the soil in the same orientation as in the field and with the flow vertical. However, sometimes the horizontal permeability, k_h, is larger than the vertical value, k_v, which usually leads to predominantly horizontal flow in the field. Laboratory specimens should be oriented to produce flow in the direction that will dominate in the field.

Indirect methods for determining coefficient of permeability

Permeabilities can be found indirectly from laboratory consolidation tests or formulas based on grain size. As a rule the permeability of most soils should be determined by direct test methods.

One dimensional consolidation testing. Data from a consolidation test can be use to calculate the permeability of a soil sample. The permeability can be calculated using the following formula:

$$k = \frac{c a \gamma_w}{1 + e}$$

where c = the coefficient of consolidation
a = coefficient of compressibility
e = void ratio.

Frequently the permeability of clays and silts is determined directly by using the consolidation test apparatus as a falling head permeameter. Values thus obtained are checked by indirect calculations using the above equation. Some engineers believe that the calculated values are more dependable than the directly determined values because calculated values are free of errors caused by piping along the sides of the soil specimens.

Grain size. Hazen developed a formula to determine the permeability of a soil based on the grain size. The following formula was developed using clean filter sand:

$$k = C_1 D_{10}^{2}$$

where k = permeability in cm/sec
D_{10} = is the effective size in centimeters
C_1 = from about 90 to 120 with a value of 100 often used.

This formula was based on clean filter sand and minute amounts of silt or clay can greatly diminish the permeability of sands.

Determination of permeability based on Hazen's formula or one on the others that have been developed should be looked at as approximations. As a rule the permeabilities of most soils should be determined by direct test methods.

Field or insitu methods for determining coefficient of permeability

No matter how carefully laboratory permeability tests are made, they represent only minute volumes of soil at individual points in large masses. Their value in solving drainage and seepage problems depends on how well they represent masses of material that actually exist in the field. In important projects it is often advisable to require field tests that measure the permeabilities in large masses of soil insitu (Cedergren, 1989).

Pumped well testing. Darcy's law and Dupuit's assumptions provide the basis for deriving the simple well formula in radial flow toward wells that penetrate the entire

water-bearing formation. When flow is unconfined, i.e. one boundary of the flow domain is a free surface, Dupuit's theory is used (see Figure 2-7). Dupuit made the following assumptions used in the calculation of the simple well formula:

1. For small inclinations of the line of seepage, the streamlines can be taken as horizontal; hence, the equipotential lines approach the vertical.

2. The hydraulic gradient is equal to the slope of the free surface and is invariant with depth.

These assumptions introduce large errors near wells but are reasonably accurate at moderate distances.

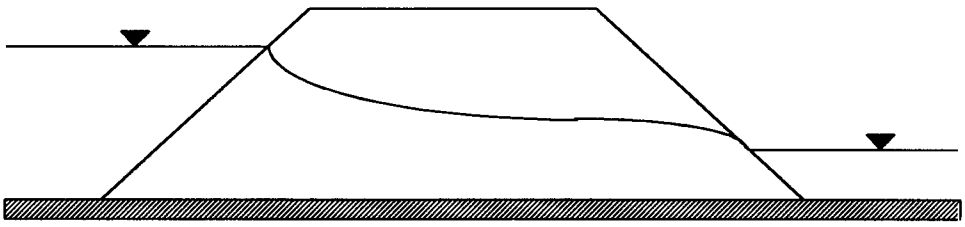

Figure 2-7. Example of unconfined flow.

Figure 2-8 shows a typical arrangement for determining soil permeability by well pumping tests. Using Figure 2-8, the simple well formula may be derived for steady-state conditions. After development of a steady state, any where from a few hours to a few days, the quantity of water flowing toward a well in unit time is

$$q = k\,i\,A$$

where q = steady pumping rate
i = dh/dr, Dupuit's assumption
A = area through water is flowing at a distance r.

After substitution, transposing, and integration the following formula is derived:

$$k = \frac{2.3\,q\log\left(r_2/r_1\right)}{\pi\left(h_2^2 - h_1^2\right)} = \frac{q\ln\left(r_2/r_1\right)}{\pi\left(h_2^2 - h_1^2\right)}$$

where r_1 = distance to first elevation observation well
r_2 = distance to second elevation observation well
h_1 = water level of first well
h_2 = water level of second well.

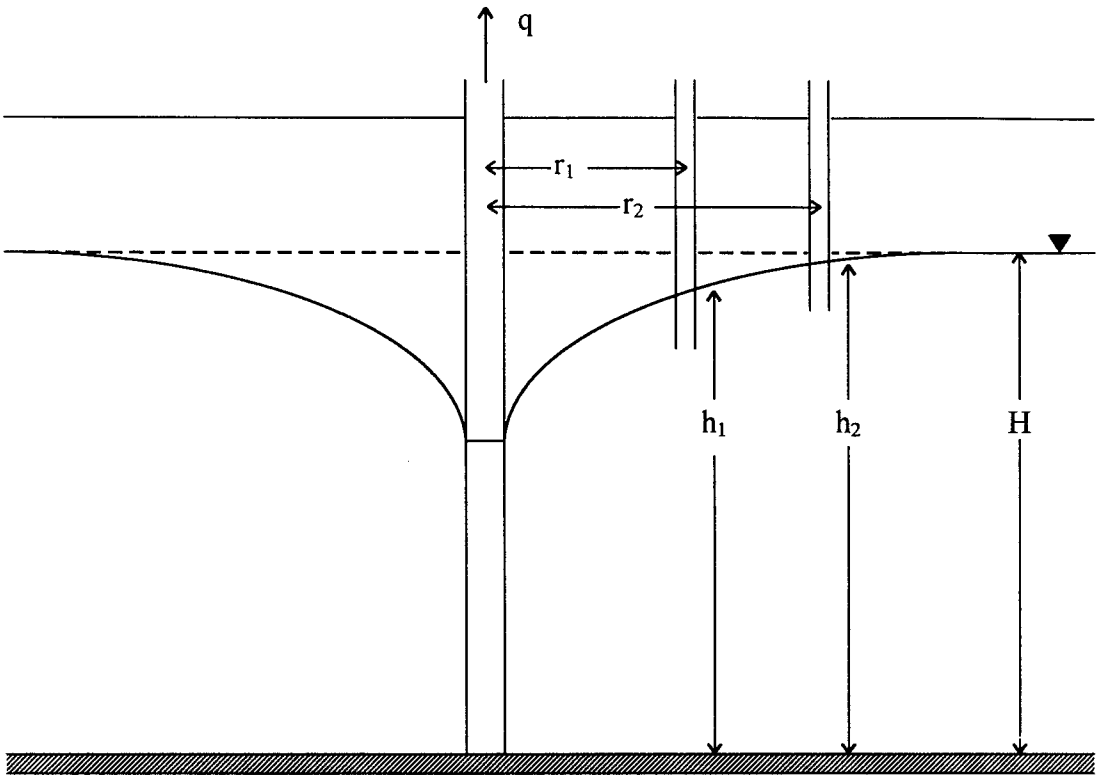

Figure 2-8. Typical arrangement for determining soil permeability by well pumping test, steady state.

The well formula is based on the following assumptions (Cedergren, 1989).

1. The pumping well penetrates the full thickness of the water-bearing formation.

2. A steady-state flow condition exists.

3. The water-bearing formation is homogeneous and isotropic and extends an infinite distance in all directions.

4. The Dupuit assumption is valid.

The reliability of well-pumping tests depends on how accurately the above assumptions are fulfilled. Pumping tests can be used for level or sloping water tables. The cost of well-pumping setup is relatively high, but normally observation wells are a comparatively small part of the total. At least four observation wells should be used; two is the minimum number in one radial line that permits a single computation of permeability.

When field permeability tests are made with the method described for steady-state flow, pumping must be continued until the water levels in observation holes have approximately stabilized. Although true equilibrium may require extremely long periods of pumping, practical results usually can be obtained by pumping at a steady rate for periods that range from a few hours to a few days, depending largely on the permeability (Cedergren, 1989).

During the period in which the water table around a pumped well is lowering, water is draining out of the aquifer. Useful solutions to seepage conditions during the nonsteady period are furnished by basic differential equations (Glover, 1966). Figure 2-9 shows the setup and variables for pumped wells in a nonsteady state. The derived equation is

$$s = \frac{q}{2\pi k D} \int_{r/\sqrt{4\alpha t}}^{\infty} \frac{e^{-u^2}}{u} du$$

where s = drawdown at time t
D = the aquifer thickness
q = pump flow
α = k D / η
η = porosity.

Tables published by the U. S. Bureau of Reclamation can be used to solve the above integral.

When field permeability tests are made by measuring the drawdown in observation wells adjacent to a pumped well, the pumping is usually continued until drawdowns are

reasonably stabilized. If the pumping is continued a number of hours or days until the rate of change in drawdown is small, errors in permeability will be within moderate limits, although, from a rigorous viewpoint, drawdowns continue to increase as long as the pumping is continued.

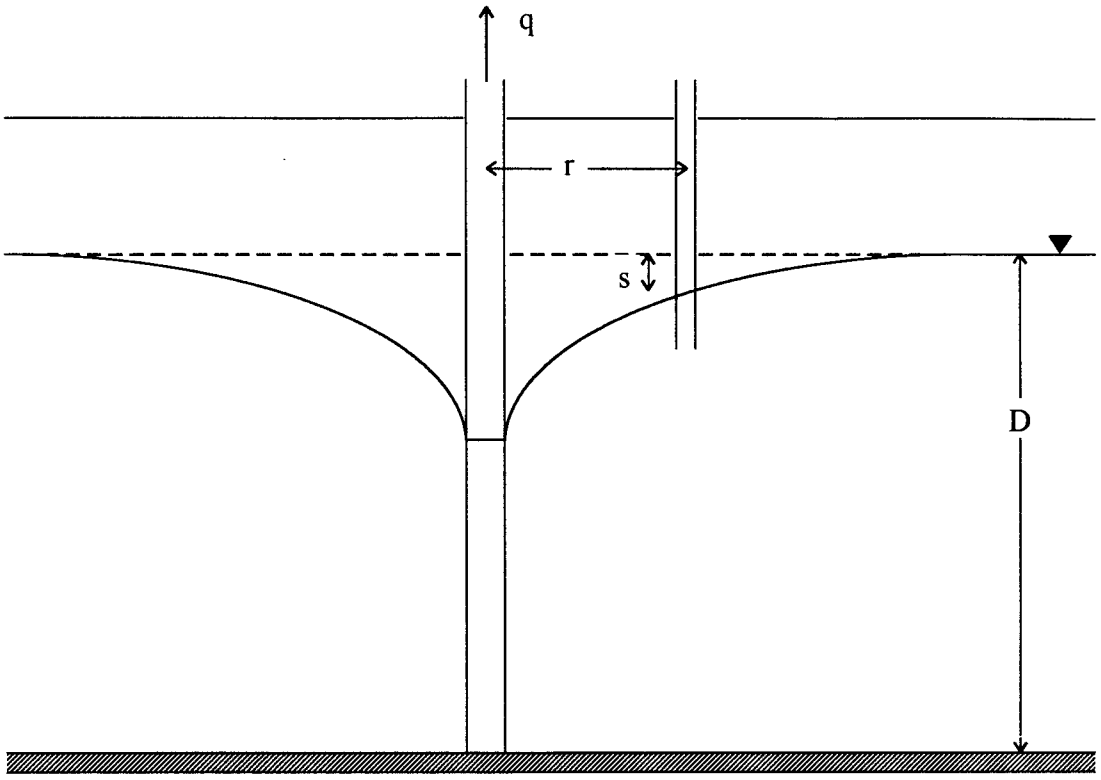

Figure 2-9. Typical arrangement for determining soil permeability by well pumping test, nonsteady state.

Borehole tests. The hydraulic conductivity is generally measured in the field by drilling a hole in the ground, measuring the rate of flow of water into or out of the hole, and using an appropriate formula to calculate the conductivity. Additional variables to be included in the equations for k must account for the presence or absence of casing, the location of the bottom of the casing in relation to the bottom of the boring, the shape of a piezometer tip if one is used, anisotropy in the soil, soil compressibility, presence of impervious surfaces near the tip, amount of air in the soil, secondary effects, and doubtless other effects as well (Olson and Daniel, 1981). In all bore hole test care must be taken to

avoid the use of amounts of head that will split formations and cause erroneously high rates of flow, thereby giving erroneously high permeabilities.

The auger method in principle is the simplest field test to perform. It is accomplished by drilling a hole, without the use of casing, and then performing either a constant head or variable head test, using either inflow or outflow. In its usual form, the method involves boring a hole beneath the water table, pumping the water level down several times to flush out the voids in the soil, and then pumping the hole down again and measuring the water level in the hole as a function of time. The relevant equation is

$$k = \frac{\pi^2 r \Delta h}{16 S d \Delta t}$$

where r = radius of the well (L)
S = a shape factor (dimensionless)
d = depth of the bottom of the hole below the water table (L)
h = height of water in the hole (L)
t = the time elapsed since the cessation of pumping (T).

The solution applies only for an incompressible soil, a hole drilled down to an impervious base, and no drawdown of the water table. To simplify analysis, most users of the auger method appear to assume the presence of an impervious base.

The auger method is generally used only near the water table because of a tendency of the soil to fail by piping or sloughing. Further, the test can be used only in moderately pervious soils because of the slow rate at which the water level rises for less pervious soils.

Another borehole method is to use cased holes, sometimes called open-ended tests. For applications in geotechnical engineering, it is common practice to case the soil either to prevent sloughing or to isolate the flow to a single layer. Testing is though the open end of a casing which has been drilled to the desired depth and carefully cleaned out

to the bottom of the casing. When desired, additional pressure head can be added to the gravity head. For a constant head test a common form is

$$k = \frac{q}{FDh}$$

where q = the flow rate (L^3/T)
F = a shape factor (dimensionless)
D = hole diameter (L)
h = the head loss (L).

For cases in which the bottom of the borehole is beneath the water table, h is the difference between the elevations of the water in the borehole and the water table. If the base of the borehole is above the water table, then h is often taken as the depth of water in the borehole. For falling head or rising head tests a common form for the equation is

$$k = \frac{A}{FDt} \ln \frac{h_1}{h_2}$$

where A = the area of the standpipe
t = the time for the head to change from h_1 to h_2.

For incompressible, homogeneous, isotropic soils, Hvorslev (1951) tabulated the shape factors that can be used in the above equations.

The Boutwell permeameter is a two-stage borehole hydraulic conductivity test developed by Boutwell. The concept is that by varying the geometry of the wetted zone, the relative effect of vertical and horizontal conductivities is varied in a calculable manner. Figure 2-10 shows the schematic for the test. The device is installed by drilling a hole, placing a casing in the hole, and sealing the annular space between the casing and borehole with grout. Falling-head tests are performed, and the permeability from stage I (k_1) is computed using the following equation:

$$k_1 = \frac{\pi d^2}{11D(t_2 - t_1)} \ln\left(\frac{H_1}{H_2}\right)$$

The values of k_1 are plotted versus time. When steady conditions are reached, stage I of the test is complete.

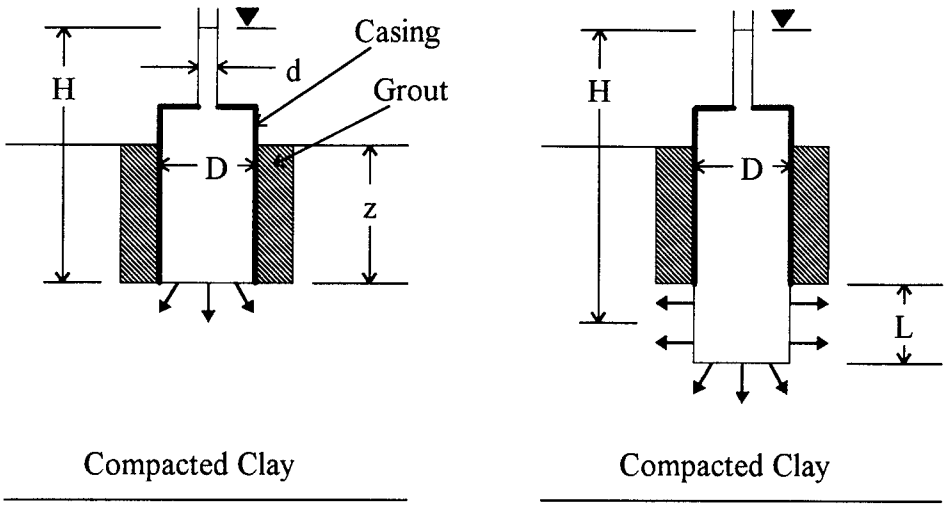

Figure 2-10. Schematic diagram of two-stage insitu hydraulic conductivity test with Boutwell permeameter for case in which potentiometric level is below base of permeameter: (a) stage I; (b) stage II. (Daniel, 1989, p. 1206.)

The next stage of the test is performed by deepening the hole by augering or by pushing a thin-walled sampling tube into the soil. Any smeared soil is removed from the surface with a wire brush. The permeameter is reassembled and falling head tests are again performed until k_2 does not change significantly. The following equations are used to compute k_2

$$k_2 = \frac{A}{B} \ln \frac{H_1}{H_2}$$

where

$$A = d^2 \left\{ \ln \left[\frac{L}{D} + \sqrt{1 + \left(\frac{L}{D} \right)^2} \right] \right\}$$

$$B = 8D \frac{L}{D} (t_2 - t_1) \left\{ 1 - 0.562 \exp \left[-1.57 \left(\frac{L}{D} \right) \right] \right\}$$

To account for anisotropy we define $m = (k_h/k_v)^{0.5}$, the relationship for m versus k_2/k_1 for various L/D values is shown in Figure 2-11. Knowing k_1, k_2, L, and D, m can be obtained from Figure 2-11. The permeability in the vertical and horizontal directions are computed as follows (Daniel, 1989):

$$k_h = m\, k_1$$

$$k_v = \frac{1}{m} k_1$$

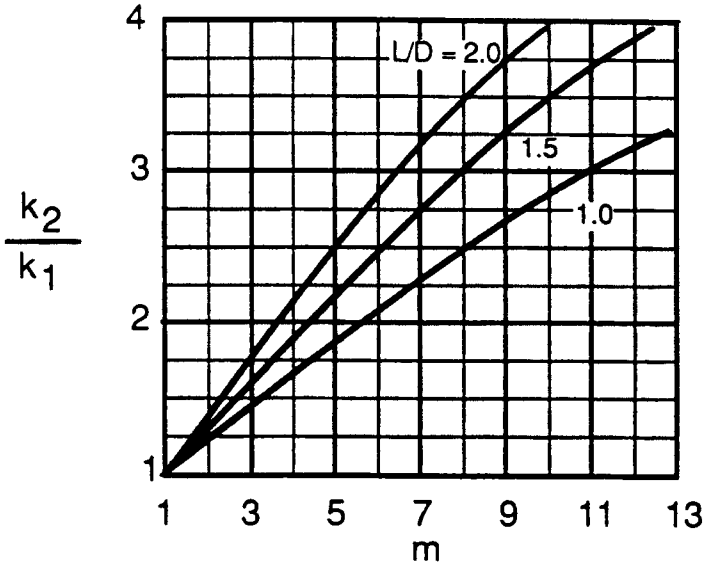

Figure 2-11. Curves of k_2/k_1 versus m for L/D = 1.0, 1.5, and 2.0. (Daniel, 1989, p. 1208.)

The constant-head permeameter is another example of a borehole test. With this permeameter a constant head of water is maintained using a Mariotte system or using a float value. The rate of flow needed to maintain a constant head is measured. Figure 2-12 shows a typical test setup. There are several different methods used to calculate the permeability using the constant-head permeameter. Some of the methods take into account the effects of soil suction and others do not. The borehole test may be continued for a second stage with a higher head. Because of soil heterogeneities it is recommended that the one-stage approach be used.

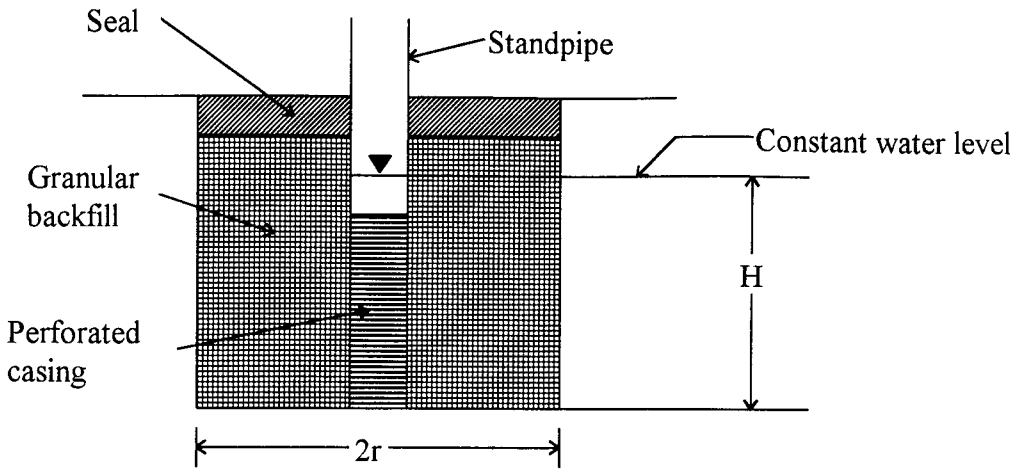

Figure 2-12. Borehole test with constant water level.
(Daniel, 1989, p. 1212.)

The packer test uses drill holes below the casing for making permeability tests. If the formation is strong enough to remain open, tests can be made above or below the water table. These tests are used for testing bedrock with the number of packers necessary to isolate the section of hole being testing. The permeabilities can be calculated using the following formulas:

$$k = \frac{q}{2\pi L h} \ln \frac{L}{r}, L \geq 10r$$

$$k = \frac{q}{2\pi L h} \sinh^{-1} \frac{L}{2r}, 10r > L \geq r$$

where q = the constant rate of flow into the hole
h = differential head
L = length of the section of hole being tested
r = radius of the hole tested.

The above equations have been found to be most valid when the thickness of the tested stratum is at least 5L and are more accurate in testing below the groundwater level than above (Cedergren, 1989).

Porous probes. Field permeability tests are probably most easily performed by sealing a more-or-less cylindrical cavity at an appropriate depth with one or two tubes

extending to the surface. The cylinder may be formed by drilling a borehole and sealing a well point or porous stone in a sand-filled lower cylindrical portion or by forcing into place a more-or-less cylindrical probe. Typically a cone-shaped probe is used with it being either pushed or driven into the soil. Constant or falling head test are then performed. Various porous probe permeameters have been used including the BAT permeameter. The self-boring pressuremeter also has applications in this area. Further discussion of porous probes can be found in Chapter 3.

Infiltrometers. There are five types of infiltrometers and each will be briefly discussed. Figure 2-13 shows conceptually four infiltrometers.

- Open single-ring infiltrometer. This simplest infiltrometer consists of embedding a ring into a trench and recording the quantity of flow over a period of time by measuring the change in water level. The main problems with this method are evaporation loss and measuring low flow rates. This method has difficulty in measuring permeabilites lower than 10^{-6} to 10^{-7} cm/s. An advantage is the low cost and unlimited size.
- Open double-ring infiltrometer. This consists of two rings sealed in the soil. The rings are then filled with water and covered to minimize evaporation. The test results may be unreliable in very porous soils ($k > 10^{-2}$ cm/s) or in low-permeability soils ($k < 10^{-6}$ cm/s). This test is also considered a low cost test.
- Sealed single-ring infiltrometer. The main problem with this system is consideration of thermal effects. There could also be lateral flow in addition to vertical flow. This device can measure low infiltration rates, down to 10^{-9} cm/s, but temperature changes and lateral spreading of water can lead to error. Testing times are long and the volume tested is somewhat small.

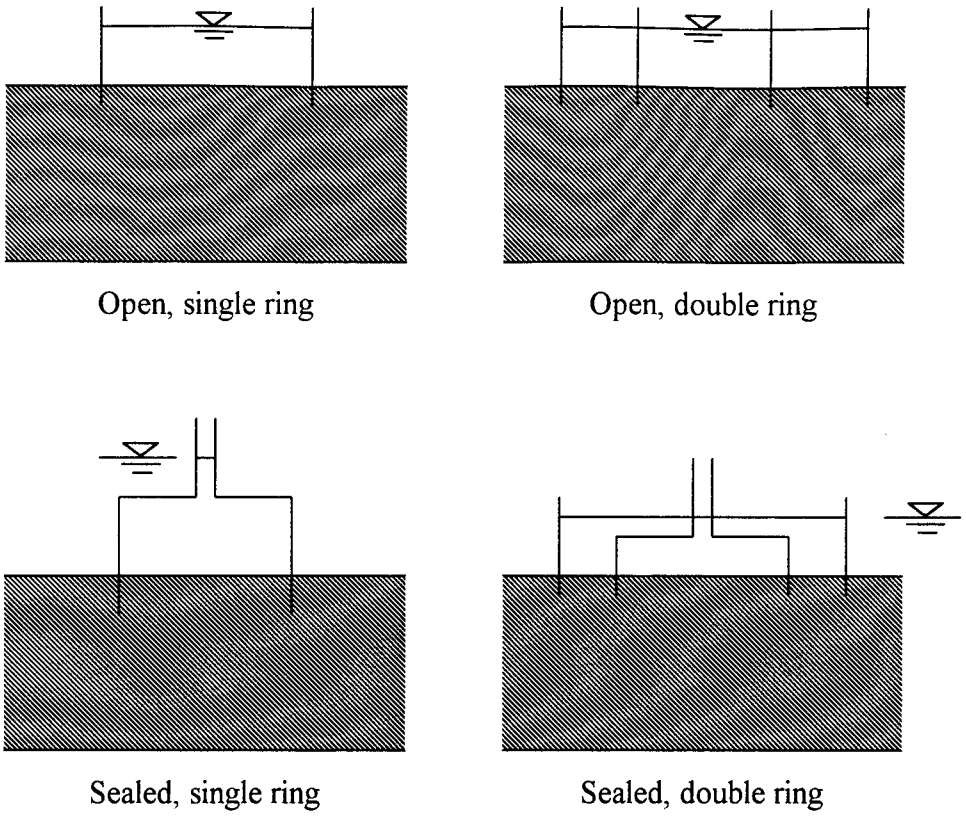

Figure 2-13. Types of infiltrometers
(Sharma and Lewis (1994) p. 187.)

- Sealed double-ring infiltrometer. This test method is applicable for soils with infiltration rates in the range of 10^{-5} to 10^{-8} cm/s. Both rings are embedded and sealed in trenches excavated in the soil. An advantage is that it minimizes most of the problems that the other types of infiltrometers have. The main disadvantage is that testing usually lasts several weeks or months.
- Air-entry permeameter. This test consists of a sealed ring embedded into the soil with the test performed in two stages. The primary advantage is the short testing time. Low permeability can be measured (10^{-8} to 10^{-9} cm/s), and permeability in the vertical direction is measured. The main disadvantages are that a relatively small volume of soil is tested and several important assumptions must be made.

Underdrains. This consists of a lysimeter pan placed as an underdrain beneath a clay liner for collecting liquid percolating through the liner. For low permeability soils (< 10^{-8} cm/s) it may take many weeks or months for steady seepage to develop, because of this it is a time consuming test. Advantages are the low cost, large volumes of soil that can be tested, and few experimental ambiguities.

CHAPTER 3
DESIGN OF INSITU PERMEABILITY DEVICE

Insitu testing offers the advantage of testing the soil while it remains relatively undistrubed. It also allows more representative properties of the material to be included. Because of the possibility of sand seams, fissures, and other macrostructures in the field which are not duplicated properly in the laboratory test, it is advantageous to perform these tests on material that is field compacted and ready for actual field loading.

The purpose of this device is to test the insitu permeability of pavement base and subbase material. It was first decided that a porous probe would be the best option to adopt. This was chosen for ease of use, repeatability, ability to test to several depths, and relatively low cost. The majority of the expense of the apparatus involved the development and initial testing of the equipment. A low cost per individual test is anticipated during actual field use.

This chapter describes the design of the insitu permeability device. The first section discusses probe theory, while the next section reviews the placement of the probe and water tanks. The final section discusses the additional equipment required to complete the unit.

Probe Theory

According to Daniel (1989), several assumptions need to be made regarding the soil properties. That is, the soil is homogeneous, isotropic, uniformly soaked (wetted), and incompressible. It is also assumed that the boundaries are infinite, soil is not smeared across the surface of the porous element, effects of soil suction are negligible (unless

efforts are made to account for suction), conditions are isothermal, and Hvorslev's (1949) equations are valid.

Daniel's assumptions for the soil properties, are essentially correct. The device is designed to test the permeability of base and subbase materials, with the material being placed generally originating from the same borrow pit. This meets the requirement of homogeneity because, the soil is relatively uniform in structure and has approximately the same physical properties throughout. Since the material is placed in layers and uniformly compacted, it meets the isotropic requirement, which means the soil exhibits the same properties in all directions at a point. The material is assumed to be uniformly soaked because the zone of influence of the probe is less than the saturated zone of the material. Because the material being tested is base material that is usually granular in structure and constitutes more than 95% of the grain size distribution, it is essentially incompressible. Incompressibility is also approached since the soil is well compacted.

The device will predominantly test the permeability in the horizontal direction, and given the direction of flow of water, the assumption that the boundaries are infinite, is met. The effects of soil smearing across the surface of the porous is a possible source of error. Thus, flow rates will be recorded before and after removal of the probe to verify that the porous element did not clog.

Because of the relatively small thickness of the layer, the development of any negative pressure gradient to cause suction is minimized. The shallow depth being tested also minimizes any significant temperature gradient that might create viscous related permeability problems within the layer.

Hvorslev's equations are based on the fundamental principle governing the theory of permeability, i.e.,the validity of Darcy's law. Darcy assumed that the flow through the soil is laminar or nonturbulent. In 1948 Taylor presented information that flow through most soils is generally laminar. Terzaghi concluded that Darcy's law is valid for a wide range of soils and hydraulic gradients. Muskat concluded that the majority of the flow

systems are governed by Darcy's law (Cedergren, 1989). Hvorslev also assumed that water and soil are incompressible. For the types of material tested, the above criteria are met.

Hvorslev's Equation

During the advance of a bore hole or immediately after a piezometer or other device is installed, the initial hydrostatic pressure recorded by the device seldom equals the surrounding porewater pressure. Water must flow to or from the hole or device until the pressure or head in the device equals that of the surrounding soil. The time required for equalization of the pressures is called the time lag. A flow also occurs with a corresponding time lag when the surrounding pore pressure increases or decreases. The magnitude of the time lag depends on the type and dimensions of the pressure measuring device, and it is inversely proportional to the permeability of the soil. Because of this, the time lag theory is a practical technique for determining the permeability of soils in the field.

Hvorslev conducted a study for the U. S. Corps of Engineers, Waterways Experiment Station, on methods of measuring hydrostatic pressure, and determining permeability in borings, observation wells, piezometers, and hydrostatic pressure cells. Derivation of the basic differential equation for determing the hydrostatic time lag, is similar to the equations for a falling-head permeability test. It is assumed that Darcy's law is valid and that water and soil are incompressible, that artesian conditions prevail or that the flow required for pressure equalization does not cause any perceptible draw-down of the ground-water level (Hvorslev, 1951). If water is flowing into or out of a casing or other pore-pressure sensing device, the flow my be expressed by the following equation (see Figure 3-1):

$$q = F k h = F k (z - y)$$

where q = flow rate (L^3/T),
F = factor that depends on the shape and size of the intake or well point, (L),
k = coefficient of permeability (L/T),
h = active head (L),
z = distance from a reference level to the outside piezometric level (L),
y = distance from the reference level to the piezometer level in the transient state (L).

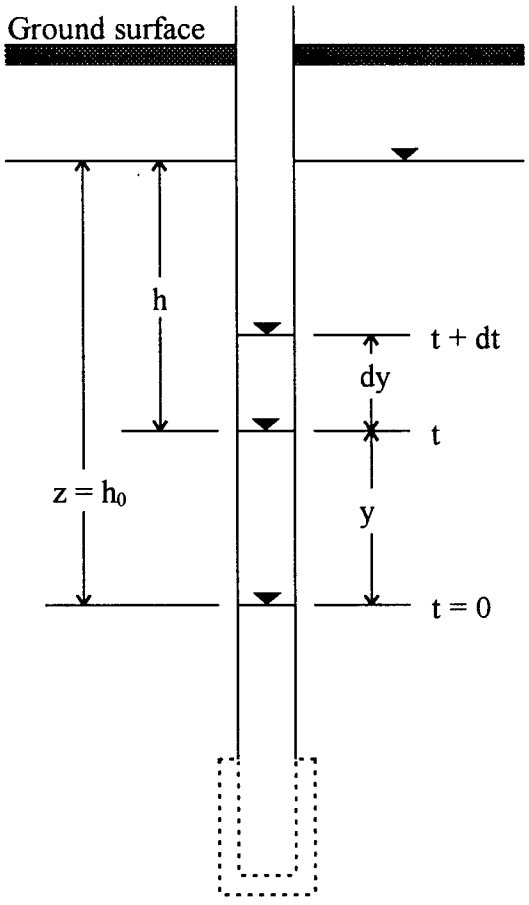

Figure 3-1. Setup for derivation of Hvorslev's equation.

It is assumed that the friction losses in the pipe are negligible for the small rates of flow occurring during pressure observations. By considering the volume of flow, the following equation is obtained:

$$q\,dt = A\,dy$$

where dt = time period considered (T),
A = cross-sectional area of the standpipe or an appropriate area representing the relationship between volume and pressure changes in a pressure cell or gage (L^2).

By taking the expression for q from the first equation and substituting it into the second equation the following differential equation is formed:

$$\frac{dy}{z-y} = \frac{F\,k}{A}\,dt$$

The volume of flow, V, required to equalize the pressure difference, h, is V = A h. Hvorslev defines the basic time lag, T, as the time required for equalization of this pressure difference when the original rate of flow q = F k h is maintained. It then follows that

$$T = \frac{V}{q} = \frac{A\,h}{F\,k\,h} = \frac{A}{F\,k}$$

The differential equation may then be rewritten as

$$\frac{dy}{z-y} = \frac{dt}{T}$$

This is the basic differential equation for the hydrostatic time lag. When the ground-water level or piezometric pressure is constant and $z = h_0$ the above equation becomes

$$\frac{dy}{h_0 - y} = \frac{dt}{T}$$

By integrating and letting y=0 for t=0 the solution is

$$\ln\frac{h_0}{h} = \frac{t}{T}$$

A plot of ln (h/h_0) versus t can be made. The plot will be a linear line with the negative slope of 1/T. The basic time lag is at the time where the head ratio, h/h_0, equals 0.37. The equalization ratio is defined as ($1-h/h_0$). An equalization ration of 0.90, which corresponds to a time lag of 2.3 times the basic time lag, is considered by Hvorslev to be adequate for many practical purposes.

Coefficient of Permeability for Proposed Probe

When the shape factor or the dimensions of a device are known, it is theoretically possible to determine the coefficient of permeability of the soil insitu. For a constant head the following equation is used:

$$k = \frac{q}{F h_c}$$

where F = shape factor for the probe (L),
h_c = constant head (L).

For a variable head with constant ground-water level or pressure the following equation is obtained:

$$t_2 - t_1 = T\left(\ln\frac{h_0}{h_2} - \ln\frac{h_0}{h_1}\right) = \frac{A}{Fk}\ln\frac{h_1}{h_2}$$

where h_0 = constant ground-water level or piezometric pressure (L),
h_1 = starting head (L),
h_2 = ending head (L),
t_1 = starting time (T),
t_2 = ending time (T).

Solving the above equation for the coefficient of permeability, the following equation is obtained:

$$k = \frac{A}{F(t_2 - t_1)}\ln\frac{h_1}{h_2}$$

Several charts are published with formulas of shape factors for various types of observation wells and piezometers. Daniel (1989) shows a probe (Figure 3-2) similar to the one developed for this project that includes a shape factor. The following equation is used to calculate the shape factor:

$$F = \frac{2\pi L}{\ln\left(\frac{L}{D} + \sqrt{1 + (L/D)^2}\right)} - 2.8D$$

where L = length of porous opening (L),
D = diameter of porous opening(L).

This will be the preliminary shape factor that will be used with the insitu permeability device developed for the FDOT. After testing of the probe, adjustments may need to be made to the shape factor.

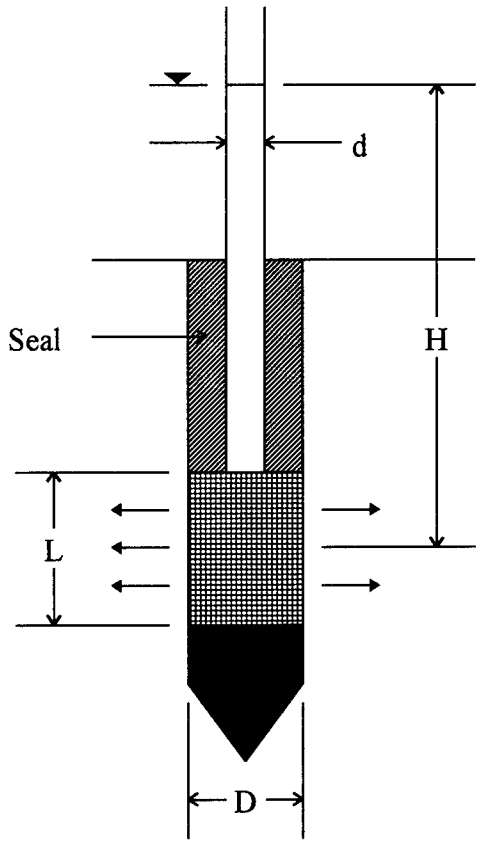

Figure 3-2. Probe with impermeable base.
(Daniel, 1989, p. 1215)

Insitu Permeability Device

The main components of the insitu permeability device developed are as follows:

1. Trailer
2. Mariotte tank
3. Water tanks
4. Coring device
5. Generator
6. Flow system
7. Control box
8. Hydraulic system
9. Probe

The insitu permeability device features will be discussed in detail in the following sections. Figure 3-3 shows the left side of the insitu device and Figure 3-4 shows the schematic of the insitu permeability device. The right side of the device is pictured in Figure 3-5.

Figure 3-3. Left side view of insitu permeability device.

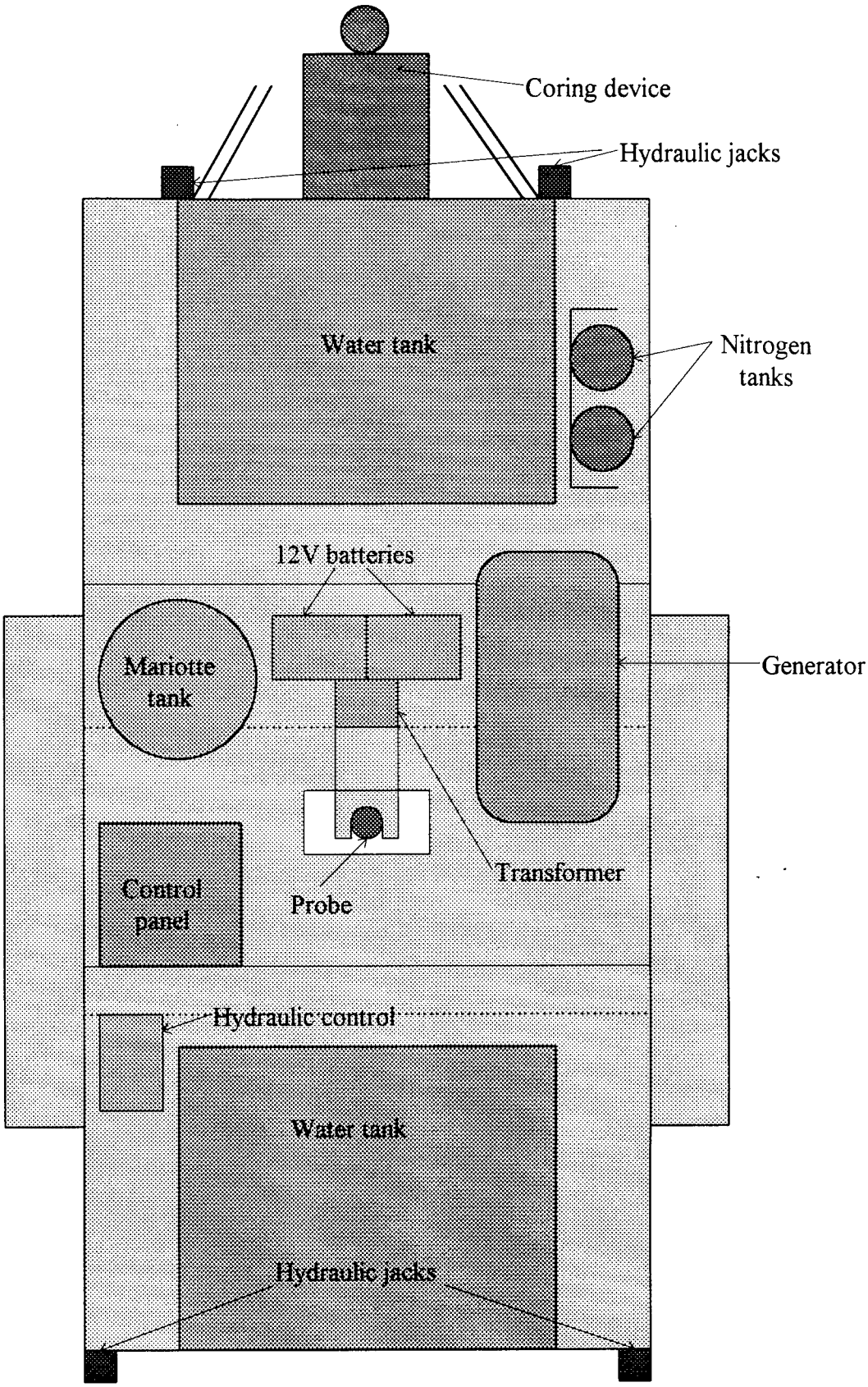

Figure 3-4. Schematic of insitu permeability device.

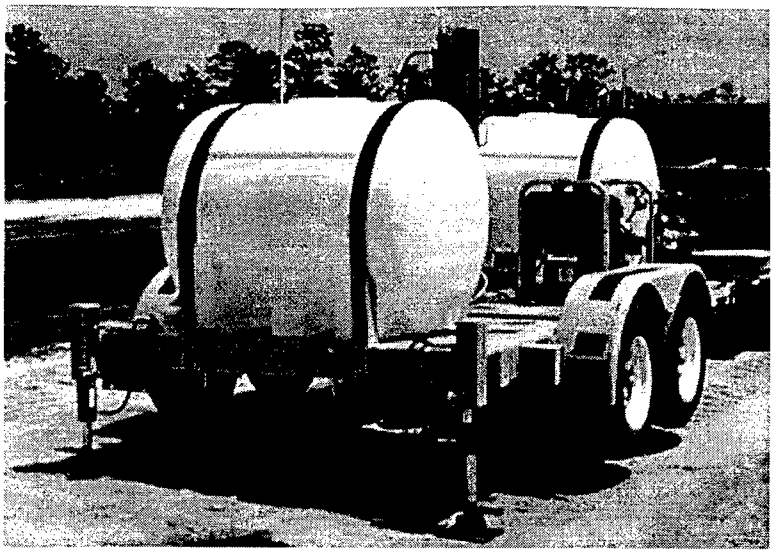

Figure 3-5. Right side view of insitu permeability device.

Trailer

A 182.88 x 365.76 cm (6 x 12 ft) trailer was purchased to be used as the base for the insitu permeability device. This trailer has a 12.7 cm (5″) channel main frame, 38.1 cm (15″) tires, and two 1589 kg (3,500 lb) capacity axles. The trailer has a 2721 kg (3 ton) capacity. The decking is made up of three 122 x 183 cm (4 x 6 ft) sections. The center panel is a 2.54 cm (1 in) thick steel plate. This adds approximately 454 kg (1,000 lb) to the trailer. The outer panels are 0.635 cm (0.25 in) diamond plate steel decking.

For safety a brake system was added to the trailer. This system is a 4-wheel surge braking system with breakaway capabilities. This was needed because of the weight of the trailer.

Mariotte Tank

A Mariotte system is used to maintain a constant head of water. Air is supplied to the tank creating a constant head that maintains a constant flow of water. The Mariotte tank is made with a 159 L (42 gal) water tank, the type used for well systems and is galvanized steel. This should prevent any potential problems with rusting. To fill the tank use the

section of hose supplied and insert it into the quick connect on the top of the tank. If the Mariotte tank becomes low while out in the field, the tank can be filled using the hose and pump supplied. Water can be removed from the large water tanks to accomplish this. Figure 3-6 shows the setup of the Mariotte tank.

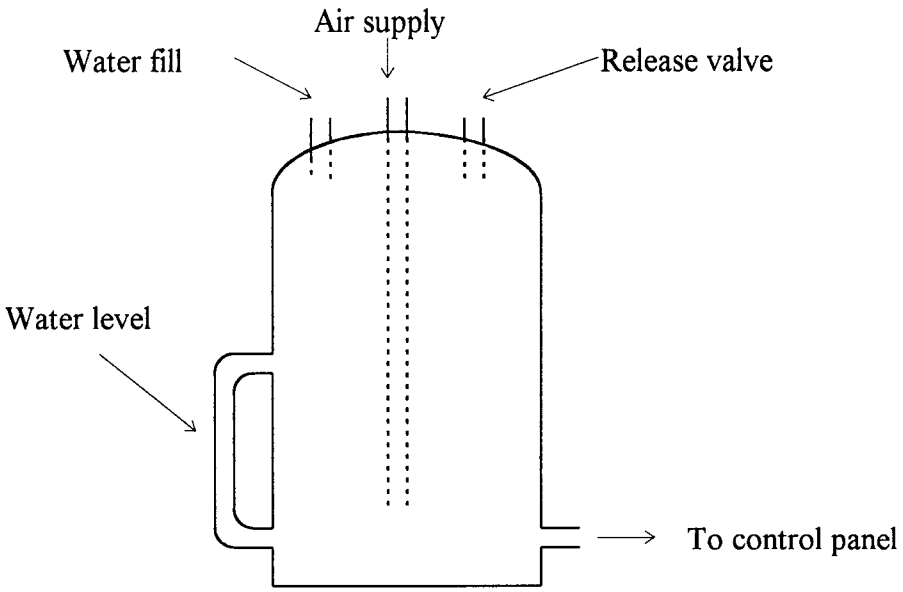

Figure 3-6. Diagram of Mariotte tank.

Water Tanks

The reaction for the probe is supplied by two 870 L (230 gal) cross-linked polyethylene water tanks. When both tanks are filled they provide up to a total of 1743 kg (3840 lb) of added mass to the trailer. The tanks can be filled from any water source. The tanks can be emptied by either opening the valve at the bottom of the tanks or by using the pump provided. Two 7.6 m (25 ft) hoses have been provided to empty the tanks.

Coring Device

To increase usability, a DD 250E coring system was purchased from Hilti (Figure 3-7). This system has a 20 amp motor and uses 115 VAC. The motor has four speeds, enabling a wide range of optimized coring diameters. The hole staring mode-switch reduces the motor speed by one-third for easy hole starting.

A 15.24 cm (6 in) diameter, 112 cm (44 in) long bit is supplied to be used with the coring device. This allows the device to be mounted on the front of trailer with the bit extending to the ground surface. The motor has a quick connect for the bit, allowing for easy removal. When using the 15.24 cm (6 in) bit the motor should be used on speed 2, this will give a motor speed of 450 RPM. This system can be used to remove pavement when insitu permeability testing is to be done on existing roadways. The system can also be used to extract samples for laboratory testing.

The water needed during the use of the coring device is supplied by the water tanks. Use the hose supplied and control the water flow with the valve on the water tank. Power for the coring device is supplied by the generator.

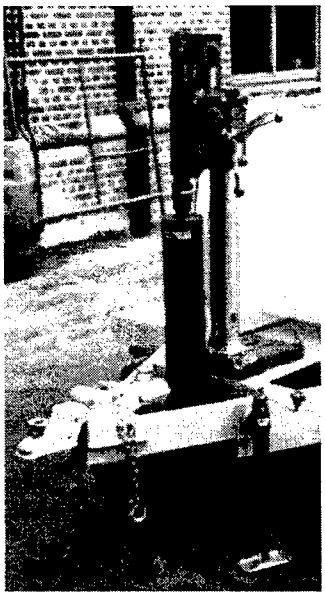

Figure 3-7. Coring Device.

Generator

The trailer is equipped with a 10,000 Watt Dyna LLC9000E generator. The generator has four 15 Amp, 120 Volt receptacles and one 30 Amp 240 Volt Twistlock. It is powered with a Briggs & Stratton Vanguard engine with electric start. There is a 17 L (4.5 gal) fuel tank and a low oil shutdown.

Because the coring device needed 20 Amps and 120 Volts a transformer was installed on the trailer, this will also protect the coring system from surges. A battery charger is also installed on the trailer in order to recharge the 12 Volt deep cycle batteries used to power the hydraulics and control panel.

Flow System

The flow system consists of two flow meters with digital/LCD displays, nitrogen tanks, and constant head and falling head systems. The flow meters have a Pelton type turbine wheel that is used to determine the flow rate of the liquid. The display units are a digital D.C. voltmeter with an analog-to-digital converter and liquid crystal display. The flow range for the meters are 50-500 ml/min. for the high range and 13-100 ml/min. for the low range. Figure 3-8 is a schematic of the flow meter electrical system. The flow meter system uses two 9-Volt batteries. The reason for the separate circuit for the flow meters is to protect them from voltage spikes from the solenoids. A water filter with a rating of five microns is installed in the water line to meet the required seven micron rating of the flow meter.

The air for the system is supplied by two 1.12 m^3 (40 ft^3) nitrogen tanks. The regulator has a 0 to 27560 kPa (0 to 4,000 psi) cylinder pressure gauge and an operating pressure of 0 to 1378 kPa (0 to 200 psi). The tanks are not connected together, when one is empty the regulator is moved to the full tank and testing can resume. The nitrogen is hooked up to the control panel with a quick connect.

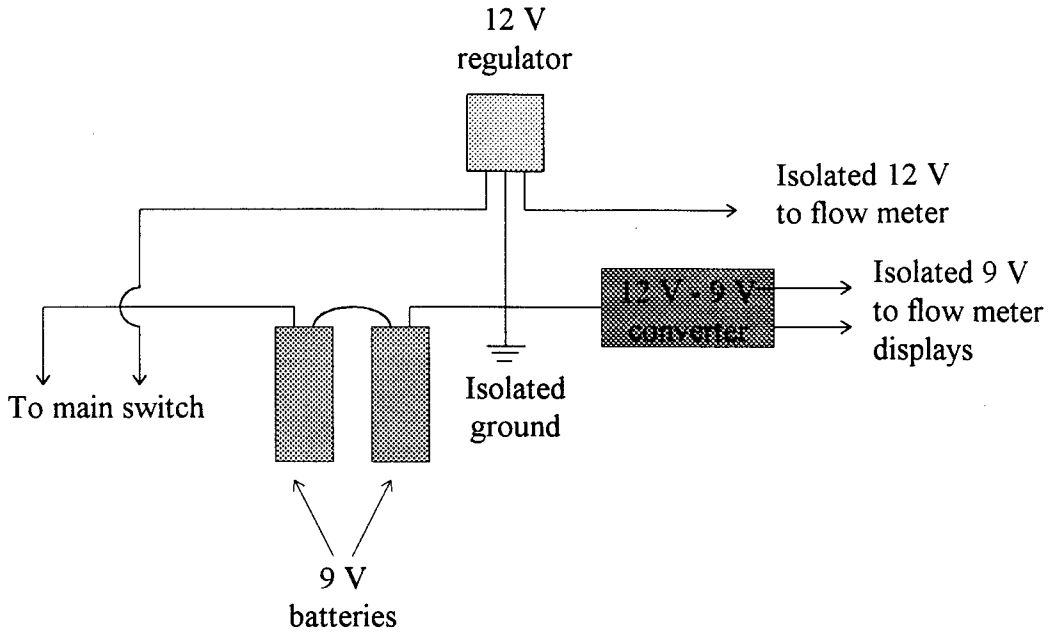

Figure 3-8. Schematic of flow meter electrical system.

The permeability of the soil can be determined by running either a constant head or falling head permeability test. The constant head is accomplished by recording the flow meter reading and the pressure gage reading. For the falling head, the time is recorded as water flows through the clear standpipe mounted on the H-beam. Instructions to run both test can be found in chapter four. Figure 3-9 is a schematic for the constant head and falling head system.

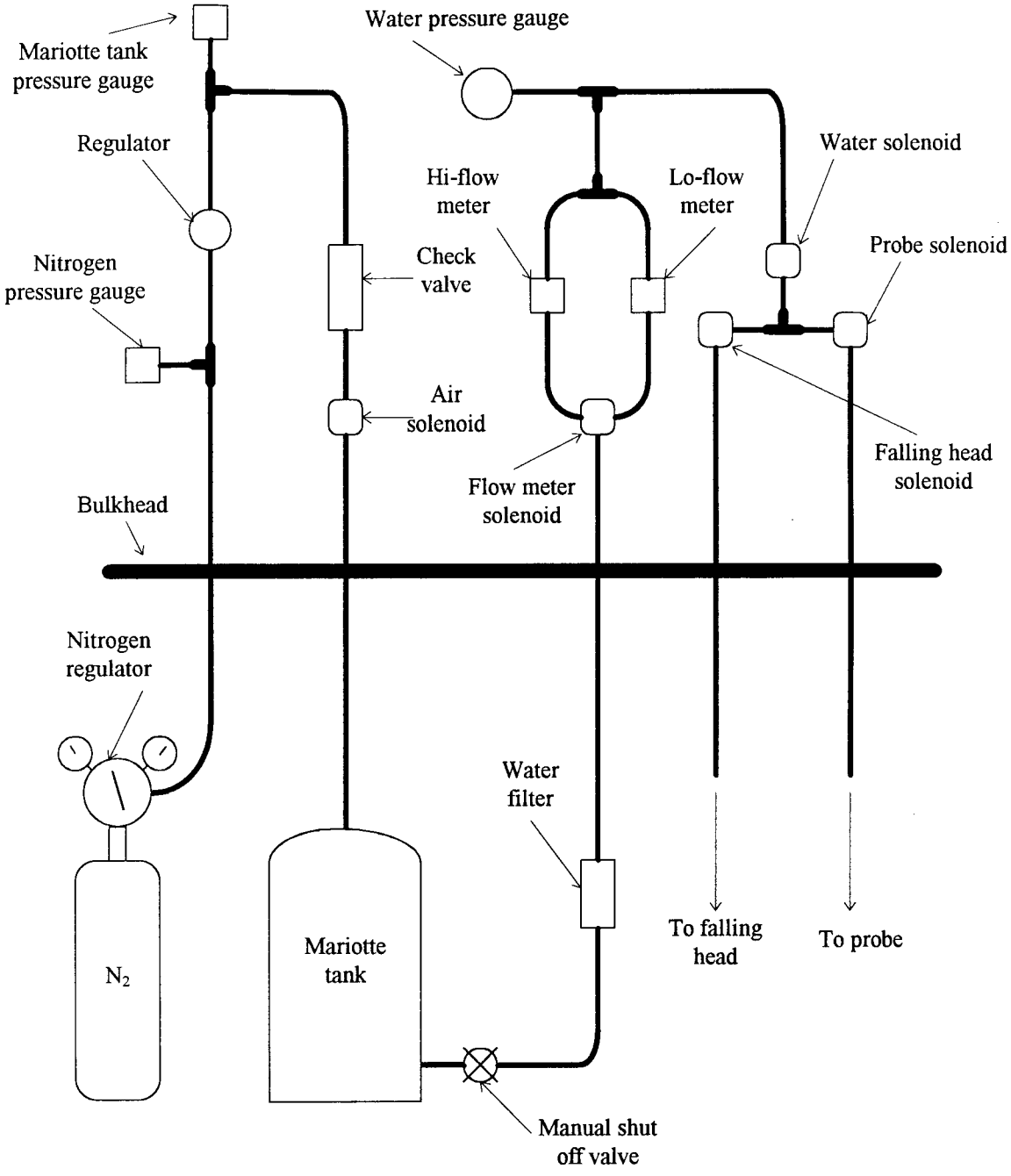

Figure 3-9. Schematic of constant and falling head systems.

Control Box

An 45.72 x 45.72 x 60.96 cm (18 x 18 x 24 in) locking tool chest is installed on the permeability trailer. This houses the solenoids, switches, flow meter, and pressure gauges (Figure 3-10). This allows for the permeability test to be run from one location. Figure 3-11 is a schematic of the control panel and Figure 3-12 is a schematic of the electrical system.

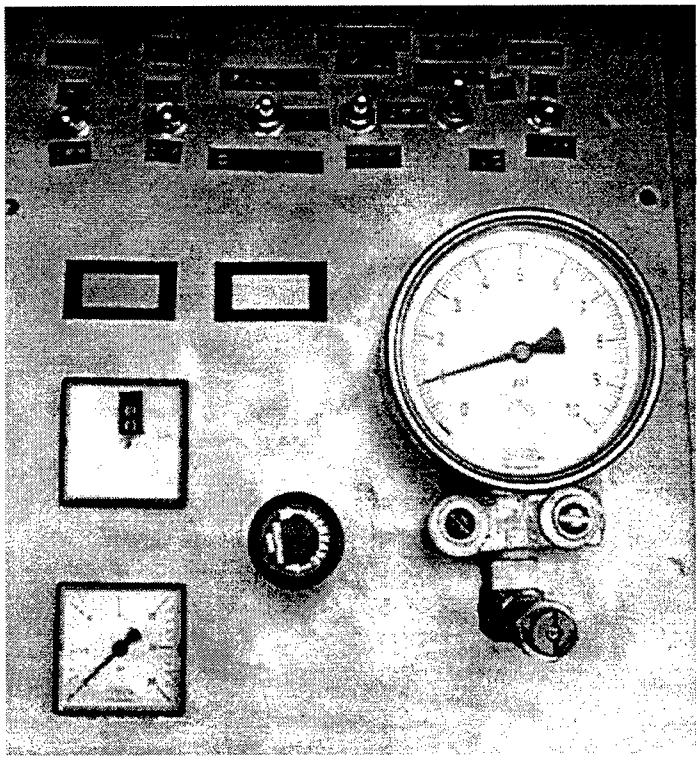

Figure 3-10. Control panel.

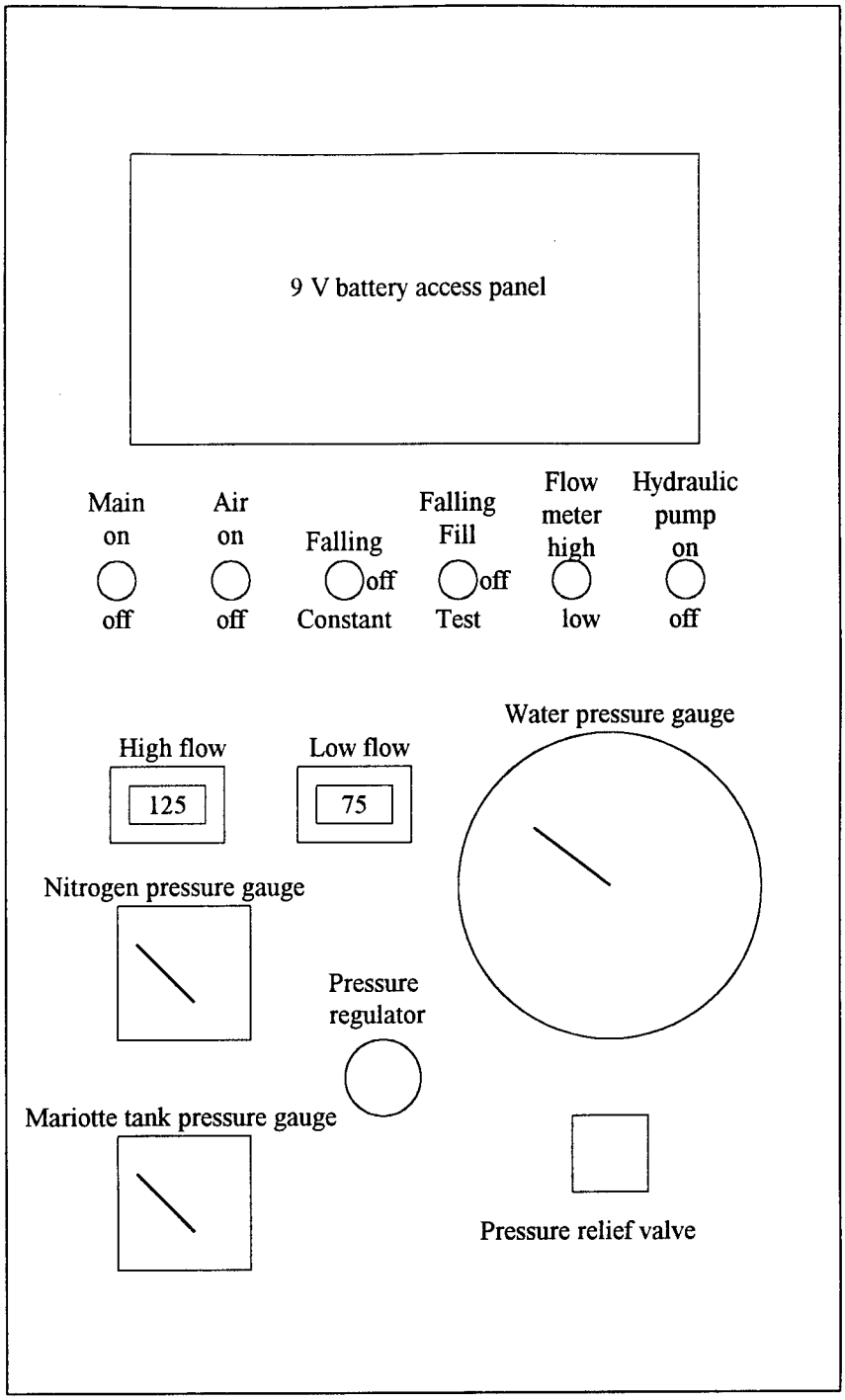

Figure 3-11. Schematic of control panel.

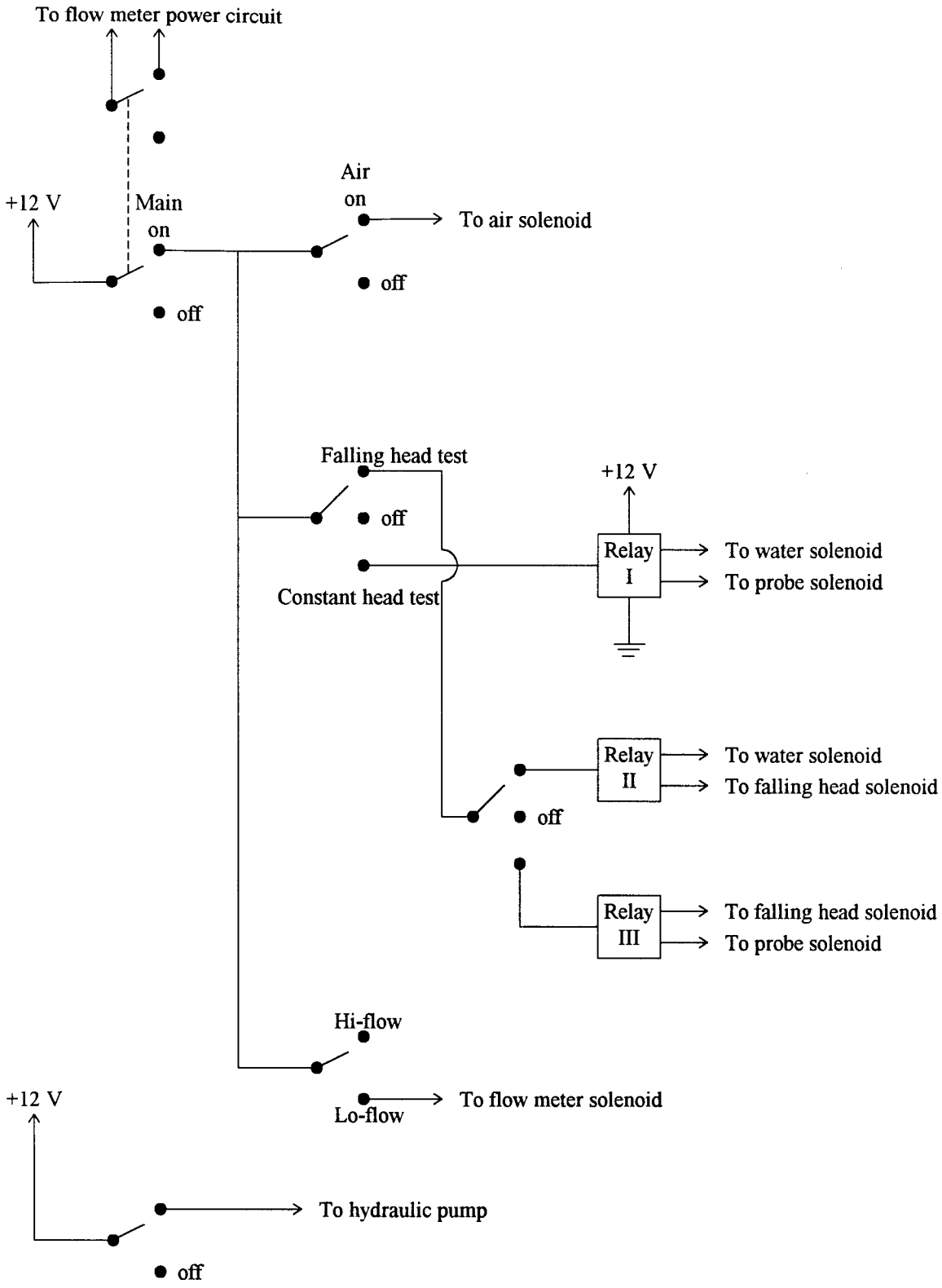

Figure 3-12. Schematic of control box electrical system.

Hydraulic System

The hydraulic system consist of the hydraulic pump, a bank of five spools, a cylinder for the probe, and four cylinders for leveling the trailer. The pump has a 12 Volt Bosch motor with an internal ground start switch. It will pump 5.3 LPM (1.4 GPM) at 13780 kPa (2000 psi). A 9.5 L (2.5 gal) reservoir is attached to the pump. The bank of control valves for the cylinders is mounted next to the control box on the trailer. The valves are 3-position spring centered. Figure 3-13 is a diagram of the control bank.

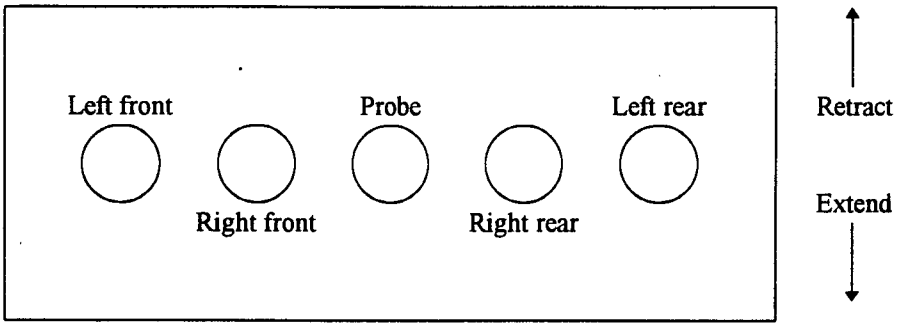

Figure 3-13. Diagram of hydraulic control bank.

The probe is attached to a hydraulic cylinder that has a 66.04 cm (26 in) stroke. This cylinder is mounted on the H-beam at the center of the trailer. The leveling system is made up of four 50.8 cm (20 in) welded tee cylinders. The cylinders have a 30.48 cm (12 in) stroke and a 3.81 cm (1.5 in) diameter shaft. Welded to the trailer at the corners are 30.48 cm (12 in) long 10.16 x 10.16 x 0.635 cm (4 x 4 x 1/4 in) steel tubes that have one side removed. To reinforce the tubes a 10.16 x 10.16 x 1.27 cm (4 x 4 x 1/2 in) plate was welded to the top. The leveling cylinders are bolted into these tubes. The base for the jacks is 30.32 x 30.32 x 1.27 cm (8 x 8 x 1/2 in), this base can rotate for uneven ground. The cylinders are swung up and chained when traveling. Figure 3-14 shown the jacks in the traveling position and Figure 3-15 is of the jacks in the down position.

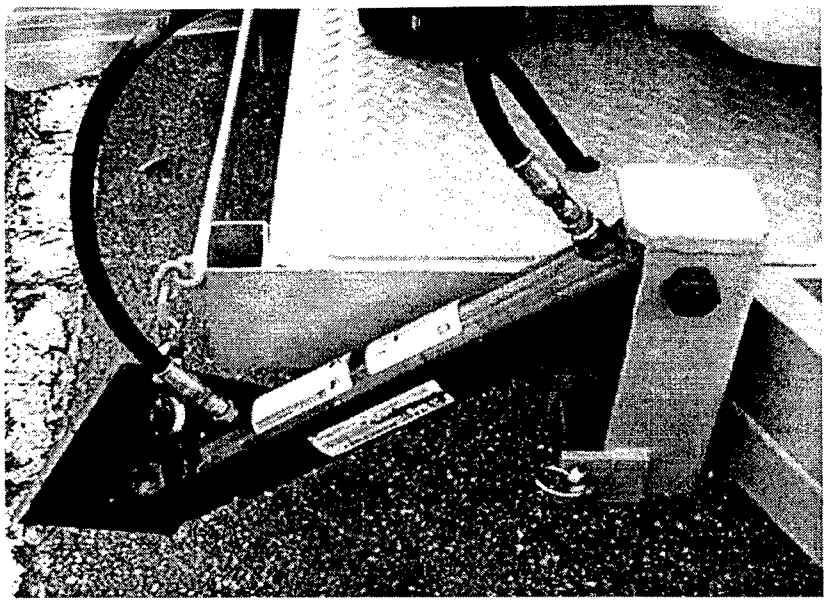

Figure 3-14. Leveling jacks in traveling position.

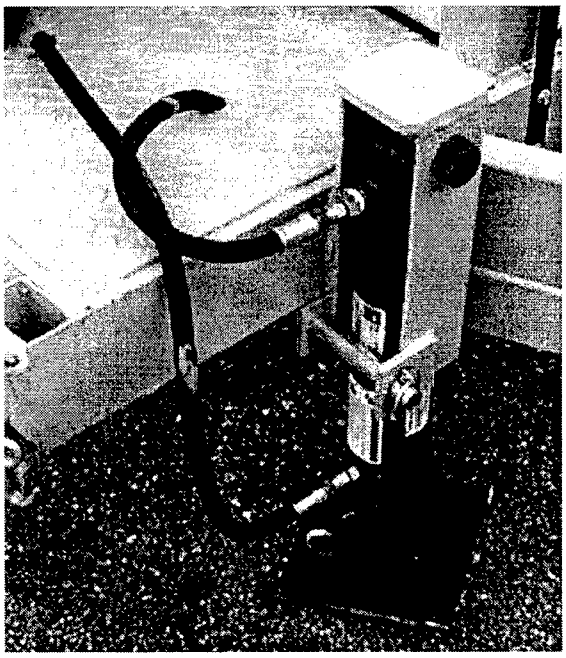

Figure 3-15. Leveling jacks in the down position.

Probe Design

After running tests on the prototype, it was decided to decrease the diameter of the probe. This was done for two reasons, the first being to decrease the amount of

disturbance to the soil. The second reason was so that standard size porous elements could be obtained for the sleeve portion of the tip.

For the sleeve, porous 316L SS seamless tubes were ordered from Mott Metallurgical Corporation. The tubes are 60.96 cm (24 in) long and will be cut into lengths of 1.7 cm (0.67 in). They have an outside diameter of 1.9 cm (0.750 in) and an inside diameter of 1.6 cm (0.650 in). Micron grades of 40 and 100 were purchased. Testing will be performed with the 100 microns with additional testing to be done in the future to determine which will perform the best for the soil types tested.

The probe consists of three parts, the extension rod, the tip, and the cone (Figure 3-16). The 91.44 cm (36 in) extension rod connects to the hydraulic unit. It has an O.D. of 3.175 cm (1.25 in) and an I.D. of 1.27 cm (0.50 in). The water line connects to the extension with a quick connect and the flow path is down the inside of it. The tip steps down from an O.D. of 3.175 cm (1.25 in) to 1.905 cm (0.75 in) with a 60 degree angle, see Figure 3-17. It has an I.D. of 0.635 cm (0.25 in) and will fit between the extension rod and the cone. The last part is the cone which has a 60 degree tip. The cone screws onto the tip. There are eight 0.305 cm (0.12 in) holes for the water to flow out. The porous sleeve will slip over the holes in the cone (see Figure 3-18).

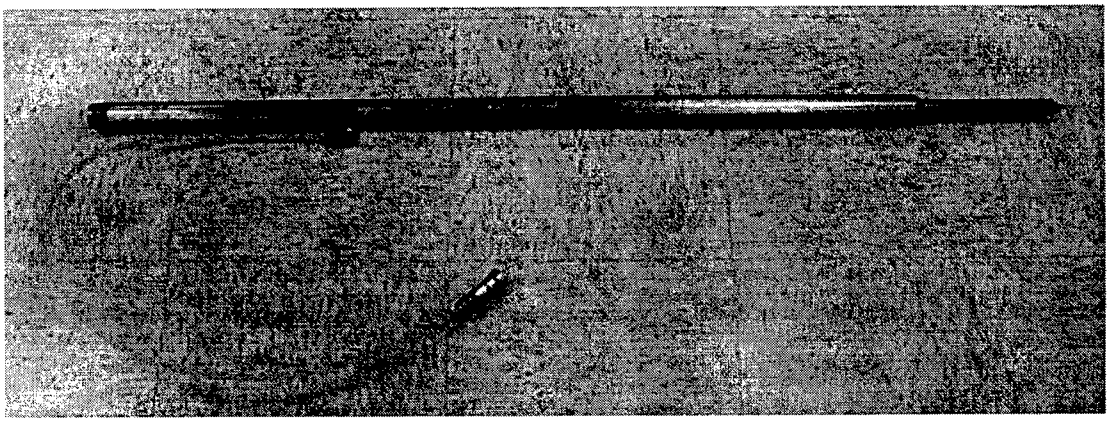

Figure 3-16. Picture of permeability probe.

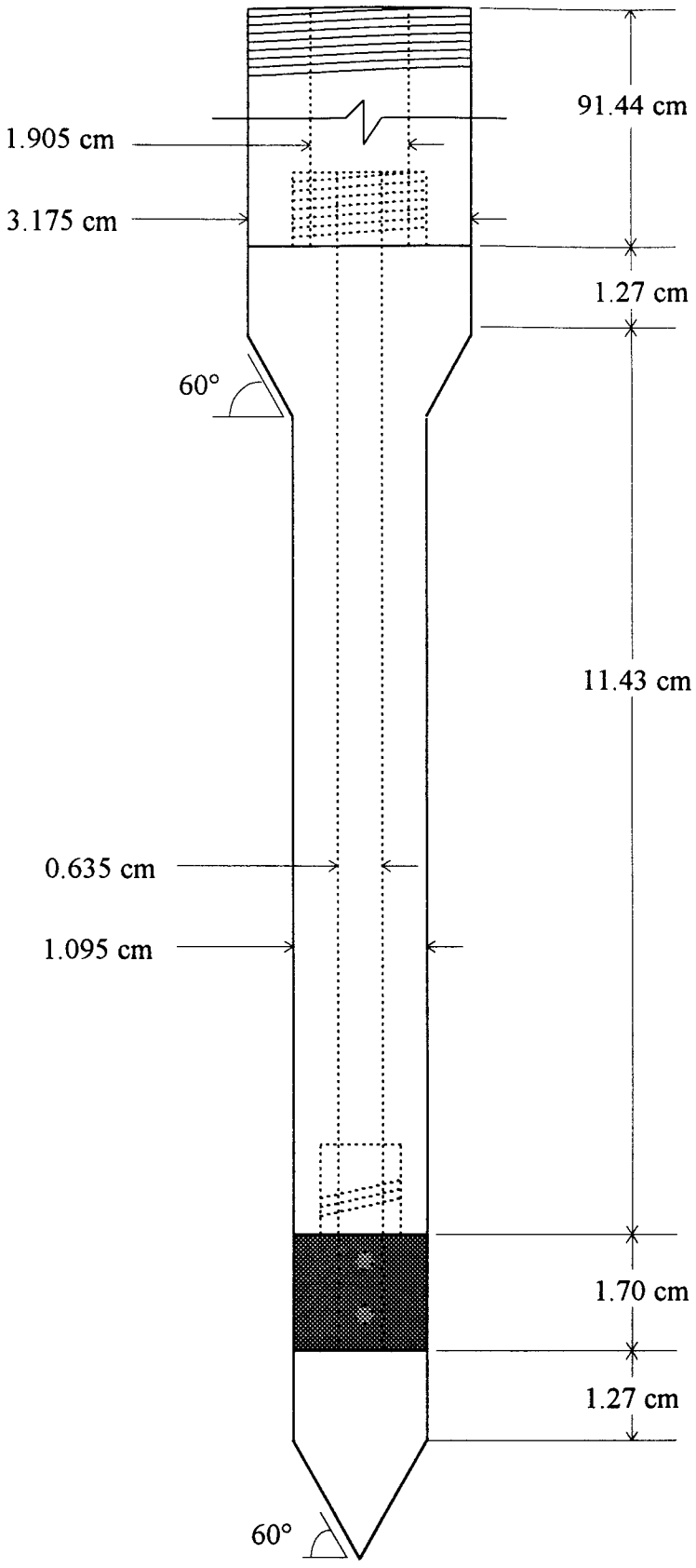

Figure 3-17. Diagram of permeability probe.

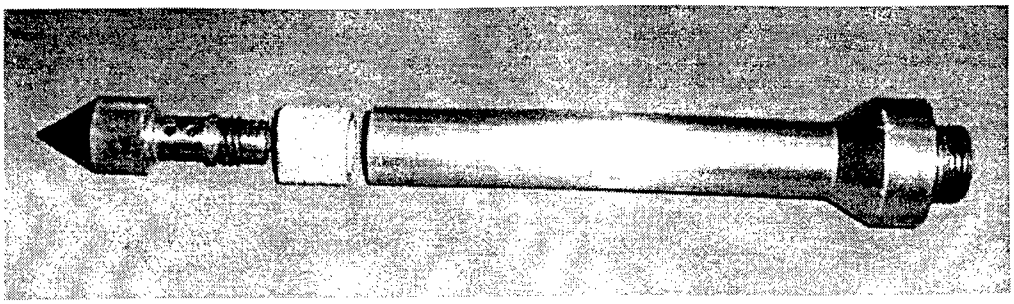

Figure 3-18. Cone, sleeve, and tip of permeability probe.

Equipment Placement

Before the water tanks, jacks, and the H-bean that supports the hydraulic cylinder for the probe were placed onto the trailer, calculations were made to determine the optimal placement for these major components. The following calculations were tried for various placements of the components. All forces are in Newtons and distances in centimeters. A reaction of 15575 N (3500 lbf), due to the maximum trailer hitch capacity, for penetration of the probe was used. Figure 3-19 places the water tanks at the ends of the trailer along with the jacks at the corners. The probe was placed at a distance x from the front of the trailer. The weight of the trailer is a distributed load which was taken as a point load at the center of the trailer. This weight includes the Mariotte tank, generator, and control box that is added to the trailer and is approximately 8900 N (2000 lbf).

The reactions at R_1 and R_2 were found by summing the moments about points A and B with the positive moment in the counterclockwise direction. This was also how the reactions for the other placement was calculated. The distance x was varied from 182.88 to 254 cm (72 to 100 in), this moves the probe from the center of the trailer to the back end near the rear water tank.

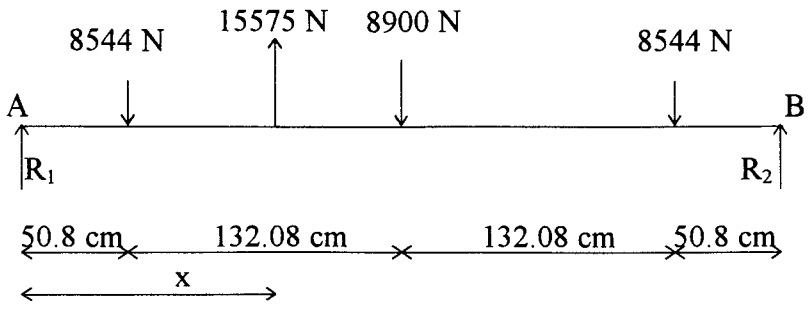

Figure 3-19. Tanks and jacks at ends with probe in center.

$$\Sigma M_A = 0: \ -50.8(8544)+x(15575)-182.88(8900)-314.96(8544)+365.76R_2 = 0$$

$$R_2 = 12994 - 42.58x$$

$$\Sigma M_B = 0: \ 50.8(8544)+182.88(8900)-(365.76-x)(15575)+314.96(8544)-365.76R_1 = 0$$

$$R_1 = 42.58x - 2581$$

If x = 182.88 cm (72 in), then $R_1 = R_2 = 5206.5$ N (1170 lbf) and when x = 254 cm (100 in) $R_1 = 8235.0$ N (1850.56 lbf) and $R_2 = 2178.0$ N (489.44 lbf). Because of the trailer bracing, the probe can not be placed in the center of the trailer. Therefore, if x = 198.12 cm (78 in) then $R_1 = 5854.5$ N (1315.83 lbf) and $R_2 = 4557.5$ N (1024.17 lbf). This placement of the probe, water tanks, and jacks gives adequate reactions and should enable penetration of the probe.

The following calculation places the probe at the rear of the trailer, see Figure 3-20. This was attempted so that viewing and inspection of the probe as it penetrated the soil could be performed. With this configuration $R_1 = 9196.67$ N (2066.67 lbf) and $R_2 =$ 1216.33 N (273.33 lbf). Even though this setup gives positive reactions it will not be used because if a force of more than 15575 N (3500 lbf) is needed to insert the probe in the soil Figure 3-19 would give the best reaction.

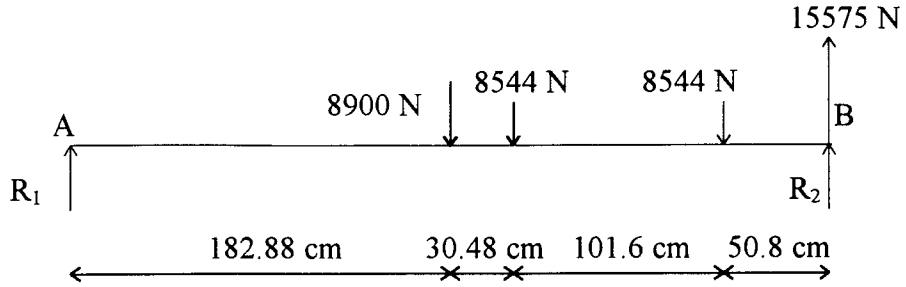

Figure 3-20. Probe at rear with jacks at corners, water tanks at rear of trailer.

$$\Sigma M_A = 0: \quad -72(2000)-84(1920)-124(1920)+144(3500)+144R_2 = 0$$

$$R_2 = 273.33 \text{ lb.}$$

$$\Sigma M_B = 0: \quad -144R_1+72(2000)+60(1920)+20(1920) = 0$$

$$R_1 = 2066.67 \text{ lb.}$$

CHAPTER 4
PRELIMINARY TESTING OF THE INSITU PERMEABILITY DEVICE

Once fabrication was completed, the device was transported to several test sites for operational check-out. This chapter includes the testing procedure, data sheet, sample calculations, testing methods, and results. Conclusions and recommendations are presented in Chapter 5.

Testing Procedure

Guidelines for the proper use and operation of the insitu permeability device are given below. The sequential observance of these guidelines is critical for proper operation of the device.

1. Hook up the trailer to the towing vehicle. Be sure that the hitch is securely locked to the towing vehicle. The safety chains and brake wire should be securely attached. Make sure that the lights are hooked up and working.

2. Make sure that the jacks are in their traveling position. If not, the following steps should be followed:
   a. Raise the trailer jacks by removing the lynch pin from the one-inch diameter hitch pin. Rotate the hydraulic cylinders up and hook the chain to the base plate of the jacks. Replace the hitch pin in the jack frame and insert the lynch pin.
   b. Raise the hitch jack by removing the pin and rotating the jack to the horizontal position, securely replace the pin.

3. The trailer is now ready to tow to the testing site. If water will not be available at the site the water tanks should be filled now or in route to the testing area.

4. If an existing road is being tested, the site should first be prepared by using the coring machine. Attach the coring motor to the stand on the trailer. The core bit should then be placed in the device. Attach the hose provided to the water tank and the coring device. After the road has been cored, line up the hydraulic cylinder for the probe with the hole.

5. Once at the site the jacks should be lowered into place following the

procedures listed below.

a. Lower the hitch jack by removing the pin and rotating the jack to the vertical position, securely replace the pin. Lower the jack so that it is touching the ground surface.
b. Remove the hitch pin from the jack frame by first removing the lynch pin.
c. Unhook the chain from the base plate and rotate the hydraulic cylinder down. Be sure not to use the hoses to lower the jacks. If the front jacks do not lower to the vertical position the trailer can be raised using the hitch jack.
d. Place the hitch pin in the jack frame. Be sure to put the lynch pin in place.
e. Turn on the hydraulic switch at the control panel. Lower the jacks with the control levers until they touch the ground.

6. The trailer can now be unhooked from the towing vehicle. Be sure to loosen the hitch from the hitch ball. Remove the safety chains, brake wire, and lights.

7. The next step is to level the trailer. First raise the trailer so that there is enough room for the probe to connect to the hydraulic ram. Place the level on the ram and adjust the jacks at the hydraulic controls until level. The hydraulic pump can now be turned off.

8. Place the probe in the guide sleeve and screw the probe into the hydraulic ram. Attach the sleeve to the deck with the bolts and nuts provided. Connect the water supply to the probe with the quick connect.

9. After turning on the hydraulic pump, lower the probe so that the tip touches the ground surface. Place a mark on the probe at the top of the guide sleeve with a marker. Turn off the hydraulic pump.

10. Turn on the main switch on the control panel. Be sure that the regulator on the control panel is turned all the way in the counterclockwise position before turning on the main switch.

11. Turn on the hydrogen tank and adjust the regulator so that the low pressure gauge on the nitrogen tank does not exceed 50 psi. Hook up the nitrogen tank to the air quick connect.

12. Verify that the water is flowing by following the procedure below.
    a. Make sure the main water valve on the Mariotte tank is open.
    b. Made sure that the flowmeter is in the high flow position.
    c. The release valve on top of the Mariotte tank should be in the open position.
    d. Turn the constant head switch to the on position.

e. Visually verify that water is flowing out of the probe and that the flowmeter is showing a flow rate.
f. Turn the constant head switch to the off position.

13. Push the probe to the desired depth following the steps below.
    a. Determine the depth of testing.
    b. Place a mark on the probe with the marker that distance above the guide sleeve.
    c. Turn on the hydraulic pump and slowly lower the probe into the soil to the depth marked on the probe.
    d. Record the depth on the data sheet.
    e. Turn the hydraulic pump off.

14. Turn the switch for the air supply to the on position. Be sure to switch the valve on the top of the Mariotte to the closed position.

15. Determine the testing pressure that will be used. This is usually low to start and then increased during testing. The pressure regulator on the control panel can now be turned on. This is done by turning the knob in the clockwise direction. Verify the test pressure on the water pressure gage.

16. For a constant head test the following steps should be followed.
    a. If the flowrate is below 50 cm^3/min switch the flow meter to the low flow rate. Be sure that the switch is not at the low flow if the flow is over 100 cm^3/min.
    b. If the flow needs to be switched from the low flow to the high flow be sure to decrease the air pressure by turning off the regulator and releasing the pressure in the Mariotte tank with the release valve.
    b. At 30 second intervals record the pressure from the water gauge and the flowmeter reading on the data sheet. This should be done until the flow stabilizes.
    c. Increase the pressure and repeat for other pressures as needed.
    d. Turn off the air pressure using the regulator on the control panel and release the pressure in the Mariotte tank with the release valve.

17. For a falling head test the following steps should be followed.
    a. Make sure that the flow meter is in the high position.
    b. Turn the switch to the falling head test on the control panel.
    c. Turn the switch to the fill position. Fill the tube past the top mark. If the tube is filling slow or it does not fill to the top mark, air pressure in the Mariotte tank can be increased.
    d. Turn the switch to the run test position.
    e. Start the stop watch at the top position and stop it at the lower mark.
    f. Turn the switch to the neutral position.
    g. Record the time on the data sheet.

h. Repeat steps 18c to 18g for a total of five times.

18. After running the constant and/or falling head test the probe can be pushed to another depth. Be sure to mark the incremental change on the probe first and record this depth on a new data sheet. At the new depth perform step 17 for the constant head test or step 18 for the falling head test.

19. After the testing is accomplished the following steps should be followed.
    a. Be sure that the flow meter is in the high flow position.
    b. Reduce the air pressure by turning the regulator knob in the counterclockwise direction and release the pressure with the release valve on the Mariotte tank.
    c. Turn off the air switch on the control panel. If no more testing is to be performed the Nitrogen tank can be turned off and unhooked at the quick connect.
    d. Raise the probe and disconnect the water supply at the quick connect.
    e. Remove the bolts and nuts from the guide sleeve. Unscrew the probe from the hydraulic cylinder.
    f. Measure the distance from the tip of the probe to the first mark on the probe and record on the data sheet(s).
    g. Remove the porous element and clean with water and the brush provided.

20. Lower the trailer and hook it up to the towing vehicle. Be sure that the hitch is securely locked to the towing vehicle. The safety chains and brake wire should be securely attached.

21. Raise the trailer jacks by removing the lynch pin from the hitch pin. Rotate the hydraulic cylinders up and hook the chain to the base plate of the jacks. Replace the hitch pin and the lynch pin in the jack frame. Raise the hitch jack and place in the traveling position.

Field Permeability Data Sheet

Figure 4-1 shows the data sheet developed for field testing. All measurements and test data must be recorded on-site to allow later permeability calculations to be performed.

FIELD PERMEABILITY Date: _____

Sample ID:
Location:
Sleeve used:
Sleeve diameter (in):
Sleeve length (in):

Depth of probe (in):
Length of probe (in):
Elevation (in):

Constant Head Test

Time (sec)	Gauge Pressure Reading (psi)	Flowmeter Reading (cm^3/min)

Time (sec)	Gauge Pressure Reading (psi)	Flowmeter Reading (cm^3/min)

Falling Head Test
H_1 (in)
H_2 (in)
Tube diameter (in)

Trial	1	2	3	4	5
Time (sec)					

Figure 4-1. Field permeability data sheet.

Sample Calculations

The following section contains the permeability calculations for both the insitu and the laboratory tests. Data from site 306 was used for the sample calculations contained in this section. The permeability was found for a constant head test with a water pressure of 0.5 psi and for the falling head results, trial one was used.

Shape factor

The shape factor (F) used in the permeability calculations, depends on the geometry of the probe. An in-depth discussion of the shape factor was presented in Chapter three. The following equation is used to calculate the shape factor:

$$F = \frac{2\pi L}{\ln\left(\frac{L}{D} + \sqrt{1 + \left(L/D\right)^2}\right)} - 2.8D$$

where D = 0.775 inch (sleeve diameter)
L = 0.685 inch (sleeve length)

$$F = \frac{2\pi(0.685\,\text{in})}{\ln\left(\frac{0.685\,\text{in}}{0.775\,\text{in}} + \sqrt{1 + \left(0.685\,\text{in}/0.775\,\text{in}\right)^2}\right)} - 2.8(0.775\,\text{in})$$

$$F = 3.231\ \text{in} = 8.208\ \text{cm}$$

Elevation head

The elevation head (h_e) is measured from the midpoint elevation of the water pressure gauge to the midpoint elevation of the porous element. Figure 4-2 shows the variables and methodology used to calculate h_e.

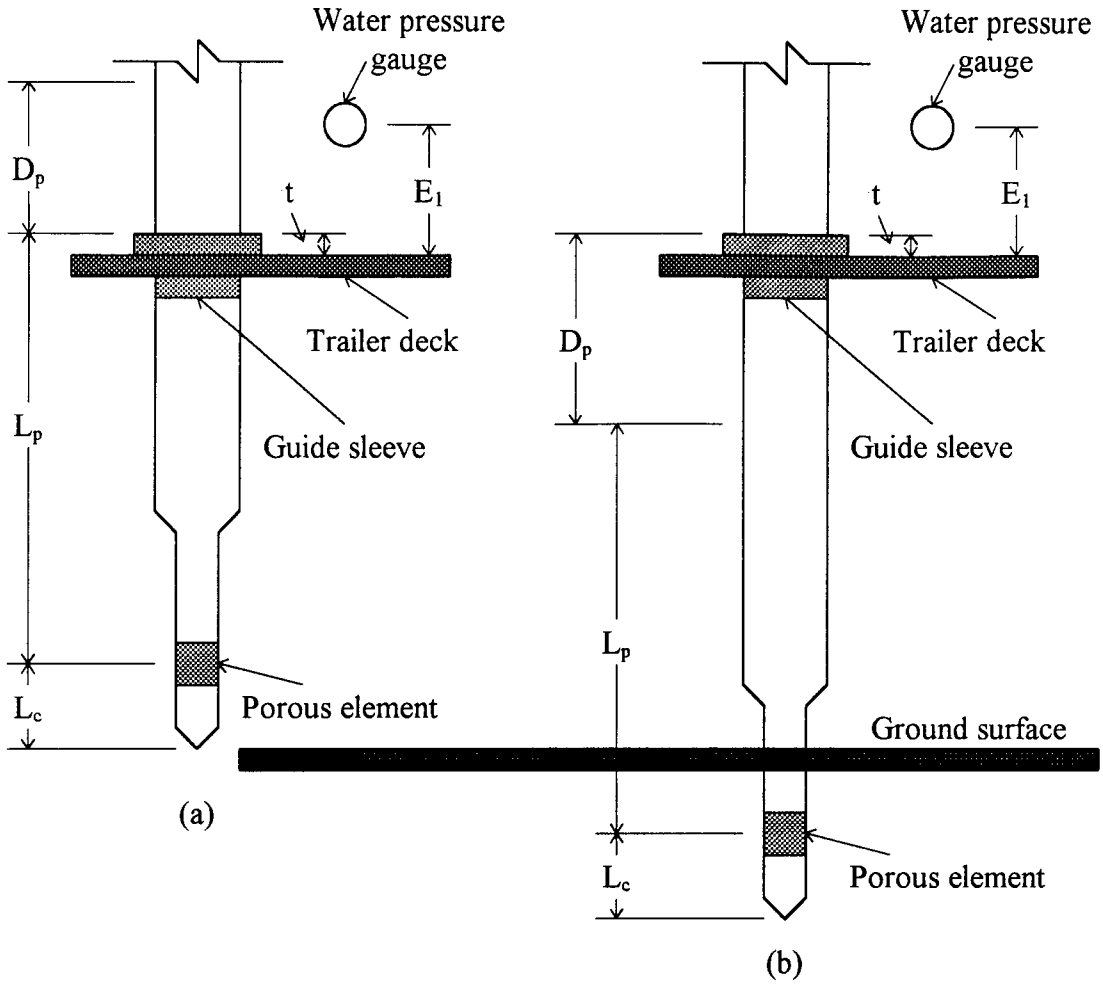

Figure 4-2. Diagram for elevation head.
(a) Before penetration of probe. (b) after penetration of probe.

The elevation head is calculated using the following equation:

$$h_e = D_p + L_p + E_1 - L_c - t$$

where D_p = depth of the probe = 9 inches
L_p = length of the probe from tip to top of guide sleeve = 25.50 inches
E_1 = distance from trailer deck to water pressure gauge = 15.5 inches
L_c = length from tip of cone to middle of porous element = 1.5 inches
t = thickness of guide sleeve = 0.687 inches

$$h_e = 9 + 25.50 + 15.5 - 1.5 - 0.687$$

$$h_e = 47.813 \text{ in} = 121.45 \text{ cm}$$

Constant head permeability

The total head is calculated by summing the elevation head and the pressure head. The pressure head (h_p) is obtained from the water pressure gauge and converted to centimeters of water. If the example gauge pressure is 0.5 psi, then:

$$h_p = 0.5 \text{ psi} \left(70.28 \frac{\text{cm } H_2O}{\text{psi}} \right)$$

$$h_p = 35.14 \text{ cm}$$

The total head (h_t) is then calculated using the following formula:

$$h_t = h_e + h_p$$

$$h_t = 121.45 \text{ cm} + 35.14 \text{ cm}$$

$$h_t = 156.59 \text{ cm}$$

Next the insitu permeability (k_c) is calculated using h_t, F, and flow rate (q). The flow rate is measured with the flowmeter.

The equation for k_c is:

$$k_c = \frac{q}{F h_t}$$

where: k_c = constant head permeability
q = flow rate = 29 cm^3/min.

$$k_c = \frac{29\,cm^3/min}{(3.231\,in)(156.59\,cm)}\left(\frac{1\,in}{2.54\,cm}\right)\left(\frac{1\,min}{60\,sec}\right)$$

$$k_c = 0.000371 \text{ cm/sec}$$

Falling head permeability

To calculate the falling head, the values for H_1 and H_2 must be known. These are the distances from the middle of the porous element to the starting and ending heights on the standpipe, respectively. The following calculations for H_1 and H_2 are made:

$$H_1 = h_e - E_1 + h_1$$

where h_1 = height from trailer deck to starting mark = 49 inches

$$H_1 = 47.813 \text{ in} - 15.5 \text{ in} + 49 \text{ in}$$

$$H_1 = 81.313 \text{ in}$$

also:

$$H_2 = h_e - E_1 + h_2$$

where h_2 = height from trailer deck the ending mark = 37 inches

$$H_2 = 47.813 \text{ in} - 15.5 \text{ in} + 37 \text{ in}$$

$$H_2 = 69.313 \text{ in}$$

The falling head insitu permeability (k_f) is then found using the following equation:

$$k_f = \frac{\pi d^2 / 4}{F t} \ln\left(\frac{H_1}{H_2}\right)$$

where d = 0.5 inches (standpipe diameter)

t = time for water the drop in standpipe = 13.6 seconds

$$k_f = \frac{\pi(0.5\text{in})^2/4}{(3.231\text{in})(13.6\text{sec})} \ln\left(\frac{81.313\text{in}}{69.313\text{in}}\right)\left(\frac{2.54\text{cm}}{1\text{in}}\right)$$

$$k_f = 0.00181 \text{ cm/sec}$$

Laboratory Permeability

Falling head and constant head permeability tests were performed in the lab on soils that were tested in the field. An attempt was then made to correlate the lab results with the insitu permeabilities.

Constant head

The constant head permeability was found using the following equation:

$$k = \frac{Q\,L}{t\,\Delta h\,A}$$

where Q = total quantity of water which flows through the sample = 16.05 cm^3
L = length of sample in permeameter = 13.3 cm
t = elapsed time = 180 seconds
Δh = total head loss = 65.2 cm
A = cross-sectional area of permeameter = 31.67 cm^2

$$k = \frac{(16.05\text{cm}^3)(13.3\text{cm})}{(180\text{sec})(65.2\text{cm})(31.67\text{cm}^2)}$$

$$k = 0.000574 \text{ cm/sec}$$

Falling head

The falling head permeability was calculated using:

$$k = 2.3\frac{a\,L}{A\,t}\log\frac{h_i}{h_f}$$

where a = cross-sectional area of standpipe = 1.65 cm^2
h_i = initial height of water above outflow = 65.1 cm
h_f = final height of water above outflow = 58.0 cm
t = time change in height of standpipe = 132.5 sec

$$k = 2.3\frac{(1.65\,cm^2)(13.3\,cm)}{(3167\,cm^2)(132.5\,sec)}\log\left(\frac{65.1\,cm}{58.0\,cm}\right)$$

0.000604 cm/sec

Back Calculated Shape Factor

The shape factor was found by back calculation, using the permeabilities found from the constant head and falling head lab tests.

Constant head shape factor

The shape factor was back calculated by using the insitu constant head formula and solving for the shape factor. The average laboratory constant head permeability was used.

$$F = \frac{q}{k\,h_t}$$

$$F = \frac{29\,cm^3/min}{(0.000575\,cm/sec)(156.59\,cm)}\left(\frac{min}{60\,sec}\right)$$

F = 5.30 cm = 2.08 in

Falling head shape factor

Calculation of the shape factor for the falling head was found by using the insitu falling head formula and solving for the shape factor.

$$F = \frac{\pi d^2 / 4}{k \Delta t} \ln \frac{H_1}{H_2}$$

$$F = \frac{\pi(0.5in)^2 / 4}{(0.000604cm/sec)(136sec)} \ln\left(\frac{81.313in}{69.313in}\right)\left(\frac{2.54cm}{in}\right)$$

$$F = 9.70 \text{ in} = 24.63 \text{ cm}$$

Testing Methodology

Testing of the insitu permeability device was accomplished in three phases. Preliminary testing of the device, corresponding to test numbers 301 through 311, was performed at the UF's coastal laboratory, an athletic (softball) field under construction, and a dormitory (Maguire village) field. The second group of tests, corresponding to test numbers 400 through 416, were performed at the State Materials Office (Waldo Road) test pit site designated by the FDOT. The third set of tests, corresponding to test numbers 500 through 504, were done on roadways under construction. Complete data for the insitu and laboratory constant head permeability can be found in Appendix A, and the complete data for the insitu and laboratory falling head permeability tests are found in Appendix B.

Preliminary Testing

Preliminary testing was carried out near campus because of the accessibility and the presence of well compacted soil. Testing in these conditions allowed the researcher to

evaluate whether the device could penetrate such stiff materials.

Constant head and falling head tests were performed at each location, except for test 301 where only a falling head test was done due to the high permeability of the soil. Table 4-1 and Figure 4-3 show the results of the constant head permeability test. A linear trendline was inserted into the plot of data points and the R^2 was found. The value for R^2 is usually referred to as the sample coefficient of determination. That is, R^2 expresses the proportion of the total variation in the values of the variable Y that can be accounted for or explained by a linear relationship with the values of the random variable X. The closer the value is to one, the better the relationship is. From Figure 4-3 a R^2 of 0.5481 was found for the constant head permeability tests.

Table 4-1. Preliminary constant head data.

Test #	Insitu Permeability (cm/s)	Laboratory Permeability (cm/s)	Location
302	7.41E-04	3.42E-04	At Coastal
303	2.48E-03	1.09E-03	At Coastal
304	3.30E-04	4.73E-04	At Coastal
305	3.83E-04	2.74E-04	At Coastal
306	4.43E-04	5.75E-04	At Coastal
308	3.88E-04	7.06E-04	Softball Field
309	9.28E-04	3.89E-04	Maguire Field
310	6.70E-04	4.00E-04	Softball Field
311	5.60E-04	2.39E-04	Maguire Field

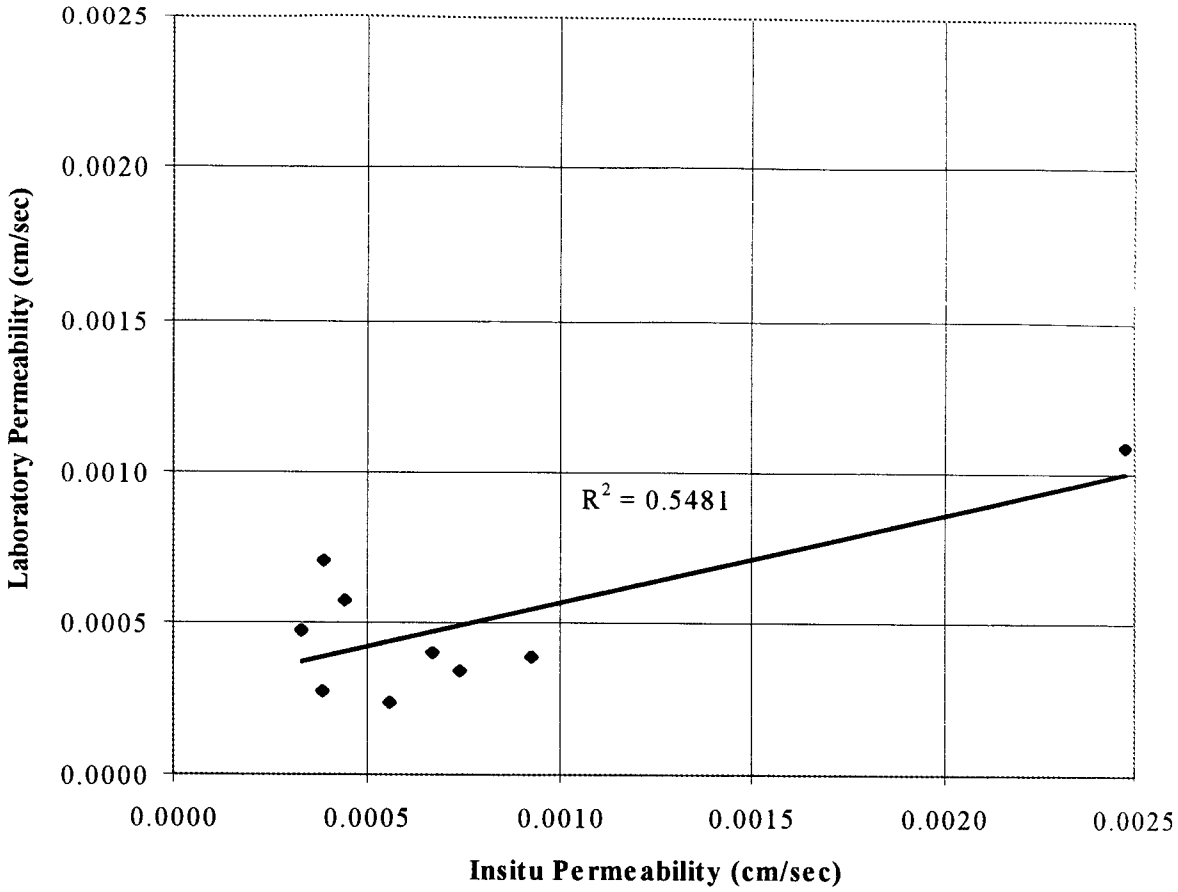

Figure 4-3. Preliminary constant head data.

The results of the falling head permeability tests can be found in Table 4-2 and Figure 4-4. From Figure 4-4 the value for R^2 was found to be 0.5206. Differences in field and laboratory densities may account for the low R^2 values. The field densities were unknown while Laboratory densities were maximized. In addition, the field device measures the horizontal permeability while in the lab, only the vertical permeability is determined. Thus, future efforts will be made to test materials in the same orientation both in the field and lab.

Table 4-2. Preliminary falling head data.

Test #	Insitu Permeability (cm/s)	Laboratory Permeability (cm/s)	Location
301	8.75E-05	1.19E-03	At Coastal
302	4.81E-04	1.43E-03	At Coastal
304	3.22E-04	1.70E-03	At Coastal
305	2.61E-04	1.33E-03	At Coastal
306	4.41E-04	6.03E-04	At Coastal
307	3.30E-04	1.11E-03	At Coastal
308	4.35E-04	2.92E-03	Softball Field
309	8.05E-04	4.55E-03	Maguire Field
310	6.70E-04	1.74E-03	Softball Field
311	8.12E-04	3.35E-03	Maguire Field

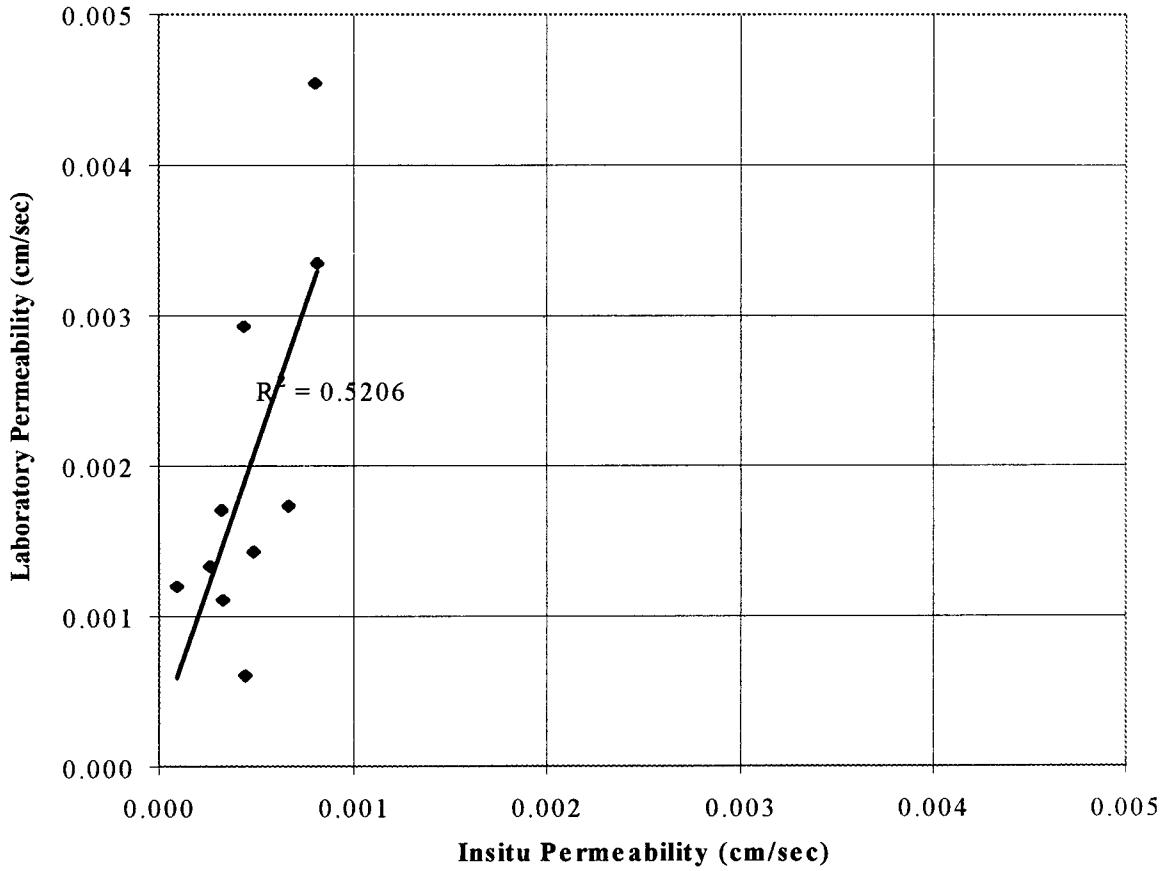

Figure 4-4. Preliminary falling head data.

FDOT Test Pit

The second phase of testing was carried out at the FDOT State Materials Office on Waldo Road. A test pit was constructed on the west side of the property. This test pit was made with two sections consisting of two layers each. Table 4-3 lists the sections and layers along with the AASHTO soil classifications.

Table 4-3. Test pit description.

Section	Layer	Classification
East	Upper	A-3
East	Lower	A-2-4
West	Upper	A-2-4
West	Lower	A-2-4

The test data obtained at the test pit are presented in Table 4-4 for the constant head and Table 4-5 for the falling head permeability tests.

Table 4-4. Test pit constant head data.

Test #	Insitu Permeability (cm/s)	Laboratory Permeability (cm/s)	Location
401	5.82E-05	6.90E-06	East Lower
402	1.68E-03	6.14E-04	East Upper
403	1.46E-03	6.14E-04	East Upper
405	1.41E-03	6.14E-04	East Upper
407	1.47E-03	6.14E-04	East Upper
409	1.40E-03	6.14E-04	East Upper
411	6.31E-05	5.37E-07	West Upper
413	1.30E-04	5.37E-07	West Upper

Table 4-5. Test pit falling head data

Test #	Insitu Permeability (cm/s)	Laboratory Permeability (cm/s)	Location
402	1.32E-03	6.14E-04	East Upper
404	1.06E-05	6.90E-06	East Lower
405	1.21E-03	6.14E-04	East Upper
406	1.04E-05	6.90E-06	East Lower
408	1.06E-05	6.90E-06	East Lower
410	6.56E-06	6.90E-06	East Lower
411	2.04E-05	5.37E-07	West Upper
412	4.13E-06	5.33E-06	West Lower
413	5.34E-05	5.37E-07	West Upper
414	9.00E-06	5.33E-06	West Lower
415	2.34E-05	5.37E-07	West Upper
416	4.71E-06	5.33E-06	West Lower

The data show a good correlation. One reason for this is that the density of the test pit was known and the laboratory permeability was performed at that density.

Road Construction Site Testing

Two different sites road construction were tested. The first site was on state road 27 near Williston and the second site was on state road 26 west of Gainesville. Constant head tests were performed at both sites. The data are presented in Table 4-6 and Figure 4-7. Results from the FDOT laboratory permeability tests have not been obtained yet, so the laboratory permeability tests were performed at the University of Florida. The R^2 value was found to be 0.5557. One reason for the low R^2 value is that the density of the test site was not obtained to simulate field conditions when performing the laboratory permeability test. If the data from number 500 is not used then the R^2 value is 0.9683.

Test 500 was performed on a section that was not compacted to density. Even though only two sites were tested, the repeatability of the device is shown.

Table 4-6. Road construction constant head data.

Test #	Insitu Permeability (cm/s)	Laboratory Permeability (cm/s)	Location
500	1.97E-03	6.81E-03	State Road 27
501	6.42E-04	6.81E-03	State Road 27
502	7.99E-04	6.81E-03	State Road 27
503	1.07E-04	1.31E-03	State Road 26
504	6.82E-05	1.31E-03	State Road 26

Summary of Data

The test data from the preliminary permeability tests and the test pit data were combined and are presented below. Table 4-7 and Figure 4-8 show the combined data for the constant head tests. An R^2 value of 0.6682 was obtained. Table 4-8 and Figure 4-9 contain the data for the falling head permeability tests. The R^2 value for the falling head tests was found to be 0.7997.

Table 4-7. Summary of constant head data.

Test #	Insitu Permeability (cm/s)	Laboratory Permeability (cm/s)	Location
302	7.41E-04	3.42E-04	At Coastal
303	2.48E-03	1.09E-03	At Coastal
304	3.30E-04	4.73E-04	At Coastal
305	3.83E-04	2.74E-04	At Coastal
306	4.43E-04	5.75E-04	At Coastal
308	3.88E-04	7.06E-04	Softball Field
309	9.28E-04	3.89E-04	Maguire Field
310	6.70E-04	4.00E-04	Softball Field
311	5.60E-04	2.39E-04	Maguire Field
401	5.82E-05	6.90E-06	East Lower
402	1.68E-03	6.14E-04	East Upper
403	1.46E-03	6.14E-04	East Upper
405	1.41E-03	6.14E-04	East Upper
407	1.47E-03	6.14E-04	East Upper
409	1.40E-03	6.14E-04	East Upper
411	6.31E-05	5.37E-07	West Upper
413	1.30E-04	5.37E-07	West Upper

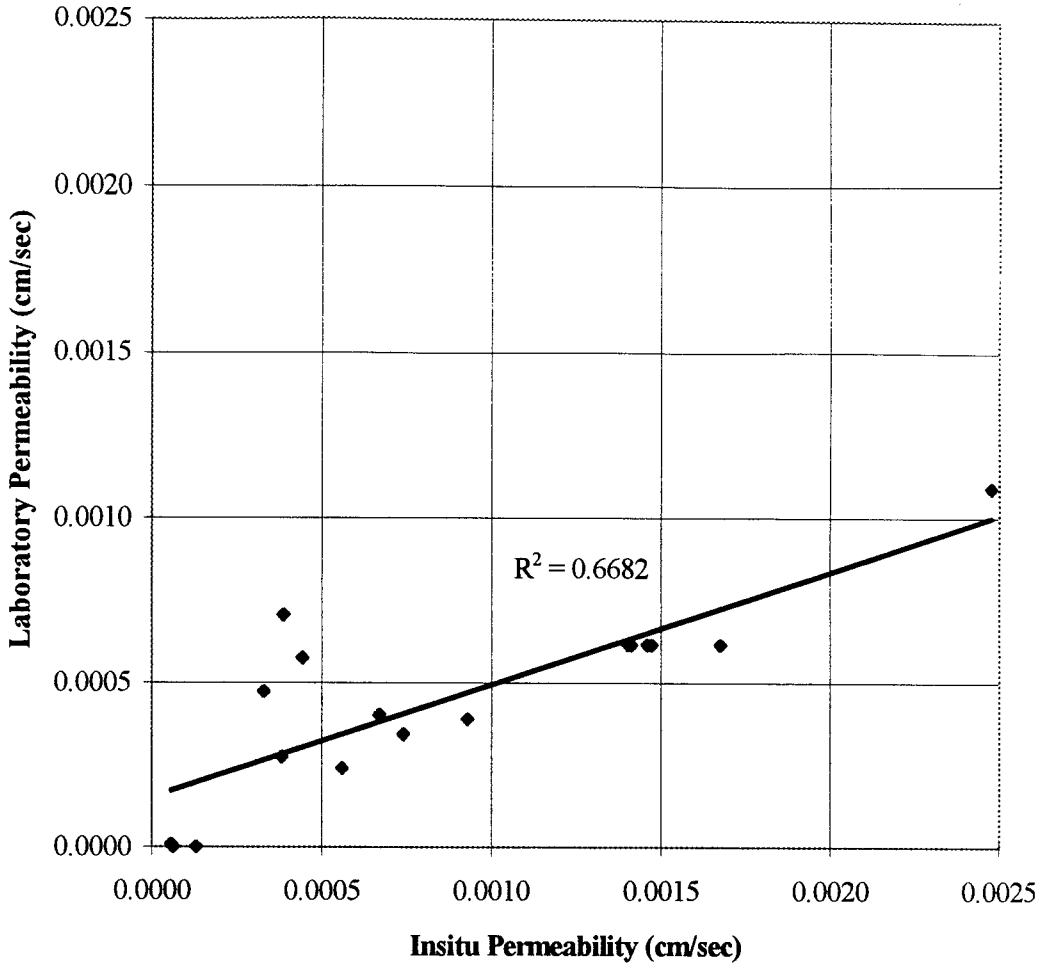

Figure 4-5 Summary of constant head data

Table 4-8. Summary of falling head data.

Test #	Insitu Permeability (cm/s)	Laboratory Permeability (cm/s)	Location
301	8.75E-05	1.19E-03	At Coastal
302	4.81E-04	1.43E-03	At Coastal
304	3.22E-04	1.70E-03	At Coastal
305	2.61E-04	1.33E-03	At Coastal
306	4.41E-04	6.03E-04	At Coastal
307	3.30E-04	1.11E-03	At Coastal
308	4.35E-04	2.92E-03	Softball Field
309	8.05E-04	4.55E-03	Maguire Field
310	6.70E-04	1.74E-03	Softball Field
311	8.12E-04	3.35E-03	Maguire Field
404	1.06E-05	6.90E-06	East Lower
406	1.04E-05	6.90E-06	East Lower
408	1.06E-05	6.90E-06	East Lower
410	6.56E-06	6.90E-06	East Lower
411	2.04E-05	5.37E-07	West Upper
412	4.13E-06	5.33E-06	West Lower
413	5.34E-05	5.37E-07	West Upper
414	9.00E-06	5.33E-06	West Lower
415	2.34E-05	5.37E-07	West Upper
416	4.71E-06	5.33E-06	West Lower

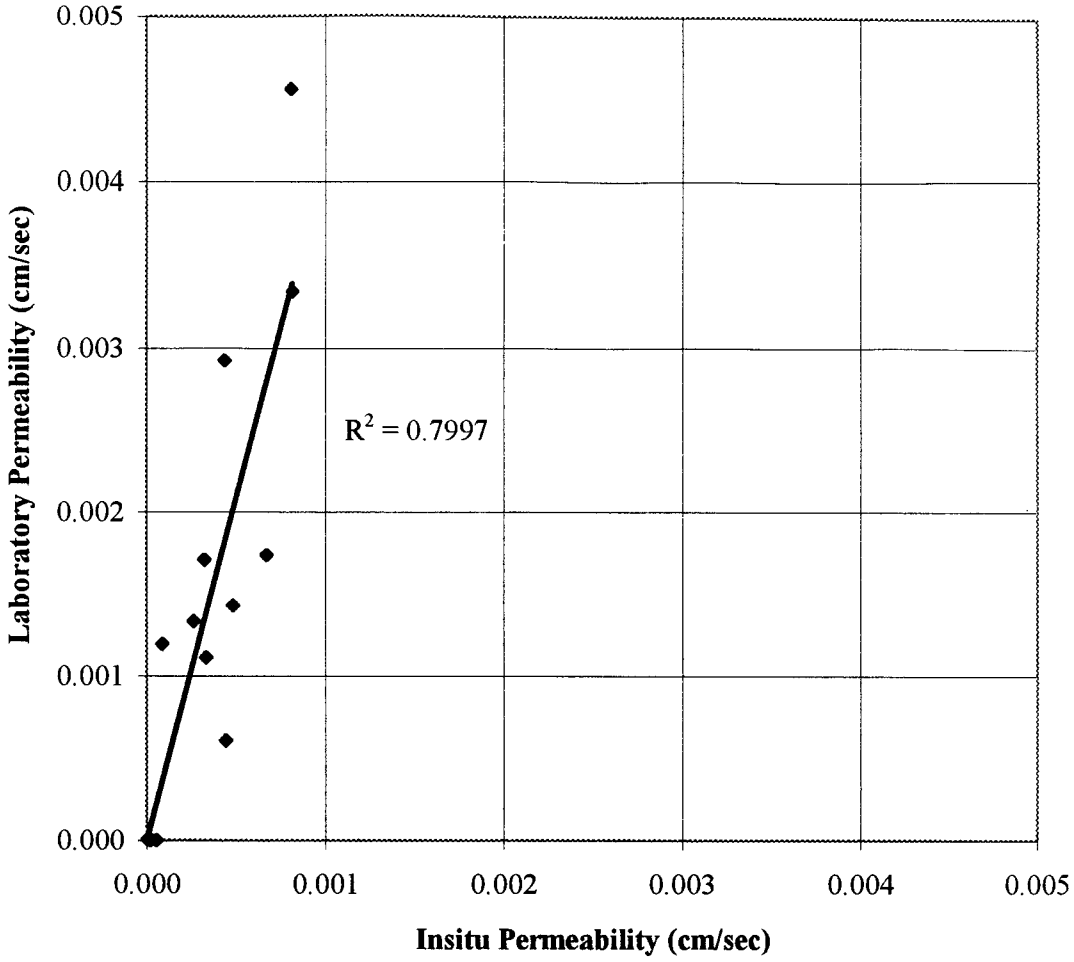

Figure 4-6. Summary of falling head data.

The average of the back calculated F values was used as the final shape factor of the probe. Table 4-9 shows the back calculated shape factor for the constant head permeability tests, with an average value of 15.44. From Table 4-10 the average back calculated shape factor for the falling head permeability test was found to be 7.46.

Table 4-9. Constant head back calculated shape factors.

Test #	Insitu Permeability (cm/s)	Laboratory Permeability (cm/s)	F (cm)
302	7.41E-04	3.42E-04	17.79
303	2.48E-03	1.09E-03	18.70
304	3.30E-04	4.73E-04	5.73
305	3.83E-04	2.74E-04	11.46
306	4.43E-04	5.75E-04	6.32
307	5.55E-04	1.15E-03	3.95
308	3.88E-04	7.06E-04	4.51
309	9.28E-04	3.89E-04	19.60
310	6.70E-04	4.00E-04	13.73
311	5.60E-04	2.39E-04	19.25
400	2.38E-03	6.14E-04	31.88
401	5.82E-05	6.90E-06	69.25
402	1.68E-03	6.14E-04	22.41
403	1.46E-03	6.14E-04	19.51
405	1.41E-03	6.14E-04	18.89
407	1.47E-03	6.14E-04	19.69
409	1.40E-03	6.14E-04	18.77
501	6.42E-04	6.81E-03	0.77
502	7.99E-04	6.81E-03	0.96
503	1.07E-04	1.31E-03	0.67
504	6.82E-05	1.31E-03	0.43
		Average F	15.44

Table 4-10. Falling head back calculated shape factors.

Test #	Insitu Permeability (cm/s)	Laboratory Permeability (cm/s)	F (cm)
301	8.75E-05	1.19E-03	0.60
302	4.81E-04	1.43E-03	2.77
303	2.53E-03	1.05E-03	19.77
304	3.22E-04	1.70E-03	1.55
305	2.61E-04	1.33E-03	1.61
306	4.41E-04	6.03E-04	6.01
307	3.30E-04	1.11E-03	2.45
308	4.35E-04	2.92E-03	1.22
309	8.05E-04	4.55E-03	1.45
310	6.70E-04	1.74E-03	3.17
311	8.12E-04	3.35E-03	1.99
402	1.32E-03	6.14E-04	17.61
404	1.06E-05	6.90E-06	12.57
405	1.21E-03	6.14E-04	16.20
406	1.04E-05	6.90E-06	12.37
408	1.06E-05	6.90E-06	12.58
410	6.56E-06	6.90E-06	7.80
412	4.13E-06	5.33E-06	6.35
414	9.00E-06	5.33E-06	13.86
416	4.71E-06	5.33E-06	7.25
		Average F	7.46

CHAPTER 5
CONCLUSIONS AND RECOMMENDATIONS

Conclusions

The main objective of this project was to design and construct an insitu device that measures the permeability of base layers beneath pavements, specifically those made of concrete. A succession of design alterations has resulted in a much improved version. For example, the original trailer did not provide sufficient reaction for penetration. Hence, a larger, twin axle trailer was purchased and the H-beam supporting the hydraulic cylinder and probe was mounted to it. This new trailer allows two water tanks and a one-inch steel plate to be added that thereby provides the necessary additional reaction when penetrating in stiff soils.

Electrical scissor jacks were originally attached to the trailer for leveling purposes. However, due to the lack of stability under certain conditions, a hydraulic jacking system was installed and no problems have occurred with the new leveling system. These jacks improve both the speed of leveling as well as providing a rigid platform from which to test. This rigidity is very important because if the trailer shifts during penetration, a void around the probe may occur. This could result in erroneous flow measurements, as the water could travel along the gap created by the lateral rod movement.

To facilitate testing, solenoids switches were added to run the constant and falling head tests. Another feature that has decreased the operator's workload was the installation of digital flow meters. These direct reading devices make it much easier to determine the flow rate and now there is no need to use conversion (voltage to flow) factors.

One item that needed to be addressed concerned the porous element. In order to see if it clogs during insertion into the soil, flow readings were taken just prior to penetration into various types of soil, and then again after removal of the probe from the soil. There was not an appreciable change in readings, therefore, it is reasonable and assumed that clogging is not occurring. The probe was also inserted into the material while water was flowing out the porous element. The elevation head was the only head applied during penetration. No noticeable change in the permeability was observed.

In order to compute the permeability, k, of the base and subbase, a characteristic shape factor for the probe is required. The shape factor was back calculated and an average value of 15.5 was determined. It is recommended that this value be used in the calculation of the insitu permeability using this field device.

The results to date show that the determination of insitu permeability is repeatable. This was one of the FDOT requirements of the device. In addition, the device is also easy to run by a single operator.

Recommendations

Continued testing of the device is recommended, specifically, additional sites under construction will allow for a more refined shape factor, F, to be determined. It is also recommended to make charts that will plot the flow rate versus pressure. Since the primary purpose of the device is to verify that the as-constructed permeability meets certain FDOT criteria, accumulation of field data is mandated. Testing of existing roads also need to be done, those with and without pumping problems. This will provide insight and allow for a realistic criteria to be developed.

Minor changes can be made to the insitu permeability device. A methods such as recharging the batteries from the towing vehicle as it is traveling to different sites should be looked into. A photovoltaic trickling charger is currently being installed which will

allow recharging to occur while the device is in operation. It is also suggested that a portable data acquisition system be included. This will read data from the digital flow meters and pressure transducers, and can prevent errors from occurring in data recording. Once acquired, the data can then be loaded into spreadsheets to calculate the permeability of the base and subbase material. The use of a laptop computer will also enable the permeability to be calculated on site.

One final suggestion deals with trailer organization. Because of the equipment arrangement on it there is limited space available to reach the probe assembly. A solution would be to remove the water tanks and place one-inch thick steels plates on the front and rear sections of the trailer. This would add approximately 2000 pounds to the gross weight. Smaller water tanks could then be placed on the trailer to obtain the needed weight for penetration. The only drawback is that this additional weight would be permanent ballast.

APPENDIX A
CONSTANT HEAD PERMEABILITY DATA

Appendix A contains the data for the insitu and laboratory constant head testing. The back calculation of the shape factor is also included on the data sheets.

INSITU CONSTANT HEAD TEST

Sample ID: 302

Location: at coastal

Sleeve diameter (in):	0.775	Depth of probe (in):	8
Sleeve length (in):	0.685	Length of probe (in):	26.00
Shape factor (in):	3.23	Elevation (in):	47.31

Gage Pressure Reading (psi)	Pressure Head (cm)	Elevation Head (cm)	Total Head (cm)	Flowmeter Reading (cm^3/min)	Permeability (cm/sec)
0.5	35.14	120.18	155.32	58	7.58E-04
0.55	38.65	120.18	158.83	56	7.16E-04
0.6	42.17	120.18	162.34	51	6.36E-04
1.0	70.28	120.18	190.46	65	6.96E-04
1.5	105.42	120.18	225.60	87	7.83E-04
2.0	140.56	120.18	260.74	110	8.57E-04
			Average k (cm/sec)		7.41E-04

LABORATORY CONSTANT HEAD TEST

Sample Length (cm):	6.6	Sample Volume (cm^3):	209.0
Sample Diameter (cm):	6.4	Sample Mass (g):	367.56
		Sample Density (g/cm^3):	1.76

Trial	1	2	3	4	5
Time (s)	120	120	120	120	120
Δ h (cm)	74.5	74.5	74.5	74.5	74.5
Q (cm^3)	14.56	14.85	14.83	14.61	14.50
k (cm/s)	3.39E-04	3.46E-04	3.46E-04	3.41E-04	3.38E-04
			Average k (cm/sec)		3.42E-04

BACK CALCULATED SHAPE FACTOR

Gauge Pressure (psi)	Total Head (cm)	Flow rate (cm^3/min)	Permeability (cm/sec)	Calculated F (cm)	Calculated F (in)
0.5	155.32	58	3.42E-04	18.20	7.17
0.6	158.83	56	3.42E-04	17.18	6.77
0.6	162.34	51	3.42E-04	15.27	6.01
1.0	190.46	65	3.42E-04	16.71	6.58
1.5	225.60	87	3.42E-04	18.79	7.40
2.0	260.74	110	3.42E-04	20.56	8.09
			Average F	17.79	7.00

INSITU CONSTANT HEAD TEST

Sample ID: 303
Location: at coastal
Sleeve used: 100 microns
Sleeve diameter (in): 0.775 Depth of probe (in): 8
Sleeve length (in): 0.685 Length of probe (in): 27.00
Shape factor (in): 3.23 Elevation (in): 48.31

Gage Pressure Reading (psi)	Pressure Head (cm)	Elevation Head (cm)	Total Head (cm)	Flowmeter Reading (cm^3/min)	Permeability (cm/sec)
0.5	35.14	122.72	157.86	170	2.19E-03
1.0	70.28	122.72	193.00	230	2.42E-03
1.5	105.42	122.72	228.14	300	2.67E-03
2.0	140.56	122.72	263.28	342	2.64E-03
			Average k (cm/sec)		2.48E-03

LABORATORY CONSTANT HEAD TEST

Sample Length (cm): 13.8 Sample Volume (cm^3): 437.0
Sample Diameter (cm): 6.4 Sample Mass (g): 734.88
Sample Density (g/cm^3): 1.68

Trial	1	2	3	4	5
Time (s)	180	180	180	180	180
Δ h (cm)	65.5	65.5	65.5	65.5	65.5
Q (cm^3)	29.60	29.50	29.37	29.34	29.24
k (cm/s)	1.09E-03	1.09E-03	1.09E-03	1.08E-03	1.08E-03
			Average k (cm/sec)		1.09E-03

BACK CALCULATED SHAPE FACTOR

Gauge Pressure (psi)	Total Head (cm)	Flow rate (cm^3/min)	Permeability (cm/sec)	Calculated F (cm)	Calculated F (in)
0.5	157.86	170	1.09E-03	16.51	6.50
1.0	193.00	230	1.09E-03	18.25	7.18
1.5	228.14	300	1.09E-03	20.13	7.92
2.0	263.28	342	1.09E-03	19.92	7.84
			Average F	18.70	7.36

INSITU CONSTANT HEAD TEST

Sample ID: 304

Location: at coastal

Sleeve diameter (in):	0.775	Depth of probe (in):	8
Sleeve length (in):	0.685	Length of probe (in):	26.25
Shape factor (in):	3.23	Elevation (in):	47.56

Gage Pressure Reading (psi)	Pressure Head (cm)	Elevation Head (cm)	Total Head (cm)	Flowmeter Reading (cm^3/min)	Permeability (cm/sec)
0.5	35.14	120.81	155.95	24	3.06E-04
1.0	70.28	120.81	191.09	32	3.39E-04
1.5	105.42	120.81	226.23	35	3.12E-04
2.0	140.56	120.81	261.37	42	3.26E-04
3.0	210.84	120.81	331.65	60	3.67E-04
			Average k (cm/sec)		3.30E-04

LABORATORY CONSTANT HEAD TEST

Sample Length (cm):	6.7	Sample Volume (cm^3):	212.2
Sample Diameter (cm):	6.4	Sample Mass (g):	342.23
		Sample Density (g/cm^3):	1.61

Trial	1	2	3	4	5
Time (s)	120	120	120	120	180
Δ h (cm)	74.5	74.5	74.5	74.5	74.5
Q (cm^3)	20.02	20.14	20.04	19.93	29.65
k (cm/s)	4.74E-04	4.77E-04	4.74E-04	4.72E-04	4.68E-04
			Average k (cm/sec)		4.73E-04

BACK CALCULATED SHAPE FACTOR

Gauge Pressure (psi)	Total Head (cm)	Flow rate (cm^3/min)	Permeability (cm/sec)	Calculated F (cm)	Calculated F (in)
0.5	155.95	24	4.73E-04	5.31	2.09
1.0	191.09	32	4.73E-04	5.89	2.32
1.5	226.23	35	4.73E-04	5.42	2.13
2.0	261.37	42	4.73E-04	5.65	2.22
3.0	331.65	60	4.73E-04	6.37	2.51
			Average F	5.73	2.26

INSITU CONSTANT HEAD TEST

Sample ID: 305

Location: at coastal

Sleeve diameter (in):	0.775	Depth of probe (in):	8
Sleeve length (in):	0.685	Length of probe (in):	25.25
Shape factor (in):	3.23	Elevation (in):	46.56

Gage Pressure Reading (psi)	Pressure Head (cm)	Elevation Head (cm)	Total Head (cm)	Flowmeter Reading (cm^3/min)	Permeability (cm/sec)
1.0	70.28	118.27	188.55	28	2.96E-04
1.5	105.42	118.27	223.69	39	3.52E-04
2.0	140.56	118.27	258.83	53	4.13E-04
2.5	175.70	118.27	293.97	68	4.70E-04
			Average k (cm/sec)		3.83E-04

LABORATORY CONSTANT HEAD TEST

Sample Length (cm):	6.7	Sample Volume (cm^3):	212.2
Sample Diameter (cm):	6.4	Sample Mass (g):	340.98
		Sample Density (g/cm^3):	1.61

Trial	1	2	3	4	5
Time (s)	120	120	120	120	120
Δ h (cm)	74.7	74.7	74.7	74.7	74.7
Q (cm^3)	11.75	11.66	11.63	11.56	11.51
k (cm/s)	2.77E-04	2.75E-04	2.74E-04	2.73E-04	2.72E-04
			Average k (cm/sec)		2.74E-04

BACK CALCULATED SHAPE FACTOR

Gauge Pressure (psi)	Total Head (cm)	Flow rate (cm^3/min)	Permeability (cm/sec)	Calculated F (cm)	Calculated F (in)
1.0	188.55	28	2.74E-04	8.86	3.49
1.5	223.69	39	2.74E-04	10.54	4.15
2.0	258.83	53	2.74E-04	12.37	4.87
2.5	293.97	68	2.74E-04	14.08	5.54
			Average F	11.46	4.51

INSITU CONSTANT HEAD TEST

Sample ID: 306

Location: at coastal

Sleeve diameter (in):	0.775	Depth of probe (in):	9
Sleeve length (in):	0.685	Length of probe (in):	25.50
Shape factor (in):	3.23	Elevation (in):	47.81

Gage Pressure Reading (psi)	Pressure Head (cm)	Elevation Head (cm)	Total Head (cm)	Flowmeter Reading (cm^3/min)	Permeability (cm/sec)
0.5	35.14	121.45	156.59	29	3.71E-04
1.5	105.42	121.45	226.87	50	4.47E-04
2.0	140.56	121.45	262.01	60	4.65E-04
2.5	175.70	121.45	297.15	72	4.89E-04
			Average k (cm/sec)		4.43E-04

LABORATORY CONSTANT HEAD TEST

Sample Length (cm):	13.3	Sample Volume (cm^3):	421.2
Sample Diameter (cm):	6.4	Sample Mass (g):	817.38
		Sample Density (g/cm^3):	1.94

Trial	1	2	3	4	5
Time (s)	180	180	180	180	180
Δ h (cm)	65.2	65.2	65.2	65.2	65.2
Q (cm^3)	16.05	16.03	16.10	16.09	16.05
k (cm/s)	5.74E-04	5.74E-04	5.76E-04	5.76E-04	5.74E-04
			Average k (cm/sec)		5.75E-04

BACK CALCULATED SHAPE FACTOR

Gauge Pressure (psi)	Total Head (cm)	Flow rate (cm^3/min)	Permeability (cm/sec)	Calculated F (cm)	Calculated F (in)
0.5	156.59	29	5.75E-04	5.30	2.08
1.5	226.87	50	5.75E-04	6.38	2.51
2.0	262.01	60	5.75E-04	6.64	2.61
2.5	297.15	72	5.75E-04	6.98	2.75
			Average F	6.32	2.49

INSITU CONSTANT HEAD TEST

Sample ID: 307

Location: at coastal

Sleeve diameter (in):	0.775	Depth of probe (in):	8
Sleeve length (in):	0.685	Length of probe (in):	25.75
Shape factor (in):	3.23	Elevation (in):	47.06

Gage Pressure Reading (psi)	Pressure Head (cm)	Elevation Head (cm)	Total Head (cm)	Flowmeter Reading (cm^3/min)	Permeability (cm/sec)
1.0	70.28	119.54	189.82	46	4.94E-04
1.5	105.42	119.54	224.96	63	5.68E-04
2.0	140.56	119.54	260.10	73	5.68E-04
2.5	175.70	119.54	295.24	86	5.89E-04
			Average k (cm/sec)		5.55E-04

LABORATORY CONSTANT HEAD TEST

Sample Length (cm):	13.6	Sample Volume (cm^3):	430.7
Sample Diameter (cm):	6.4	Sample Mass (g):	850.14
		Sample Density (g/cm^3):	1.97

Trial	1	2	3	4	5
Time (s)	180	120	180	120	120
Δ h (cm)	65.3	65.3	65.3	65.3	65.3
Q (cm^3)	31.68	21.05	31.53	21.00	20.99
k (cm/s)	1.16E-03	1.15E-03	1.15E-03	1.15E-03	1.15E-03
			Average k (cm/sec)		1.15E-03

BACK CALCULATED SHAPE FACTOR

Gauge Pressure (psi)	Total Head (cm)	Flow rate (cm^3/min)	Permeability (cm/sec)	Calculated F (cm)	Calculated F (in)
1.0	189.82	46	1.15E-03	3.52	1.39
1.5	224.96	63	1.15E-03	4.04	1.59
2.0	260.10	73	1.15E-03	4.05	1.59
2.5	295.24	86	1.15E-03	4.20	1.65
			Average F	3.95	1.56

INSITU CONSTANT HEAD TEST

Sample ID: 308

Location: by the softball field

Sleeve diameter (in):	0.775	Depth of probe (in):	14
Sleeve length (in):	0.685	Length of probe (in):	26.13
Shape factor (in):	3.23	Elevation (in):	53.44

Gage Pressure Reading (psi)	Pressure Head (cm)	Elevation Head (cm)	Total Head (cm)	Flowmeter Reading (cm^3/min)	Permeability (cm/sec)
1.0	70.28	135.73	206.01	22	2.21E-04
1.5	105.42	135.73	241.15	35	2.91E-04
2.5	175.70	135.73	311.43	56	3.65E-04
2.5	175.70	135.73	311.43	88	5.73E-04
3.0	210.84	135.73	346.57	83	4.89E-04
			Average k (cm/sec)		3.88E-04

LABORATORY CONSTANT HEAD TEST

Sample Length (cm):	7	Sample Volume (cm^3):	221.7
Sample Diameter (cm):	6.4	Sample Mass (g):	370.04
		Sample Density (g/cm^3):	1.67

Trial	1	2	3	4	5
Time (s)	90	90	90	95	90
Δ h (cm)	73.8	73.8	73.8	73.8	73.8
Q (cm^3)	21.96	20.85	20.53	23.59	20.43
k (cm/s)	7.31E-04	6.94E-04	6.83E-04	7.44E-04	6.80E-04
			Average k (cm/sec)		7.06E-04

BACK CALCULATED SHAPE FACTOR

Gauge Pressure (psi)	Total Head (cm)	Flow rate (cm^3/min)	Permeability (cm/sec)	Calculated F (cm)	Calculated F (in)
1.0	206.01	22	7.06E-04	2.57	1.01
1.5	241.15	35	7.06E-04	3.39	1.33
2.5	311.43	56	7.06E-04	4.24	1.67
2.5	311.43	88	7.06E-04	6.66	2.62
3.0	346.57	83	7.06E-04	5.68	2.24
			Average F	4.51	1.77

INSITU CONSTANT HEAD TEST

Sample ID: 309

Location: Maguire field

Sleeve diameter (in):	0.775	Depth of probe (in):	8
Sleeve length (in):	0.685	Length of probe (in):	25.75
Shape factor (in):	3.23	Elevation (in):	47.06

Gage Pressure Reading (psi)	Pressure Head (cm)	Elevation Head (cm)	Total Head (cm)	Flowmeter Reading (cm^3/min)	Permeability (cm/sec)
0.5	35.14	119.54	154.68	52	6.80E-04
1.0	70.28	119.54	189.82	80	8.52E-04
1.5	105.42	119.54	224.96	115	1.04E-03
2.0	140.56	119.54	260.10	147	1.14E-03
			Average k (cm/sec)		9.28E-04

LABORATORY CONSTANT HEAD TEST

Sample Length (cm):	6.7	Sample Volume (cm^3):	212.2
Sample Diameter (cm):	6.4	Sample Mass (g):	378.74
		Sample Density (g/cm^3):	1.78

Trial	1	2	3	4	5
Time (s)	180	180	180	180	180
Δ h (cm)	72.9	72.9	72.9	72.9	72.9
Q (cm^3)	24.22	24.17	24.10	24.10	23.96
k (cm/s)	3.90E-04	3.90E-04	3.89E-04	3.89E-04	3.86E-04
			Average k (cm/sec)		3.89E-04

BACK CALCULATED SHAPE FACTOR

Gauge Pressure (psi)	Total Head (cm)	Flow rate (cm^3/min)	Permeability (cm/sec)	Calculated F (cm)	Calculated F (in)
0.5	154.68	52	3.89E-04	14.36	5.65
1.0	189.82	80	3.89E-04	17.98	7.08
1.5	224.96	115	3.89E-04	21.90	8.62
2.0	260.10	147	3.89E-04	24.17	9.51
			Average F	19.60	7.72

INSITU CONSTANT HEAD TEST

Sample ID: 310

Location: by the softball field

Sleeve diameter (in):	0.775	Depth of probe (in):	9
Sleeve length (in):	0.685	Length of probe (in):	26.44
Shape factor (in):	3.23	Elevation (in):	48.75

Gage Pressure Reading (psi)	Pressure Head (cm)	Elevation Head (cm)	Total Head (cm)	Flowmeter Reading (cm^3/min)	Permeability (cm/sec)
0.5	35.14	123.83	158.97	43	5.51E-04
1.0	70.28	123.83	194.11	58	6.11E-04
1.5	105.42	123.83	229.25	81	7.14E-04
2.0	140.56	123.83	264.39	105	8.03E-04
			Average k (cm/sec)		6.70E-04

LABORATORY CONSTANT HEAD TEST

Sample Length (cm):	6.6	Sample Volume (cm^3):	209.0
Sample Diameter (cm):	6.4	Sample Mass (g):	352.15
		Sample Density (g/cm^3):	1.68

Trial	1	2	3	4	5
Time (s)	180	180	180	180	180
Δ h (cm)	73.0	73.0	73.0	73.0	73.0
Q (cm^3)	24.85	25.63	25.44	25.29	25.04
k (cm/s)	3.94E-04	4.06E-04	4.03E-04	4.01E-04	3.97E-04
			Average k (cm/sec)		4.00E-04

BACK CALCULATED SHAPE FACTOR

Gauge Pressure (psi)	Total Head (cm)	Flow rate (cm^3/min)	Permeability (cm/sec)	Calculated F (cm)	Calculated F (in)
0.5	158.97	43	4.00E-04	11.28	4.44
1.0	194.11	58	4.00E-04	12.52	4.93
1.5	229.25	81	4.00E-04	14.63	5.76
2.0	264.39	105	4.00E-04	16.47	6.48
			Average F	13.73	5.40

INSITU CONSTANT HEAD TEST

Sample ID: 311

Location: Maguire field

Sleeve diameter (in):	0.775	Depth of probe (in):	9
Sleeve length (in):	0.685	Length of probe (in):	27.44
Shape factor (in):	3.23	Elevation (in):	49.75

Gage Pressure Reading (psi)	Pressure Head (cm)	Elevation Head (cm)	Total Head (cm)	Flowmeter Reading (cm^3/min)	Permeability (cm/sec)
0.5	35.14	126.37	161.51	37	4.60E-04
1.0	70.28	126.37	196.65	54	5.56E-04
1.5	105.42	126.37	231.79	76	6.65E-04
			Average k (cm/sec)		5.60E-04

LABORATORY CONSTANT HEAD TEST

Sample Length (cm):	6.5	Sample Volume (cm^3):	205.8
Sample Diameter (cm):	6.4	Sample Mass (g):	349.14
		Sample Density (g/cm^3):	1.70

Trial	1	2	3	4	5
Time (s)	180	180	180	180	180
Δ h (cm)	72.7	72.7	72.7	72.7	72.7
Q (cm^3)	14.22	14.70	14.67	14.71	17.86
k (cm/s)	2.23E-04	2.31E-04	2.30E-04	2.31E-04	2.80E-04
			Average k (cm/sec)		2.39E-04

BACK CALCULATED SHAPE FACTOR

Gauge Pressure (psi)	Total Head (cm)	Flow rate (cm^3/min)	Permeability (cm/sec)	Calculated F (cm)	Calculated F (in)
0.5	161.51	37	2.39E-04	15.81	6.22
1.0	196.65	54	2.39E-04	19.09	7.51
1.5	231.79	76	2.39E-04	22.84	8.99
			Average F	19.25	7.58

INSITU CONSTANT HEAD TEST

Sample ID: 400

Location: East upper

Sleeve diameter (in):	0.775	Depth of probe (in):	8
Sleeve length (in):	0.685	Length of probe (in):	26.81
Shape factor (in):	3.23	Elevation (in):	48.13

Gage Pressure Reading (psi)	Pressure Head (cm)	Elevation Head (cm)	Total Head (cm)	Flowmeter Reading (cm^3/min)	Permeability (cm/sec)
0.5	35.14	122.24	157.38	171	2.20E-03
1.0	70.28	122.24	192.52	236	2.49E-03
1.5	105.42	122.24	227.66	276	2.46E-03
			Average k (cm/sec)		2.38E-03

LABORATORY CONSTANT HEAD TEST

Test performed by the FDOT

Average k (cm/sec) 6.14E-04

BACK CALCULATED SHAPE FACTOR

Gauge Pressure (psi)	Total Head (cm)	Flow rate (cm^3/min)	Permeability (cm/sec)	Calculated F (cm)	Calculated F (in)
0.5	157.38	171	6.14E-04	29.43	11.59
1.0	192.52	236	6.14E-04	33.32	13.12
1.5	227.66	276	6.14E-04	32.88	12.95
			Average F	31.88	12.55

INSITU CONSTANT HEAD TEST

Sample ID: 401

Location: East lower

Sleeve diameter (in):	0.775	Depth of probe (in):	16
Sleeve length (in):	0.685	Length of probe (in):	26.81
Shape factor (in):	3.23	Elevation (in):	56.13

Gage Pressure Reading (psi)	Pressure Head (cm)	Elevation Head (cm)	Total Head (cm)	Flowmeter Reading (cm^3/min)	Permeability (cm/sec)
4.5	316.26	142.56	458.82	12.6	5.58E-05
5.0	351.40	142.56	493.96	14.8	6.07E-05
			Average k (cm/sec)		5.82E-05

LABORATORY CONSTANT HEAD TEST

Test performed by the FDOT

Average k (cm/sec)	6.90E-06

BACK CALCULATED SHAPE FACTOR

Gauge Pressure (psi)	Total Head (cm)	Flow rate (cm^3/min)	Permeability (cm/sec)	Calculated F (cm)	Calculated F (in)
4.5	458.82	13	6.90E-06	66.33	26.12
5.0	493.96	15	6.90E-06	72.18	28.42
			Average F	69.25	27.27

INSITU CONSTANT HEAD TEST

Sample ID: 402

Location: East upper

Sleeve diameter (in):	0.775	Depth of probe (in):	8
Sleeve length (in):	0.685	Length of probe (in):	26.44
Shape factor (in):	3.23	Elevation (in):	47.75

Gage Pressure Reading (psi)	Pressure Head (cm)	Elevation Head (cm)	Total Head (cm)	Flowmeter Reading (cm^3/min)	Permeability (cm/sec)
0.5	35.14	121.29	156.43	122	1.59E-03
1.0	70.28	121.29	191.57	149	1.58E-03
1.5	105.42	121.29	226.71	187	1.68E-03
2.0	140.56	121.29	261.85	225	1.74E-03
2.5	175.70	121.29	296.99	262	1.79E-03
			Average k (cm/sec)		1.68E-03

LABORATORY CONSTANT HEAD TEST

Test performed by the FDOT

Average k (cm/sec) 6.14E-04

BACK CALCULATED SHAPE FACTOR

Gauge Pressure (psi)	Total Head (cm)	Flow rate (cm^3/min)	Permeability (cm/sec)	Calculated F (cm)	Calculated F (in)
0.5	156.43	122	6.14E-04	21.25	8.37
1.0	191.57	149	6.14E-04	21.14	8.32
1.5	226.71	187	6.14E-04	22.45	8.84
2.0	261.85	225	6.14E-04	23.31	9.18
2.5	296.99	262	6.14E-04	23.91	9.41
			Average F	22.41	8.82

INSITU CONSTANT HEAD TEST

Sample ID: 403

Location: East upper

Sleeve diameter (in):	0.775	Depth of probe (in):	8
Sleeve length (in):	0.685	Length of probe (in):	25.38
Shape factor (in):	3.23	Elevation (in):	46.69

Gage Pressure Reading (psi)	Pressure Head (cm)	Elevation Head (cm)	Total Head (cm)	Flowmeter Reading (cm^3/min)	Permeability (cm/sec)
0.5	35.14	118.59	153.73	103	1.37E-03
1.0	70.28	118.59	188.87	136	1.46E-03
1.5	105.42	118.59	224.01	172	1.55E-03
			Average k (cm/sec)		1.46E-03

LABORATORY CONSTANT HEAD TEST

Test performed by the FDOT

Average k (cm/sec) 6.14E-04

BACK CALCULATED SHAPE FACTOR

Gauge Pressure (psi)	Total Head (cm)	Flow rate (cm^3/min)	Permeability (cm/sec)	Calculated F (cm)	Calculated F (in)
0.5	153.73	103	6.14E-04	18.27	7.19
1.0	188.87	136	6.14E-04	19.48	7.67
1.5	224.01	172	6.14E-04	20.79	8.19
			Average F	19.51	7.68

INSITU CONSTANT HEAD TEST

Sample ID: 405

Location: East upper

Sleeve diameter (in):	0.775	Depth of probe (in):	8
Sleeve length (in):	0.685	Length of probe (in):	26.25
Shape factor (in):	3.23	Elevation (in):	47.56

Gage Pressure Reading (psi)	Pressure Head (cm)	Elevation Head (cm)	Total Head (cm)	Flowmeter Reading (cm^3/min)	Permeability (cm/sec)
1.0	70.28	120.81	191.09	124	1.32E-03
1.5	105.42	120.81	226.23	158	1.42E-03
2.0	140.56	120.81	261.37	193	1.50E-03
			Average k (cm/sec)		1.41E-03

LABORATORY CONSTANT HEAD TEST

Test performed by the FDOT

Average k (cm/sec) 6.14E-04

BACK CALCULATED SHAPE FACTOR

Gauge Pressure (psi)	Total Head (cm)	Flow rate (cm^3/min)	Permeability (cm/sec)	Calculated F (cm)	Calculated F (in)
1.0	191.09	124	6.14E-04	17.65	6.95
1.5	226.23	158	6.14E-04	18.94	7.46
2.0	261.37	193	6.14E-04	20.07	7.90
			Average F	18.89	7.44

INSITU CONSTANT HEAD TEST

Sample ID: 407

Location: East upper

Sleeve diameter (in):	0.775	Depth of probe (in):	8
Sleeve length (in):	0.685	Length of probe (in):	26.75
Shape factor (in):	3.23	Elevation (in):	48.06

Gage Pressure Reading (psi)	Pressure Head (cm)	Elevation Head (cm)	Total Head (cm)	Flowmeter Reading (cm^3/min)	Permeability (cm/sec)
1.0	70.28	122.08	192.36	133	1.41E-03
1.5	105.42	122.08	227.50	166	1.48E-03
2.0	140.56	122.08	262.64	198	1.53E-03
			Average k (cm/sec)		1.47E-03

LABORATORY CONSTANT HEAD TEST

Test performed by the FDOT

Average k (cm/sec) 6.14E-04

BACK CALCULATED SHAPE FACTOR

Gauge Pressure (psi)	Total Head (cm)	Flow rate (cm^3/min)	Permeability (cm/sec)	Calculated F (cm)	Calculated F (in)
1.0	192.36	133	6.14E-04	18.83	7.41
1.5	227.50	166	6.14E-04	19.81	7.80
2.0	262.64	198	6.14E-04	20.43	8.04
			Average F	19.69	7.75

INSITU CONSTANT HEAD TEST

Sample ID: 409

Location: East upper

Sleeve diameter (in):	0.775	Depth of probe (in):	8
Sleeve length (in):	0.685	Length of probe (in):	25.81
Shape factor (in):	3.23	Elevation (in):	47.13

Gage Pressure Reading (psi)	Pressure Head (cm)	Elevation Head (cm)	Total Head (cm)	Flowmeter Reading (cm^3/min)	Permeability (cm/sec)
1.0	70.28	119.70	189.98	127	1.35E-03
1.5	105.42	119.70	225.12	153	1.38E-03
2.0	140.56	119.70	260.26	181	1.41E-03
2.5	175.70	119.70	295.40	214	1.47E-03
			Average k (cm/sec)		1.40E-03

LABORATORY CONSTANT HEAD TEST

Test performed by the FDOT

Average k (cm/sec)	6.14E-04

BACK CALCULATED SHAPE FACTOR

Gauge Pressure (psi)	Total Head (cm)	Flow rate (cm^3/min)	Permeability (cm/sec)	Calculated F (cm)	Calculated F (in)
1.0	189.98	127	6.14E-04	18.10	7.12
1.5	225.12	153	6.14E-04	18.46	7.27
2.0	260.26	181	6.14E-04	18.84	7.42
2.5	295.40	214	6.14E-04	19.67	7.75
			Average F	18.77	7.39

INSITU CONSTANT HEAD TEST

Sample ID: 411

Location: West upper

Sleeve diameter (in):	0.775	Depth of probe (in):	8
Sleeve length (in):	0.685	Length of probe (in):	27.13
Shape factor (in):	3.23	Elevation (in):	48.44

Gage Pressure Reading (psi)	Pressure Head (cm)	Elevation Head (cm)	Total Head (cm)	Flowmeter Reading (cm^3/min)	Permeability (cm/sec)
5.0	351.40	123.03	474.43	13.5	5.79E-05
5.5	386.54	123.03	509.57	16.3	6.51E-05
6.0	421.68	123.03	544.71	16.8	6.24E-05
6.5	456.82	123.03	579.85	19.1	6.70E-05
			Average k (cm/sec)		6.31E-05

LABORATORY CONSTANT HEAD TEST

Test performed by the FDOT

Average k (cm/sec) 5.37E-07

BACK CALCULATED SHAPE FACTOR

Gauge Pressure (psi)	Total Head (cm)	Flow rate (cm^3/min)	Permeability (cm/sec)	Calculated F (cm)	Calculated F (in)
5.0	474.43	13.5	5.37E-07	885.11	348.47
5.5	509.57	16.3	5.37E-07	994.61	391.58
6.0	544.71	16.8	5.37E-07	954.38	375.74
6.5	579.85	19.1	5.37E-07	1024.47	403.33
			Average F	964.64	379.78

INSITU CONSTANT HEAD TEST

Sample ID: 413

Location: West upper

Sleeve diameter (in):	0.775	Depth of probe (in):	8
Sleeve length (in):	0.685	Length of probe (in):	25.25
Shape factor (in):	3.23	Elevation (in):	46.56

Gage Pressure Reading (psi)	Pressure Head (cm)	Elevation Head (cm)	Total Head (cm)	Flowmeter Reading (cm^3/min)	Permeability (cm/sec)
3.0	210.84	118.27	329.11	16.4	1.01E-04
3.5	245.98	118.27	364.25	21.3	1.19E-04
4.0	281.12	118.27	399.39	25.8	1.31E-04
4.5	316.26	118.27	434.53	36.2	1.69E-04
			Average k (cm/sec)		1.30E-04

LABORATORY CONSTANT HEAD TEST

Test performed by the FDOT

Average k (cm/sec)	5.37E-07

BACK CALCULATED SHAPE FACTOR

Gauge Pressure (psi)	Total Head (cm)	Flow rate (cm^3/min)	Permeability (cm/sec)	Calculated F (cm)	Calculated F (in)
3.0	329.11	16.4	5.37E-07	1549.43	610.01
3.5	364.25	21.3	5.37E-07	1815.76	714.87
4.0	399.39	25.8	5.37E-07	2002.59	788.42
4.5	434.53	36.2	5.37E-07	2586.63	1018.36
			Average F	1988.60	782.91

INSITU CONSTANT HEAD TEST

Sample ID: 500

Location: State road 27, soil not compacted to density

Sleeve diameter (in):	0.775	Depth of probe (in):	8
Sleeve length (in):	0.685	Length of probe (in):	25.94
Shape factor (in):	3.23	Elevation (in):	47.25

Gage Pressure Reading (psi)	Pressure Head (cm)	Elevation Head (cm)	Total Head (cm)	Flowmeter Reading (cm^3/min)	Permeability (cm/sec)
0.5	35.14	120.02	155.16	131	1.72E-03
1.0	70.28	120.02	190.30	181	1.93E-03
1.5	105.42	120.02	225.44	229	2.06E-03
2.0	140.56	120.02	260.58	280	2.18E-03
			Average k (cm/sec)		1.97E-03

LABORATORY CONSTANT HEAD TEST

Sample Length (cm):	13.8	Sample Volume (cm^3):	437.0
Sample Diameter (cm):	6.4	Sample Mass (g):	709.43
		Sample Density (g/cm^3):	1.62

Trial	1	2	3	4	5
Time (s)	120	120	120	120	120
Δ h (cm)	69.0	69.0	69.0	69.0	69.0
Q (cm^3)	127.28	128.10	129.74	130.84	131.18
k (cm/s)	6.70E-03	6.74E-03	6.83E-03	6.89E-03	6.90E-03
			Average k (cm/sec)		6.81E-03

BACK CALCULATED SHAPE FACTOR

Gauge Pressure (psi)	Total Head (cm)	Flow rate (cm^3/min)	Permeability (cm/sec)	Calculated F (cm)	Calculated F (in)
0.5	155.16	131	6.81E-03	2.07	0.82
1.0	190.30	181	6.81E-03	2.32	0.91
1.5	225.44	229	6.81E-03	2.49	0.98
2.0	260.58	280	6.81E-03	2.63	1.03
			Average F	2.38	0.94

INSITU CONSTANT HEAD TEST

Sample ID: 501

Location: State road 27

Sleeve diameter (in):	0.775	Depth of probe (in):	9
Sleeve length (in):	0.685	Length of probe (in):	26.75
Shape factor (in):	3.23	Elevation (in):	49.06

Gage Pressure Reading (psi)	Pressure Head (cm)	Elevation Head (cm)	Total Head (cm)	Flowmeter Reading (cm^3/min)	Permeability (cm/sec)
0.5	35.14	124.62	159.76	25.6	3.26E-04
1.0	70.28	124.62	194.90	46.4	4.84E-04
1.5	105.42	124.62	230.04	63.5	5.61E-04
2.0	140.56	124.62	265.18	116	8.88E-04
2.5	175.70	124.62	300.32	141	9.51E-04
			Average k (cm/sec)		6.42E-04

LABORATORY CONSTANT HEAD TEST

Sample Length (cm):	13.8	Sample Volume (cm^3):	437.0
Sample Diameter (cm):	6.4	Sample Mass (g):	709.43
		Sample Density (g/cm^3):	1.62

Trial	1	2	3	4	5
Time (s)	120	120	120	120	120
Δ h (cm)	69.0	69.0	69.0	69.0	69.0
Q (cm^3)	127.28	128.10	129.74	130.84	131.18
k (cm/s)	6.70E-03	6.74E-03	6.83E-03	6.89E-03	6.90E-03
			Average k (cm/sec)		6.81E-03

BACK CALCULATED SHAPE FACTOR

Gauge Pressure (psi)	Total Head (cm)	Flow rate (cm^3/min)	Permeability (cm/sec)	Calculated F (cm)	Calculated F (in)
0.5	159.76	26	6.81E-03	0.39	0.15
1.0	194.90	46	6.81E-03	0.58	0.23
1.5	230.04	64	6.81E-03	0.68	0.27
2.0	265.18	116	6.81E-03	1.07	0.42
2.5	300.32	141	6.81E-03	1.15	0.45
			Average F	0.77	0.30

INSITU CONSTANT HEAD TEST

Sample ID: 502

Location: State road 27

Sleeve diameter (in):	0.775	Depth of probe (in):	9
Sleeve length (in):	0.685	Length of probe (in):	27.38
Shape factor (in):	3.23	Elevation (in):	49.69

Gage Pressure Reading (psi)	Pressure Head (cm)	Elevation Head (cm)	Total Head (cm)	Flowmeter Reading (cm^3/min)	Permeability (cm/sec)
0.5	35.14	126.21	161.35	45.4	5.71E-04
1.0	70.28	126.21	196.49	66.3	6.85E-04
1.5	105.42	126.21	231.63	93.9	8.23E-04
2.0	140.56	126.21	266.77	120	9.14E-04
2.5	175.70	126.21	301.91	149	1.00E-03
			Average k (cm/sec)		7.99E-04

LABORATORY CONSTANT HEAD TEST

Sample Length (cm):	13.8	Sample Volume (cm^3):	437.0
Sample Diameter (cm):	6.4	Sample Mass (g):	709.43
		Sample Density (g/cm^3):	1.62

Trial	1	2	3	4	5
Time (s)	120	120	120	120	120
Δ h (cm)	69.0	69.0	69.0	69.0	69.0
Q (cm^3)	127.28	128.10	129.74	130.84	131.18
k (cm/s)	6.70E-03	6.74E-03	6.83E-03	6.89E-03	6.90E-03
			Average k (cm/sec)		6.81E-03

BACK CALCULATED SHAPE FACTOR

Gauge Pressure (psi)	Total Head (cm)	Flow rate (cm^3/min)	Permeability (cm/sec)	Calculated F (cm)	Calculated F (in)
0.5	161.35	45	6.81E-03	0.69	0.27
1.0	196.49	66	6.81E-03	0.83	0.32
1.5	231.63	94	6.81E-03	0.99	0.39
2.0	266.77	120	6.81E-03	1.10	0.43
2.5	301.91	149	6.81E-03	1.21	0.48
			Average F	0.96	0.38

INSITU CONSTANT HEAD TEST

Sample ID: 503

Location: State road 26

Sleeve diameter (in):	0.775	Depth of probe (in):	8
Sleeve length (in):	0.685	Length of probe (in):	27.00
Shape factor (in):	3.23	Elevation (in):	48.31

Gage Pressure Reading (psi)	Pressure Head (cm)	Elevation Head (cm)	Total Head (cm)	Flowmeter Reading (cm^3/min)	Permeability (cm/sec)
2.0	140.56	122.72	263.28	13.6	1.05E-04
2.5	175.70	122.72	298.42	16.1	1.10E-04
			Average k (cm/sec)		1.07E-04

LABORATORY CONSTANT HEAD TEST

Sample Length (cm):	6.3	Sample Volume (cm^3):	199.5
Sample Diameter (cm):	6.4	Sample Mass (g):	341.99
		Sample Density (g/cm^3):	1.71

Trial	1	2	3	4	5
Time (s)	120	120	120	120	120
Δ h (cm)	74.5	74.5	74.5	74.5	74.5
Q (cm^3)	59.21	59.14	58.70	58.73	58.69
k (cm/s)	1.32E-03	1.32E-03	1.31E-03	1.31E-03	1.31E-03
			Average k (cm/sec)		1.31E-03

BACK CALCULATED SHAPE FACTOR

Gauge Pressure (psi)	Total Head (cm)	Flow rate (cm^3/min)	Permeability (cm/sec)	Calculated F (cm)	Calculated F (in)
2.0	263.28	14	1.31E-03	0.66	0.26
2.5	298.42	16	1.31E-03	0.69	0.27
			Average F	0.67	0.26

INSITU CONSTANT HEAD TEST

Sample ID: 504

Location: State road 26

Sleeve diameter (in):	0.775	Depth of probe (in):	8
Sleeve length (in):	0.685	Length of probe (in):	26.13
Shape factor (in):	3.23	Elevation (in):	47.44

Gage Pressure Reading (psi)	Pressure Head (cm)	Elevation Head (cm)	Total Head (cm)	Flowmeter Reading (cm^3/min)	Permeability (cm/sec)
4.5	316.26	120.49	436.75	14.1	6.56E-05
5.0	351.40	120.49	471.89	16.0	6.87E-05
5.6	393.57	120.49	514.06	17.3	6.85E-05
6.0	421.68	120.49	542.17	18.7	7.00E-05
			Average k (cm/sec)		6.82E-05

LABORATORY CONSTANT HEAD TEST

Sample Length (cm):	6.3	Sample Volume (cm^3):	199.5
Sample Diameter (cm):	6.4	Sample Mass (g):	341.99
		Sample Density (g/cm^3):	1.71

Trial	1	2	3	4	5
Time (s)	120	120	120	120	120
Δ h (cm)	74.5	74.5	74.5	74.5	74.5
Q (cm^3)	59.21	59.14	58.70	58.73	58.69
k (cm/s)	1.32E-03	1.32E-03	1.31E-03	1.31E-03	1.31E-03
			Average k (cm/sec)		1.31E-03

BACK CALCULATED SHAPE FACTOR

Gauge Pressure (psi)	Total Head (cm)	Flow rate (cm^3/min)	Permeability (cm/sec)	Calculated F (cm)	Calculated F (in)
4.5	436.75	14	1.31E-03	0.41	0.16
5.0	471.89	16	1.31E-03	0.43	0.17
5.6	514.06	17	1.31E-03	0.43	0.17
6.0	542.17	19	1.31E-03	0.44	0.17
			Average F	0.43	0.17

APPENDIX B
FALLING HEAD PERMEABILITY DATA

Appendix B contains the data for the insitu and laboratory falling head testing. The back calculation of the shape factor is also included on the data sheets.

INSITU FALLING HEAD TEST

Sample ID: 301

Location: at coastal

Sleeve diameter (in):	0.775	Depth of probe (in):	8
Sleeve length (in):	0.685	Length of probe (in):	25.63
Shape factor (in):	3.23	H_1 (in):	80.44
Tube diameter (in):	0.25	H_2 (in):	68.44

Trial	1	2	3	4	5
Time (sec)	75.0	69.2	70.0	70.2	72.0
Permeability (cm/sec)	8.31E-05	9.01E-05	8.91E-05	8.88E-05	8.66E-05
			Average k (cm/sec)		8.75E-05

LABORATORY FALLING HEAD TEST

Sample Length (cm):	13.6	Standpipe Area (cm^2):	1.65
Sample Diameter (cm):	6.4	Sample Mass (g):	760.34
Standpipe Dia. (cm):	1.45	Sample Density (g/cm^3):	1.77

Trial	1	2	3	4	5
h_i (cm)	64.8	64.8	64.8	64.8	64.8
h_f (cm)	50.8	50.8	50.8	50.8	50.8
Time (s)	143.0	144.0	144.7	145.0	145.7
k (cm/s)	1.21E-03	1.20E-03	1.19E-03	1.19E-03	1.18E-03
			Average k (cm/sec)		1.19E-0

BACK CALCULATED SHAPE FACTOR

Trial	H_1 (in)	H_2 (in)	Time (sec)	Perm. (cm/sec)	Calculated F (cm)	Calculated F (in)
1	80.44	68.44	75.0	1.19E-03	0.57	0.23
2	80.44	68.44	69.2	1.19E-03	0.62	0.24
3	80.44	68.44	70.0	1.19E-03	0.61	0.24
4	80.44	68.44	70.2	1.19E-03	0.61	0.24
5	80.44	68.44	72.0	1.19E-03	0.60	0.23
				Average F	0.60	0.24

INSITU FALLING HEAD TEST

Sample ID: 302

Location: at coastal

Sleeve diameter (in):	0.775	Depth of probe (in):	8
Sleeve length (in):	0.685	Length of probe (in):	26.00
Shape factor (in):	3.23	H_1 (in):	80.81
Tube diameter (in):	0.25	H_2 (in):	44.81

Trial	1	2	3	4	5
Time (sec)	46.6	47.2	46.2	47.2	49.2
Permeability (cm/sec)	4.88E-04	4.82E-04	4.92E-04	4.82E-04	4.62E-04
			Average k (cm/sec)		4.81E-04

LABORATORY FALLING HEAD TEST

Sample Length (cm):	13.6	Standpipe Area (cm^2):	1.65
Sample Diameter (cm):	6.4	Sample Mass (g):	830.46
Standpipe Dia. (cm):	1.45	Sample Density (g/cm^3):	1.93

Trial	1	2	3	4	5
h_i (cm)	71.9	71.9	71.9	71.9	71.9
h_f (cm)	57.0	57.0	57.0	57.0	57.0
Time (s)	115.6	115.2	115.2	115.3	115.3
k (cm/s)	1.42E-03	1.43E-03	1.43E-03	1.43E-03	1.43E-03
			Average k (cm/sec)		1.43E-0

BACK CALCULATED SHAPE FACTOR

Trial	H_1 (in)	H_2 (in)	Time (sec)	Perm. (cm/sec)	Calculated F (cm)	Calculated F (in)
1	80.81	44.81	46.6	1.43E-03	2.81	1.11
2	80.81	44.81	47.2	1.43E-03	2.77	1.09
3	80.81	44.81	46.2	1.43E-03	2.83	1.12
4	80.81	44.81	47.2	1.43E-03	2.77	1.09
5	80.81	44.81	49.2	1.43E-03	2.66	1.05
				Average F	2.77	1.09

INSITU FALLING HEAD TEST

Sample ID: 303

Location: at coastal

Sleeve diameter (in):	0.775	Depth of probe (in):	8
Sleeve length (in):	0.685	Length of probe (in):	27.00
Shape factor (in):	3.23	H_1 (in):	81.81
Tube diameter (in):	0.25	H_2 (in):	45.81

Trial	1	2	3	4	5
Time (sec)	9.2	8.8	8.8	8.6	8.8
Permeability (cm/sec)	2.43E-03	2.54E-03	2.54E-03	2.60E-03	2.54E-03
			Average k (cm/sec)		2.53E-03

LABORATORY FALLING HEAD TEST

Sample Length (cm):	13.8	Standpipe Area (cm^2):	1.65
Sample Diameter (cm):	6.4	Sample Mass (g):	734.88
Standpipe Dia. (cm):	1.45	Sample Density (g/cm^3):	1.68

Trial	1	2	3	4	5
h_i (cm)	65.0	65.0	65.0	65.0	65.0
h_f (cm)	51.0	51.0	51.0	51.0	51.0
Time (s)	164.7	165.2	165.9	166.2	167.2
k (cm/s)	1.06E-03	1.06E-03	1.05E-03	1.05E-03	1.04E-03
			Average k (cm/sec)		1.05E-0

BACK CALCULATED SHAPE FACTOR

Trial	H_1 (in)	H_2 (in)	Time (sec)	Perm. (cm/sec)	Calculated F (cm)	Calculated F (in)
1	81.81	45.81	9.2	1.05E-03	18.99	7.48
2	81.81	45.81	8.8	1.05E-03	19.85	7.81
3	81.81	45.81	8.8	1.05E-03	19.85	7.81
4	81.81	45.81	8.6	1.05E-03	20.31	8.00
5	81.81	45.81	8.8	1.05E-03	19.85	7.81
				Average F	19.77	7.78

INSITU FALLING HEAD TEST

Sample ID: 304

Location: at coastal

Sleeve diameter (in):	0.775	Depth of probe (in):	8
Sleeve length (in):	0.685	Length of probe (in):	26.25
Shape factor (in):	3.23	H_1 (in):	81.06
Tube diameter (in):	0.25	H_2 (in):	69.06

Trial	1	2	3	4	5
Time (sec)	18.6	18.8	19.2	19.6	19.8
Permeability (cm/sec)	3.32E-04	3.29E-04	3.22E-04	3.15E-04	3.12E-04
			Average k (cm/sec)		3.22E-04

LABORATORY FALLING HEAD TEST

Sample Length (cm):	13.3	Standpipe Area (cm^2):	1.65
Sample Diameter (cm):	6.4	Sample Mass (g):	820.12
Standpipe Dia. (cm):	1.45	Sample Density (g/cm^3):	1.95

Trial	1	2	3	4	5
h_i (cm)	65.0	65.0	65.0	65.0	65.0
h_f (cm)	50.8	50.8	50.8	50.8	50.8
Time (s)	100.0	100.0	100.0	101.0	100.0
k (cm/s)	1.71E-03	1.71E-03	1.71E-03	1.69E-03	1.71E-03
			Average k (cm/sec)		1.70E-0

BACK CALCULATED SHAPE FACTOR

Trial	H_1 (in)	H_2 (in)	Time (sec)	Perm. (cm/sec)	Calculated F (cm)	Calculated F (in)
1	81.06	69.06	18.6	1.70E-03	1.60	0.63
2	81.06	69.06	18.8	1.70E-03	1.58	0.62
3	81.06	69.06	19.2	1.70E-03	1.55	0.61
4	81.06	69.06	19.6	1.70E-03	1.52	0.60
5	81.06	69.06	19.8	1.70E-03	1.50	0.59
				Average F	1.55	0.61

INSITU FALLING HEAD TEST

Sample ID: 305

Location: at coastal

Sleeve diameter (in):	0.775	Depth of probe (in):	8
Sleeve length (in):	0.685	Length of probe (in):	25.25
Shape factor (in):	3.23	H_1 (in):	80.06
Tube diameter (in):	0.25	H_2 (in):	68.06

Trial	1	2	3	4	5
Time (sec)	22.8	23.2	24.0	25.0	25.0
Permeability (cm/sec)	2.75E-04	2.70E-04	2.61E-04	2.51E-04	2.51E-04
			Average k (cm/sec)		2.61E-04

LABORATORY FALLING HEAD TEST

Sample Length (cm):	13.4	Standpipe Area (cm^2):	1.65
Sample Diameter (cm):	6.4	Sample Mass (g):	774.14
Standpipe Dia. (cm):	1.45	Sample Density (g/cm^3):	1.82

Trial	1	2	3	4	5
h_i (cm)	57.9	57.9	50.8	50.8	50.8
h_f (cm)	43.6	43.6	43.6	43.6	43.6
Time (s)	148.5	150.0	78.6	80.2	81.0
k (cm/s)	1.33E-03	1.32E-03	1.36E-03	1.33E-03	1.32E-03
			Average k (cm/sec)		1.33E-0

BACK CALCULATED SHAPE FACTOR

Trial	H_1 (in)	H_2 (in)	Time (sec)	Perm. (cm/sec)	Calculated F (cm)	Calculated F (in)
1	80.06	68.06	22.8	1.33E-03	1.69	0.67
2	80.06	68.06	23.2	1.33E-03	1.66	0.66
3	80.06	68.06	24.0	1.33E-03	1.61	0.63
4	80.06	68.06	25.0	1.33E-03	1.54	0.61
5	80.06	68.06	25.0	1.33E-03	1.54	0.61
				Average F	1.61	0.63

INSITU FALLING HEAD TEST

Sample ID: 306

Location: at coastal

Sleeve diameter (in):	0.775	Depth of probe (in):	9
Sleeve length (in):	0.685	Length of probe (in):	25.50
Shape factor (in):	3.23	H_1 (in):	81.31
Tube diameter (in):	0.25	H_2 (in):	69.31

Trial	1	2	3	4	5
Time (sec)	13.6	14.0	14.0	14.0	14.2
Permeability (cm/sec)	4.53E-04	4.40E-04	4.40E-04	4.40E-04	4.34E-04
			Average k (cm/sec)		4.41E-04

LABORATORY FALLING HEAD TEST

Sample Length (cm):	13.3	Standpipe Area (cm^2):	1.65
Sample Diameter (cm):	6.4	Sample Mass (g):	817.38
Standpipe Dia. (cm):	1.45	Sample Density (g/cm^3):	1.94

Trial	1	2	3	4	5
h_i (cm)	65.1	65.1	65.1	65.1	65.1
h_f (cm)	58.0	58.0	58.0	58.0	58.0
Time (s)	132.5	132.4	132.7	133.1	133.1
k (cm/s)	6.04E-04	6.04E-04	6.03E-04	6.01E-04	6.01E-04
			Average k (cm/sec)		6.03E-0

BACK CALCULATED SHAPE FACTOR

Trial	H_1 (in)	H_2 (in)	Time (sec)	Perm. (cm/sec)	Calculated F (cm)	Calculated F (in)
1	81.31	69.31	13.6	6.03E-04	6.17	2.43
2	81.31	69.31	14.0	6.03E-04	5.99	2.36
3	81.31	69.31	14.0	6.03E-04	5.99	2.36
4	81.31	69.31	14.0	6.03E-04	5.99	2.36
5	81.31	69.31	14.2	6.03E-04	5.91	2.33
				Average F	6.01	2.37

INSITU FALLING HEAD TEST

Sample ID: 307

Location: at coastal

Sleeve diameter (in):	0.775	Depth of probe (in):	8
Sleeve length (in):	0.685	Length of probe (in):	25.75
Shape factor (in):	3.23	H_1 (in):	80.56
Tube diameter (in):	0.25	H_2 (in):	44.56

Trial	1	2	3	4	5
Time (sec)	67.8	68.8	70.8	69.4	69.0
Permeability (cm/sec)	3.37E-04	3.32E-04	3.23E-04	3.29E-04	3.31E-04
			Average k (cm/sec)		3.30E-04

LABORATORY FALLING HEAD TEST

Sample Length (cm):	13.6	Standpipe Area (cm^2):	1.65
Sample Diameter (cm):	6.4	Sample Mass (g):	850.14
Standpipe Dia. (cm):	1.45	Sample Density (g/cm^3):	1.97

Trial	1	2	3	4	5
h_i (cm)	65.0	65.0	65.0	65.0	65.0
h_f (cm)	50.8	50.8	50.8	50.8	50.8
Time (s)	156.7	157.0	157.7	158.1	158.2
k (cm/s)	1.11E-03	1.11E-03	1.11E-03	1.10E-03	1.10E-03
			Average k (cm/sec)		1.11E-0

BACK CALCULATED SHAPE FACTOR

Trial	H_1 (in)	H_2 (in)	Time (sec)	Perm. (cm/sec)	Calculated F (cm)	Calculated F (in)
1	80.56	44.56	67.8	1.11E-03	2.50	0.98
2	80.56	44.56	68.8	1.11E-03	2.46	0.97
3	80.56	44.56	70.8	1.11E-03	2.39	0.94
4	80.56	44.56	69.4	1.11E-03	2.44	0.96
5	80.56	44.56	69.0	1.11E-03	2.45	0.97
				Average F	2.45	0.96

INSITU FALLING HEAD TEST

Sample ID: 308

Location: by the softball field

Sleeve diameter (in):	0.775	Depth of probe (in):	14
Sleeve length (in):	0.685	Length of probe (in):	26.13
Shape factor (in):	3.23	H_1 (in):	86.94
Tube diameter (in):	0.25	H_2 (in):	50.94

Trial	1	2	3	4	5
Time (sec)	51.6	47.8	46.2	46.2	46.0
Permeability (cm/sec)	4.00E-04	4.32E-04	4.46E-04	4.46E-04	4.48E-04
			Average k (cm/sec)		4.35E-04

LABORATORY FALLING HEAD TEST

Sample Length (cm):	13.8	Standpipe Area (cm^2):	1.65
Sample Diameter (cm):	6.4	Sample Mass (g):	809.65
Standpipe Dia. (cm):	1.45	Sample Density (g/cm^3):	1.85

Trial	1	2	3	4	5
h_i (cm)	64.8	64.8	64.8	64.8	64.8
h_f (cm)	50.7	50.7	50.7	50.7	50.7
Time (s)	60.2	60.2	60.3	60.3	60.7
k (cm/s)	2.93E-03	2.93E-03	2.92E-03	2.92E-03	2.91E-03
			Average k (cm/sec)		2.92E-0

BACK CALCULATED SHAPE FACTOR

Trial	H_1 (in)	H_2 (in)	Time (sec)	Perm. (cm/sec)	Calculated F (cm)	Calculated F (in)
1	86.94	50.94	51.6	2.92E-03	1.12	0.44
2	86.94	50.94	47.8	2.92E-03	1.21	0.48
3	86.94	50.94	46.2	2.92E-03	1.25	0.49
4	86.94	50.94	46.2	2.92E-03	1.25	0.49
5	86.94	50.94	46.0	2.92E-03	1.26	0.50
				Average F	1.22	0.48

INSITU FALLING HEAD TEST

Sample ID: 309

Location: Maguire field

Sleeve diameter (in):	0.775	Depth of probe (in):	8
Sleeve length (in):	0.685	Length of probe (in):	25.75
Shape factor (in):	3.23	H_1 (in):	80.56
Tube diameter (in):	0.25	H_2 (in):	44.56

Trial	1	2	3	4	5
Time (sec)	29.2	27.8	28.2	27.6	29.2
Permeability (cm/sec)	7.82E-04	8.22E-04	8.10E-04	8.28E-04	7.82E-04
			Average k (cm/sec)		8.05E-04

LABORATORY FALLING HEAD TEST

Sample Length (cm):	13.6	Standpipe Area (cm^2):	1.65
Sample Diameter (cm):	6.4	Sample Mass (g):	776.05
Standpipe Dia. (cm):	1.45	Sample Density (g/cm^3):	1.80

Trial	1	2	3	4	5
h_i (cm)	65.0	65.0	65.0	65.0	65.0
h_f (cm)	50.9	50.9	50.9	50.9	50.9
Time (s)	38.1	38.0	38.2	38.0	38.2
k (cm/s)	4.55E-03	4.56E-03	4.53E-03	4.56E-03	4.53E-03
			Average k (cm/sec)		4.55E-0

BACK CALCULATED SHAPE FACTOR

Trial	H_1 (in)	H_2 (in)	Time (sec)	Perm. (cm/sec)	Calculated F (cm)	Calculated F (in)
1	80.56	44.56	29.2	4.55E-03	1.41	0.56
2	80.56	44.56	27.8	4.55E-03	1.48	0.58
3	80.56	44.56	28.2	4.55E-03	1.46	0.58
4	80.56	44.56	27.6	4.55E-03	1.49	0.59
5	80.56	44.56	29.2	4.55E-03	1.41	0.56
				Average F	1.45	0.57

INSITU FALLING HEAD TEST

Sample ID: 310

Location: by the softball field

Sleeve diameter (in):	0.775	Depth of probe (in):	9
Sleeve length (in):	0.685	Length of probe (in):	26.44
Shape factor (in):	3.23	H_1 (in):	82.25
Tube diameter (in):	0.25	H_2 (in):	46.25

Trial	1	2	3	4	5
Time (sec)	33.6	33.2	32.6	33.2	33.2
Permeability (cm/sec)	6.61E-04	6.69E-04	6.81E-04	6.69E-04	6.69E-04
			Average k (cm/sec)		6.70E-04

LABORATORY FALLING HEAD TEST

Sample Length (cm):	13.8	Standpipe Area (cm^2):	1.65
Sample Diameter (cm):	6.4	Sample Mass (g):	847.95
Standpipe Dia. (cm):	1.45	Sample Density (g/cm^3):	1.94

Trial	1	2	3	4	5
h_i (cm)	52.5	52.5	52.5	52.5	52.5
h_f (cm)	44.0	44.0	44.0	44.0	44.0
Time (s)	72.9	73.0	73.0	73.1	73.5
k (cm/s)	1.74E-03	1.74E-03	1.74E-03	1.74E-03	1.73E-03
			Average k (cm/sec)		1.74E-0

BACK CALCULATED SHAPE FACTOR

Trial	H_1 (in)	H_2 (in)	Time (sec)	Perm. (cm/sec)	Calculated F (cm)	Calculated F (in)
1	82.25	46.25	33.6	1.74E-03	3.12	1.23
2	82.25	46.25	33.2	1.74E-03	3.16	1.24
3	82.25	46.25	32.6	1.74E-03	3.22	1.27
4	82.25	46.25	33.2	1.74E-03	3.16	1.24
5	82.25	46.25	33.2	1.74E-03	3.16	1.24
				Average F	3.17	1.25

INSITU FALLING HEAD TEST

Sample ID: 311

Location: Maguire field

Sleeve diameter (in):	0.775	Depth of probe (in):	9
Sleeve length (in):	0.685	Length of probe (in):	27.44
Shape factor (in):	3.23	H_1 (in):	83.25
Tube diameter (in):	0.25	H_2 (in):	47.25

Trial	1	2	3	4	5
Time (sec)	27.4	27.2	27.0	26.8	26.2
Permeability (cm/sec)	7.98E-04	8.03E-04	8.09E-04	8.15E-04	8.34E-04
			Average k (cm/sec)		8.12E-04

LABORATORY FALLING HEAD TEST

Sample Length (cm):	14.8	Standpipe Area (cm^2):	1.65
Sample Diameter (cm):	6.4	Sample Mass (g):	765.45
Standpipe Dia. (cm):	1.45	Sample Density (g/cm^3):	1.63

Trial	1	2	3	4	5
h_i (cm)	48.5	48.5	48.5	48.5	48.5
h_f (cm)	43.7	43.7	43.7	43.7	43.7
Time (s)	24.0	24.0	24.0	24.0	24.0
k (cm/s)	3.35E-03	3.35E-03	3.35E-03	3.35E-03	3.35E-03
			Average k(cm/sec)		3.35E-0

BACK CALCULATED SHAPE FACTOR

Trial	H_1 (in)	H_2 (in)	Time (sec)	Perm. (cm/sec)	Calculated F (cm)	Calculated F (in)
1	83.25	47.25	27.4	3.35E-03	1.96	0.77
2	83.25	47.25	27.2	3.35E-03	1.97	0.78
3	83.25	47.25	27.0	3.35E-03	1.98	0.78
4	83.25	47.25	26.8	3.35E-03	2.00	0.79
5	83.25	47.25	26.2	3.35E-03	2.05	0.81
				Average F	1.99	0.78

INSITU FALLING HEAD TEST

Sample ID: 402

Location: East upper

Sleeve diameter (in):	0.775	Depth of probe (in):	8
Sleeve length (in):	0.685	Length of probe (in):	26.44
Shape factor (in):	3.23	H_1 (in):	81.25
Tube diameter (in):	0.25	H_2 (in):	45.25

Trial	1	2	3	4	5
Time (sec)	17.8	17.2	17.0	16.6	17.2
Permeability (cm/sec)	1.27E-03	1.31E-03	1.33E-03	1.36E-03	1.31E-03
			Average k (cm/sec)		1.32E-03

LABORATORY PERMEABILITY TEST

Test performed by the FDOT

Average k (cm/sec) 6.14E-0

BACK CALCULATED SHAPE FACTOR

Trial	H_1 (in)	H_2 (in)	Time (sec)	Perm. (cm/sec)	Calculated F (cm)	Calculated F (in)
1	81.25	45.25	17.8	6.14E-04	16.97	6.68
2	81.25	45.25	17.2	6.14E-04	17.56	6.91
3	81.25	45.25	17.0	6.14E-04	17.77	6.99
4	81.25	45.25	16.6	6.14E-04	18.19	7.16
5	81.25	45.25	17.2	6.14E-04	17.56	6.91
				Average F	17.61	6.93

INSITU FALLING HEAD TEST

Sample ID: 404

Location: East lower

Sleeve diameter (in):	0.775	Depth of probe (in):	16
Sleeve length (in):	0.685	Length of probe (in):	25.38
Shape factor (in):	3.23	H_1 (in):	88.19
Tube diameter (in):	0.25	H_2 (in):	82.19

Trial	1	2	3	4	5
Time (sec)	270.3	277.3	266.9	246.6	230.9
Permeability (cm/sec)	1.01E-05	9.80E-06	1.02E-05	1.10E-05	1.18E-05
			Average k (cm/sec)		1.06E-05

LABORATORY PERMEABILITY TEST

Test performed by the FDOT

Average k (cm/sec) 6.90E-0

BACK CALCULATED SHAPE FACTOR

Trial	H_1 (in)	H_2 (in)	Time (sec)	Perm. (cm/sec)	Calculated F (cm)	Calculated F (in)
1	88.19	82.19	270.3	6.90E-06	11.96	4.71
2	88.19	82.19	277.3	6.90E-06	11.66	4.59
3	88.19	82.19	266.9	6.90E-06	12.12	4.77
4	88.19	82.19	246.6	6.90E-06	13.11	5.16
5	88.19	82.19	230.9	6.90E-06	14.01	5.51
				Average F	12.57	4.95

INSITU FALLING HEAD TEST

Sample ID: 405

Location: East upper

Sleeve diameter (in):	0.775	Depth of probe (in):	8
Sleeve length (in):	0.685	Length of probe (in):	26.25
Shape factor (in):	3.23	H_1 (in):	81.06
Tube diameter (in):	0.25	H_2 (in):	45.06

Trial	1	2	3	4	5
Time (sec)	19.1	19.3	17.9	18.9	18.4
Permeability (cm/sec)	1.19E-03	1.17E-03	1.27E-03	1.20E-03	1.23E-03
			Average k (cm/sec)		1.21E-03

LABORATORY PERMEABILITY TEST

Test performed by the FDOT

Average k (cm/sec) 6.14E-0

BACK CALCULATED SHAPE FACTOR

Trial	H_1 (in)	H_2 (in)	Time (sec)	Perm. (cm/sec)	Calculated F (cm)	Calculated F (in)
1	81.06	45.06	19.1	6.14E-04	15.86	6.25
2	81.06	45.06	19.3	6.14E-04	15.70	6.18
3	81.06	45.06	17.9	6.14E-04	16.93	6.66
4	81.06	45.06	18.9	6.14E-04	16.03	6.31
5	81.06	45.06	18.4	6.14E-04	16.47	6.48
				Average F	16.20	6.38

INSITU FALLING HEAD TEST

Sample ID: 406

Location: East lower

Sleeve diameter (in):	0.775	Depth of probe (in):	16
Sleeve length (in):	0.685	Length of probe (in):	25.25
Shape factor (in):	3.23	H_1 (in):	88.06
Tube diameter (in):	0.25	H_2 (in):	82.06

Trial	1	2	3	4	5
Time (sec)	273.9	254.2	261.2	263.0	257.3
Permeability (cm/sec)	9.94E-06	1.07E-05	1.04E-05	1.04E-05	1.06E-05
			Average k (cm/sec)		1.04E-05

LABORATORY PERMEABILITY TEST

Test performed by the FDOT

Average k (cm/sec) 6.90E-0

BACK CALCULATED SHAPE FACTOR

Trial	H_1 (in)	H_2 (in)	Time (sec)	Perm. (cm/sec)	Calculated F (cm)	Calculated F (in)
1	88.06	82.06	273.9	6.90E-06	11.82	4.66
2	88.06	82.06	254.2	6.90E-06	12.74	5.02
3	88.06	82.06	261.2	6.90E-06	12.40	4.88
4	88.06	82.06	263.0	6.90E-06	12.31	4.85
5	88.06	82.06	257.3	6.90E-06	12.59	4.96
				Average F	12.37	4.87

INSITU FALLING HEAD TEST

Sample ID: 408

Location: East lower

Sleeve diameter (in):	0.775	Depth of probe (in):	16
Sleeve length (in):	0.685	Length of probe (in):	26.75
Shape factor (in):	3.23	H_1 (in):	89.56
Tube diameter (in):	0.25	H_2 (in):	83.56

Trial	1	2	3	4	5
Time (sec)	283.8	248.7	252.3	243.0	241.3
Permeability (cm/sec)	9.43E-06	1.08E-05	1.06E-05	1.10E-05	1.11E-05
			Average k (cm/sec)		1.06E-05

LABORATORY PERMEABILITY TEST

Test performed by the FDOT

Average k (cm/sec) 6.90E-0

BACK CALCULATED SHAPE FACTOR

Trial	H_1 (in)	H_2 (in)	Time (sec)	Perm. (cm/sec)	Calculated F (cm)	Calculated F (in)
1	89.56	83.56	283.8	6.90E-06	11.21	4.42
2	89.56	83.56	248.7	6.90E-06	12.80	5.04
3	89.56	83.56	252.3	6.90E-06	12.61	4.97
4	89.56	83.56	243.0	6.90E-06	13.10	5.16
5	89.56	83.56	241.3	6.90E-06	13.19	5.19
				Average F	12.58	4.95

INSITU FALLING HEAD TEST

Sample ID: 410

Location: East lower

Sleeve diameter (in):	0.775	Depth of probe (in):	16
Sleeve length (in):	0.685	Length of probe (in):	25.81
Shape factor (in):	3.23	H_1 (in):	88.63
Tube diameter (in):	0.25	H_2 (in):	82.63

Trial	1	2	3	4	5
Time (sec)	473.8	437.8	410.2	369.8	386.5
Permeability (cm/sec)	5.71E-06	6.18E-06	6.59E-06	7.31E-06	7.00E-06
			Average k (cm/sec)		6.56E-06

LABORATORY PERMEABILITY TEST

Test performed by the FDOT

Average k (cm/sec) 6.90E-0

BACK CALCULATED SHAPE FACTOR

Trial	H_1 (in)	H_2 (in)	Time (sec)	Perm. (cm/sec)	Calculated F (cm)	Calculated F (in)
1	88.63	82.63	473.8	6.90E-06	6.79	2.67
2	88.63	82.63	437.8	6.90E-06	7.35	2.89
3	88.63	82.63	410.2	6.90E-06	7.84	3.09
4	88.63	82.63	369.8	6.90E-06	8.70	3.43
5	88.63	82.63	386.5	6.90E-06	8.32	3.28
				Average F	7.80	3.07

INSITU FALLING HEAD TEST

Sample ID: 411

Location: West upper

Sleeve diameter (in):	0.775	Depth of probe (in):	8
Sleeve length (in):	0.685	Length of probe (in):	27.13
Shape factor (in):	3.23	H_1 (in):	81.94
Tube diameter (in):	0.25	H_2 (in):	75.94

Trial	1	2	3	4	5
Time (sec)	137.2	152.0	138.0	140.4	151.6
Permeability (cm/sec)	2.14E-05	1.93E-05	2.13E-05	2.09E-05	1.94E-05
			Average k (cm/sec)		2.04E-05

LABORATORY PERMEABILITY TEST

Test performed by the FDOT

Average k (cm/sec) 5.37E-0

BACK CALCULATED SHAPE FACTOR

Trial	H_1 (in)	H_2 (in)	Time (sec)	Perm. (cm/sec)	Calculated F (cm)	Calculated F (in)
1	81.94	75.94	137.2	5.37E-07	326.88	128.69
2	81.94	75.94	152.0	5.37E-07	295.05	116.16
3	81.94	75.94	138.0	5.37E-07	324.98	127.95
4	81.94	75.94	140.4	5.37E-07	319.43	125.76
5	81.94	75.94	151.6	5.37E-07	295.83	116.47
				Average F	312.43	123.00

INSITU FALLING HEAD TEST

Sample ID: 412

Location: West lower

Sleeve diameter (in):	0.775	Depth of probe (in):	15.75
Sleeve length (in):	0.685	Length of probe (in):	27.13
Shape factor (in):	3.23	H_1 (in):	89.69
Tube diameter (in):	0.25	H_2 (in):	83.69

Trial	1	2	3	4	5
Time (sec)	547.5	615.6	676.2	736.5	697.0
Permeability (cm/sec)	4.88E-06	4.34E-06	3.95E-06	3.63E-06	3.83E-06
			Average k (cm/sec)		4.13E-06

LABORATORY PERMEABILITY TEST

Test performed by the FDOT

Average k (cm/sec) 5.33E-0

BACK CALCULATED SHAPE FACTOR

Trial	H_1 (in)	H_2 (in)	Time (sec)	Perm. (cm/sec)	Calculated F (cm)	Calculated F (in)
1	89.69	83.69	547.5	5.33E-06	7.51	2.96
2	89.69	83.69	615.6	5.33E-06	6.68	2.63
3	89.69	83.69	676.2	5.33E-06	6.08	2.39
4	89.69	83.69	736.5	5.33E-06	5.58	2.20
5	89.69	83.69	697.0	5.33E-06	5.90	2.32
				Average F	6.35	2.50

INSITU FALLING HEAD TEST

Sample ID: 413

Location: West upper

Sleeve diameter (in):	0.775	Depth of probe (in):	8
Sleeve length (in):	0.685	Length of probe (in):	25.25
Shape factor (in):	3.23	H_1 (in):	80.06
Tube diameter (in):	0.25	H_2 (in):	74.06

Trial	1	2	3	4	5
Time (sec)	61.7	51.7	54.4	56.8	57.8
Permeability (cm/sec)	4.87E-05	5.81E-05	5.53E-05	5.29E-05	5.20E-05
			Average k (cm/sec)		5.34E-05

LABORATORY PERMEABILITY TEST

Test performed by the FDOT

Average k (cm/sec) 5.37E-0

BACK CALCULATED SHAPE FACTOR

Trial	H_1 (in)	H_2 (in)	Time (sec)	Perm. (cm/sec)	Calculated F (cm)	Calculated F (in)
1	80.06	74.06	61.7	5.37E-07	744.57	293.14
2	80.06	74.06	51.7	5.37E-07	888.58	349.84
3	80.06	74.06	54.4	5.37E-07	844.48	332.47
4	80.06	74.06	56.8	5.37E-07	808.80	318.42
5	80.06	74.06	57.8	5.37E-07	794.80	312.91
				Average F	816.25	321.36

INSITU FALLING HEAD TEST

Sample ID: 414

Location: West lower

Sleeve diameter (in):	0.775	Depth of probe (in):	17.375
Sleeve length (in):	0.685	Length of probe (in):	25.25
Shape factor (in):	3.23	H_1 (in):	89.44
Tube diameter (in):	0.25	H_2 (in):	86.44

Trial	1	2	3	4	5
Time (sec)	167.0	142.9	144.9	145.2	135.0
Permeability (cm/sec)	7.88E-06	9.21E-06	9.09E-06	9.07E-06	9.75E-06
			Average k (cm/sec)		9.00E-06

LABORATORY PERMEABILITY TEST

Test performed by the FDOT

Average k (cm/sec) 5.33E-0

BACK CALCULATED SHAPE FACTOR

Trial	H_1 (in)	H_2 (in)	Time (sec)	Perm. (cm/sec)	Calculated F (cm)	Calculated F (in)
1	89.44	86.44	167.0	5.33E-06	12.14	4.78
2	89.44	86.44	142.9	5.33E-06	14.18	5.58
3	89.44	86.44	144.9	5.33E-06	13.99	5.51
4	89.44	86.44	145.2	5.33E-06	13.96	5.50
5	89.44	86.44	135.0	5.33E-06	15.01	5.91
				Average F	13.86	5.46

INSITU FALLING HEAD TEST

Sample ID: 415

Location: West upper

Sleeve diameter (in):	0.775	Depth of probe (in):	8
Sleeve length (in):	0.685	Length of probe (in):	28.31
Shape factor (in):	3.23	H_1 (in):	83.13
Tube diameter (in):	0.25	H_2 (in):	77.13

Trial	1	2	3	4	5
Time (sec)	142.0	109.8	121.4	121.4	127.4
Permeability (cm/sec)	2.04E-05	2.63E-05	2.38E-05	2.38E-05	2.27E-05
			Average k (cm/sec)		2.34E-05

LABORATORY PERMEABILITY TEST

Test performed by the FDOT

Average k (cm/sec) 5.37E-0

BACK CALCULATED SHAPE FACTOR

Trial	H_1 (in)	H_2 (in)	Time (sec)	Perm. (cm/sec)	Calculated F (cm)	Calculated F (in)
1	83.13	77.13	142.0	5.37E-07	311.14	122.50
2	83.13	77.13	109.8	5.37E-07	402.39	158.42
3	83.13	77.13	121.4	5.37E-07	363.94	143.28
4	83.13	77.13	121.4	5.37E-07	363.94	143.28
5	83.13	77.13	127.4	5.37E-07	346.80	136.53
				Average F	357.64	140.80

INSITU FALLING HEAD TEST

Sample ID: 416

Location: West lower

Sleeve diameter (in):	0.775	Depth of probe (in):	14.5
Sleeve length (in):	0.685	Length of probe (in):	28.31
Shape factor (in):	3.23	H_1 (in):	89.63
Tube diameter (in):	0.25	H_2 (in):	86.63

Trial	1	2	3	4	5
Time (sec)	280.4	302.4	264.6	270.8	279.7
Permeability (cm/sec)	4.68E-06	4.34E-06	4.96E-06	4.85E-06	4.70E-06
			Average k (cm/sec)		4.71E-06

LABORATORY PERMEABILITY TEST

Test performed by the FDOT

Average k (cm/sec) 5.33E-0

BACK CALCULATED SHAPE FACTOR

Trial	H_1 (in)	H_2 (in)	Time (sec)	Perm. (cm/sec)	Calculated F (cm)	Calculated F (in)
1	89.63	86.63	280.4	5.33E-06	7.21	2.84
2	89.63	86.63	302.4	5.33E-06	6.69	2.63
3	89.63	86.63	264.6	5.33E-06	7.64	3.01
4	89.63	86.63	270.8	5.33E-06	7.47	2.94
5	89.63	86.63	279.7	5.33E-06	7.23	2.85
				Average F	7.25	2.85

LIST OF REFERENCES

Bowles, J.E., Engineering Properties of Soils and Their Measurements (4th ed.), McGraw-Hill, Inc., New York, 1992.

Cedergren, H.R., Drainage of Highway and Airfield Pavements, Robert E. Krieger Publishing Company, Malabar, Florida, 1987.

Cedergren, H.R., Seepage, Drainage, and Flow Nets (3rd ed.), Wiley-Interscience, New York, 1989.

Daniel, D.E., "In Situ Hydraulic Conductivity Tests for Compacted Clay," Journal of Geotechnical Engineering, ASCE, Vol. 115, No. 9,1989, pp. 1205-1225.

Das, B.M., Principles of Foundation Engineering (2nd ed.), PWS-Kent Publishing Company, Boston, 1990.

Davidson, J.L., Class notes for Groundwater and Seepage Problems in Geotechnical Engineering. University of Florida, Gainesville, Summer 1996a.

Davidson, J.L., Soil Mechanics Laboratory Manual, University of Florida, Gainesville Spring 1996b.

Glover, R.E., "Ground-water Movement," Engineering Monograph No. 31 (2nd printing), U.S. Department of the Interior, Bureau of Reclamation, Denver, April 1966.

Highway Research Board, "Final Report of Project Committee No. 1, Maintenance of Concrete Pavements as Related to the Pumping Action of slabs," Proceedings, Highway Research Board, 28th Annual Meeting, 1948, p. 282.

Hvorslev, M.J., Time Lag in the Observation of Ground-water Levels and Pressures, U.S. Army Engineers Waterways Experiment Station, Vicksburg, Mississippi, 1949.

Hvorslev, M.J., "Time Lag and Soil Permeability in Ground-Water Observations," Bulletin No. 36, Waterways Experiment Station, Corps of Engineers, Vicksburg, Mississippi, 1951.

Lambe, T.W, & Whitman, R.V., Soil Mechanics, John Wiley & Sons, Inc., New York, 1969.

Olson, R.E., & Daniel, D.E., "Measurement of the Hydraulic Conductivity of Fine-Grained Soils," ASTM STP 746, American Society for Testing and Materials, 1981, pp. 18-64.

Sharma, H.D., & Lewis, S.P., Waste Containment Systems, Waste Stabilization, and Landfills Design and Evaluation, Wiley-Interscience, New York, 1994.

Spellman, D.L., "Faulting of Concrete Pavements," Highway Research Record No. 407, Highway Research Board, 1972.

Standard Specifications for Road and Bridge Construction, Florida Department of Transportation, Tallahassee, 1991

Terzaghi, K., & Peck, R.B., Soil Mechanics in Engineering Practice (2nd ed.), John Wiley & Sons, Inc., New York, 1967.

Wright, P.H, & Paquette, R.J., Highway Engineering (5th ed.), John Wiley & Sons Inc., New York, 1987